DISTRIBUTED DETECTION AND ESTIMATION WITH RELIABILITY-BASED SPLITTING ALGORITHMS IN RANDOM-ACCESS NETWORKS

A Dissertation
Presented to
The Academic Faculty

by

Seksan Laitrakun

In Partial Fulfillment
of the Requirements for the Degree
Doctor of Philosophy in the
School of Electrical and Computer Engineering

Georgia Institute of Technology
December 2014

DISTRIBUTED DETECTION AND ESTIMATION WITH RELIABILITY-BASED SPLITTING ALGORITHMS IN RANDOM-ACCESS NETWORKS

Approved by:

Professor Edward J. Coyle, Advisor
School of Electrical and Computer Engineering
Georgia Institute of Technology

Professor Douglas M. Blough
School of Electrical and Computer Engineering
Georgia Institute of Technology

Professor Xiaoli Ma
School of Electrical and Computer Engineering
Georgia Institute of Technology

Professor Fumin Zhang
School of Electrical and Computer Engineering
Georgia Institute of Technology

Professor Yajun Mei
School of Industrial and Systems Engineering
Georgia Institute of Technology

Date Approved: August 12, 2014

To my parents, my wife, and my family.

ACKNOWLEDGEMENTS

I would like to express my sincere gratitude to my advisor, Dr. Edward J. Coyle, for his tireless guidance, support, and encouragement. I have learned a lot from his insightful comments, keen vision, and professional approach to research and education. Our meetings are what I always look forward to – not only enlightening suggestions but also many funny stories. He is one of the most clam and patient human beings I have ever met. It has been a great honor to work with him.

I would also like to thank my dissertation committee members: Dr. Douglas M. Blough, Dr. Xiaoli Ma, Dr. Fumin Zhang, and Dr. Yajun Mei, for their effort and time spent on my dissertation. Their comments and suggestions have improved and reshaped the research in this dissertation.

I would like to thank my friends for their help and friendship: Dr. Daniel Lertprachaya, Pisit Jarumaneeroj, Dr. Soravit Vitoontus, Kasemsit Teeyapan, Napol Chaisilwattana, Dr. Vibhav Kapnadak, Dr. Xusheng Sun, Ghaith Matalkah, Dr. Zhenhua Yu, and Deepa Phanish.

Last but not least, I would like to express my deepest gratitude to my parents, my wife, and my family for their endless love and support. All I have accomplished is really from them.

TABLE OF CONTENTS

LIST OF TABLES

LIST OF FIGURES

SUMMARY

We design, analyze, and optimize distributed detection and estimation algorithms in a large, shared-channel, single-hop wireless sensor network (WSN). The fusion center (FC) is allocated a shared transmission channel to collect local decisions/estimates but cannot collect all of them because of limited energy, bandwidth, or time. A strategy for this situation that is based on a combination of probabilistic node selection and probabilistic transmission scheduling is developed to improve the performance of distributed detection and estimation algoirthms. Specifically, we propose a reliability-based splitting algorithm that enables the FC to collect local decisions/estimates in descending order of their reliabilities through a shared channel. The algorithm divides the transmission channel into time frames and the sensor nodes into groups based on their observation reliabilities. Only nodes with a specified range of reliabilities compete for the channel using slotted ALOHA within each frame. Nodes with the most reliable decisions/estimates attempt transmission in the first frame; nodes with the next most reliable set of decisions/estimates attempt in the next frame; etc. The set of reliability thresholds used to divide the nodes into groups affects the performance of distributed detection/estimation applications by controlling a tradeoff between channel throughput and the quality of local decisions/estimates.

The performance of the reliability-based splitting algorithm is analyzed in three scenarios: time-constrained distributed detection; sequential distributed detection; and time-constrained estimation. Performance measures of interest – including detection error probability, efficacy, asymptotic relative efficiency, and estimator variance – are derived and used to determine optimal and suboptimal reliability thresholds. We also propose and analyze algorithms that exploit information from the occurrence of collisions to improve the performance of both time-constrained distributed detection and sequential distributed detection.

CHAPTER I

INTRODUCTION

Advances in electronics and wireless communications have enabled the creation of cost-effective wireless sensor networks (WSNs). In these networks, a number of small, inexpensive, often battery-powered sensor nodes are deployed in a geographic area. The network's sensor nodes perform such functions as environmental monitoring, surveillance, event detection, etc., in which they make observations of their local environments, process those observations, and share the results with each other or a fusion center (FC) over a wireless communication channel. The existence of such WSNs has renewed interest in distributed/decentralized signal processing algorithms that support the detection and estimation tasks these networks are asked to perform. The focus of this thesis is the development of new signal processing algorithms and the analysis of the improvements they enable in the performance of distributed detection and estimation tasks.

An overview of prior research in this area is provided in Section 1.1. It focuses on prior efforts in the design, analysis, and optimization of distributed detection/estimation algorithms. In these distributed detection/estimation algorithms, a number of sensor nodes are grouped together to monitor the state of an event. They then wirelessly send their individual decisions/estimates/observations to the FC. Based on the received local decisions/estimates/observations, the FC computes a global decision/estimate.

The objective of this dissertation is to design, analyze, and optimize distributed detection/estimation algorithms in a *large*, *shared-channel*[1], *single-hop* WSN in which

[1]A data packet is transmitted successfully if no other packets are transmitted during this time.

the FC cannot collect local decisions/estimates from all of the nodes to produce a global decision/estimate. This can occur if the time allowed for making a global decision is limited, if the FC does not have sufficient energy, or if the communication channel is very limited or unreliable. When this does occur, the immediate challenge is to develop a strategy to collect the "best" local decisions, which would be the ones that are least corrupted by noise, nearest to an event being observed, or have reliable communications with the FC. In other words, a *node-selection* strategy is required. In addition, since all local decisions/estimates/observations are sent through a shared channel, a suitable *transmission-scheduling* strategy is necessary. We address these challenges through *probabilistic* selection and scheduling. The scope and organization of the dissertation are provided in Section 1.2.

1.1 Background and Literature Review

In this section, we provide an overview of prior work that is closely related to the topic of this thesis.

1.1.1 Single-Hop Distributed Detection with a Centralized Fusion Center

A simple single-hop centralized fusion system for distributed detection is shown in Fig. 1, where g_n and η_n are the observation gain and additive noise of the nth sensor node, respectively. The sensor nodes observe an event through *observation channels* that experience additive noise and/or observation gains. Based on these observations, the sensor nodes might either make and transmit local decisions or quantize and transmit their observations. These transmissions are then received by the FC via a shared wireless communication channel. Upon receiving these local decisions/observations, the FC uses either a fixed-sample-size (FSS) detector or a sequential detector to fuse the received data to compute a global decision. If local decisions are sent, the FC's fusing process is called *decision fusion*. If local observations are sent, the FC's fusing process is called *data fusion*. Clearly, the performance of a data fusion algorithm will

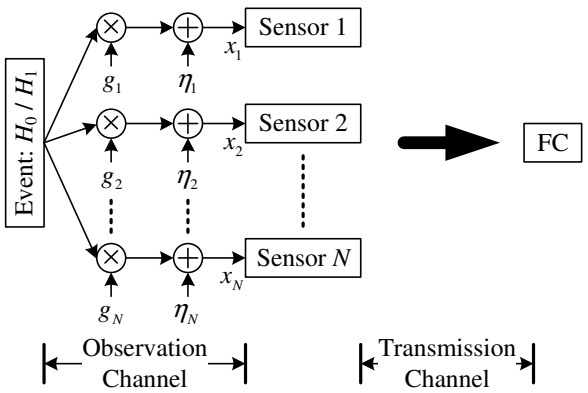

Figure 1: A model of single-hop distributed detection with a centralized FC.

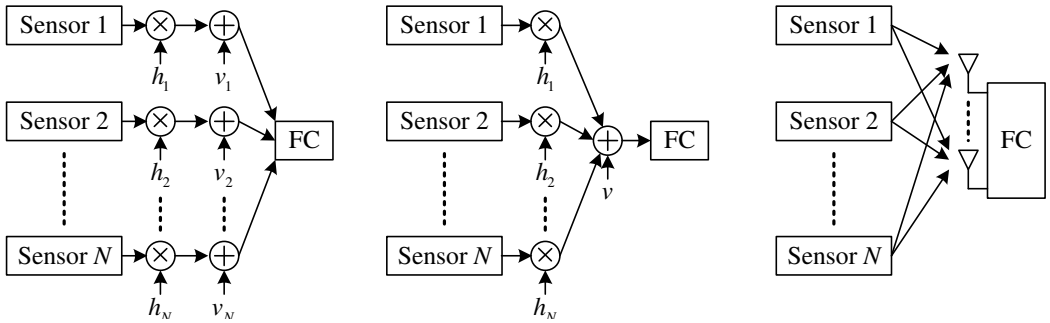

(a) PAC (b) MAC (c) MIMO

Figure 2: Types of transmission channels. Note that we do not show channel gains and additive noise in the MIMO channel model.

be at least as good as the performance of a decision fusion algorithm.

The transmission channels that the nodes use to send their local decisions/observations to the FC can be categorized into four types:

1. *Parallel Access Channel (PAC):* In the PAC, the local decisions/observations are sent to the FC via orthogonal channels, such as in TDMA or FDMA. The model of the PAC is shown in Fig. 2(a). Mathematically, the received signal y at the FC can be written as $y = \sum_{n=1}^{N} \left(h_n b_n + v_n\right)$, where h_n, b_n, and v_n are the channel gain, the transmitted decision/observation, and the additive noise of the nth node, respectively. Therefore, the effect of the additive noise increases as N increases. Note that a special case of the PAC with no knowledges of

the channel gains and the additive noise is studied in [68, 75], where the local decisions received at the FC will have bits flipped according to a known cross-over probability.

2. *Multiple Access Channel (MAC):* In the MAC, the local decisions/observations are modulated with different and orthogonal waveforms and then sent to the FC. One example of a MAC is the CDMA channel. A model of this type of MAC is shown in Fig. 2(b). Mathematically, the received signal y at the FC can be written as $y = \sum_{n=1}^{N} h_n b_n \phi_n + v$, where ϕ_n is the nth orthogonal waveform and v is a common additive noise. In the MAC, the effect of the additive noise does not increase as N increases.

3. *Multiple-Input Multiple-Output (MIMO) channel:* A model of the MIMO channel is shown in Fig. 2(c), where the FC is equipped with multiple antennas. The MIMO channel can be thought as a combination between the PAC and MAC.

4. *Random Multiple Access (RMA) channel:* In the RMA channel, time on a single channel is divided into time slots. Each sensor node will send its local decision/observation to the FC by transmitting in these slots according to the slotted ALOHA protocol, a CSMA-based protocol, or some other RMA protocols. The nodes randomly and independently choose slots in which to transmit, so collisions will occur. In the most typical collision model, a node will successfully send its decision/observation to the FC only if it is the only one that transmits in that time slot; otherwise, its packet is lost and is either dropped or retransmitted later. An RMA channel is used when it is not possible for the system to schedule the nodes' transmissions in advance.

Examples of the work on distributed detection categorized by the FC's detectors and type of transmission channels are shown in Table 1.

Table 1: Examples of the work on distributed detection categorized by the FC's detectors and the transmission channels.

Detector	PAC	MAC	MIMO	RMA
FSS	[4, 6, 20, 22, 50, 57]	[6, 46, 48, 50, 74, 96]	[23, 24, 56, 98]	[5, 19]
Sequential	[77, 95]	-	-	[2, 53, 92, 93]

Generally speaking, there are two mandatory derivations in distributed detection: optimal fusion rules and performance measures. The optimal fusion rules depend on the transmission channel used, and can be found in the papers provided in the table. The performance measures that are typically used include: probability of a false alarm, probability of a miss, and probability of detection error. Unfortunately, closed-form expressions for these performance measures are often difficult or impossible to obtain. Approximations and asymptotic performance measures are thus derived instead. Typically, the central-limit theorem is extensively used to compute approximations of these performance measures, such as in [2,5,24,46,70]. On the other hand, some asymptotic measures can be obtained in closed-form, including:

- *Error exponent* (when the number of collected decisions/observations approaches infinity) [5, 48, 50, 68],
- *Kullback-Leibler divergence* [54, 83],
- *Efficacy* (when the observation SNR approaches zero),
- *Asymptotic relative efficiency* (a relative performance between two schemes when the observation SNR approaches zeros) [29, 32, 67].

Distributed detection can be extended to multi-hop topologies, where the local decisions/observations must be forwarded by one or more other nodes before they can reach the FC [4, 49, 60, 68, 71, 72]. The optimal distributed detection rule in a serial/tandem network was derived in [71, 72]. However, asymptotically, the performance of the serial distributed detection algorithm is worse than that of the

parallel distributed detection algorithm [60]. Aggregation strategies to reduce the traffic load in multi-hop distributed detection were studied in [68]. In addition to multi-hop strategies, distributed detection with a mobile FC has been proposed in [2, 53, 70], where the FC moves around the area of interest to collect the local decisions/observations via single-hop transmissions.

1.1.2 Distributed Estimation

In distributed estimation [91], the FC computes a global parameter estimate from the sensor nodes' local estimates, which are quantized versions of the observations. Many efforts have focused on designing the sensor nodes' optimal quantizers. Binary quantizers (i.e., binary local estimates) minimizing the Cramer-Rao lower bound (CRLB) were studied in [66], while adaptive binary quantizers were proposed in [30, 39]. The performance degradation caused by use of binary local estimates was derived in [21]. The optimal quantizers for multiple-bit estimates were investigated in [51, 78].

Many fusion rules for distributed estimation have been studied in [91]. A popular approach is the best linear unbiased estimator (BLUE) [90]. The global estimate under a BLUE approach is obtained from a weighted sum of the local estimates, where the weights are computed from the sensor nodes' noise variances. Under resource constraints on, for example, power and number of bits, [47, 69, 88] formulated optimization problems to find optimal allocation strategies, all of which depend on the local noise variances.

1.1.3 Sensor-Selection Strategies

In distributed detection/estimation, the local decisions/estimates possess different reliabilities (probabilities of correct decision/estimate) because of observation noise or other error sources. Strategies used to collecting only the most reliable decisions/estimates can help to improve the WSN's performance and reduce energy consumption. Indeed, there are two interesting sensor-selection strategies: censoring

sensors [65] and ordered transmissions [13], which we now summarize.

The censoring-sensor strategy introduced by [65] for distributed detection demonstrates that only reliable decisions should be collected and fused by the FC. In this strategy, only the nodes with likelihood-ratio (LR) values greater than a predetermined threshold send their LR values to the FC. A global decision is then made from these very reliable LR values. On the other hand, the nodes with LR values below the preset threshold do not transmit their local decisions and can sleep in order to save energy. The censoring-sensor strategy has been applied and studied in many scenarios where either LR values or binary decisions are sent to the FC; see, for example, a scenario [2] with a mobile FC and a scenario in [22] with a multi-level censoring-sensor strategy. An example of distributed estimation using a censoring-sensor strategy has been introduced in [55].

An ordered-transmission strategy, introduced by [13], combines the censoring-sensor strategy with a sequential detector. The LR values computed from the nodes' observations are sent in descending order of their magnitude to the FC; i.e., the most reliable decisions are sent first. It can be conjectured that this strategy provides the fastest way to reach a required performance measure. Examples of algorithms using the ordered-transmission strategy can be found in [11, 15, 37, 52, 94].

1.1.4 Random-Access Protocols

Under resource constraints such as time, bandwidth, and energy, not all local decisions/estimates/observations will be collected. A sensor-selection strategy might then be applied. In this case, the perfect transmission scheduling is not applicable. Therefore, a random-access protocol, which is a *probabilistic* transmission-scheduling method, must be exploited instead.

Random-access protocols consist of two parts: *channel access* and *collision resolution*. *Channel access* determines how nodes transmit their packets. For example, in

ALOHA [1] the nodes send their packets immediately upon receipt, while in carrier sense multiple access (CSMA) [42] the nodes sense whether the channel is in use before sending their packets. Because of a lack of perfect scheduling/coordination amongst the nodes, packet collisions are inherent in any system using a random-access protocol. Therefore, a *collision resolution* strategy is used to retransmit collided packets. Examples of collision resolution strategies include: tree algorithms [17,82], probabilistic-backoff strategies [10,36], and heuristic-backoff strategies [43]. Probabilistic back-off strategies are used extensively in industrial standards for wireless networks, including IEEE 802.11.a/b/g/n/etc. (WiFi) and IEEE 802.15.4 (ZigBee).

Likewise, applications that use random-access protocols in distributed detection and estimation have been studied in many scenarios, especially when there is no information on which nodes will be active at any given time. In [2,53,70], a mobile FC moves around the area of interest to collect the local decisions. Since the FC does not know which nodes are within the current communication range, they cannot schedule the transmission of local-decision transmissions, and slotted ALOHA or CSMA/CA is used as the channel-access protocol. In [19,92,93], the censoring-sensor and ordered-transmission strategies[2] are applicable for distributed detection/estimation using a shared channel by exploiting slotted ALOHA. These schemes proposed threshold-based slotted-ALOHA protocols, where local decisions whose reliabilities are larger than a threshold are sent to the FC during a particular time frame.

1.2 Scope and Organization

We propose a *reliability-based splitting algorithm* for a large, shared-channel, single-hop distributed detection/estimation whose FC is not able to collect local decisions/estimates/observations from all sensor nodes. The principles and assumptions underlying the reliability-based splitting algorithm are as follows:

[2]The censoring-sensor [65] and ordered-transmission strategies [13] require a complete knowledge of decisions/estimates' reliabilities to properly schedule the nodes' transmissions.

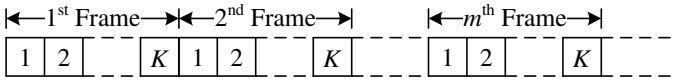

Figure 3: The transmission channel is divided into frames. Each frame consists of K time slots.

1. *Frame-based transmission channel:* We assume that a single shared channel is provided for the considered distributed detection/estimation application. The transmission channel is divided into frames, where each frame consists of K time slots, as shown in Fig. 3, unless we specify otherwise.

2. *Reliability-based splitting strategy:* The sensor nodes are divided into $M + 1$ groups according to a set of reliability thresholds $\{\hat{r}_1, \hat{r}_2, \ldots, \hat{r}_M\}$. The mth group contains the nodes whose observations have reliabilities $r \in [\hat{r}_m, \hat{r}_{m-1})$. The reliability thresholds $\{\hat{r}_m\}$ and the observation reliability r depend on applications and will be defined in the chapters that follow. Note that the $(M+1)$st group contains the nodes whose observations have reliabilities $r < \hat{r}_M$.

3. *Sensor processing:* A node collects an observation and computes its observation's reliability. If its observation's reliability r is such that $r \in [\hat{r}_m, \hat{r}_{m-1})$, then it schedules the transmission of its local decision/estimate/observation within the mth frame.

4. *Channel access protocol:* When the mth frame arrives, each node with $r \in [\hat{r}_m, \hat{r}_{m-1})$ will use slotted ALOHA to send their decisions/estimates/observations.

5. *Fusion center processing:* Upon receipt of the local decisions/estimates/observations, the FC computes a global decision/estimate using a specified fusion rule.

We apply the the reliability-based splitting algorithm in distributed detection/estimation with constraints. Two types of constraints are considered in this dissertation: time and performance. For the time constraint, the FC has to make a global decision/estimation

		Time Constraint	Performance Constraint
Detection	Not Collision-Aware	Chapter 2	Chapter 4
	Collision-Aware	Chapter 3	Chapter 5
Estimation		Chapter 6	

Figure 4: Dissertation organization.

at the end of a specific collection time. This is equivalent to a *fixed-sample-size analysis*. On the other hand, for the performance constraint, the FC continues collecting local decisions/estimates/observations until the required performance level is reached. This is equivalent to a *sequential analysis*. As a result, we organize the chapters as shown in Fig. 4 and summarize the details as follows.

- *Chapter 2:* We apply the reliability-based splitting algorithm in distributed detection applications in which the FC has a *limited time* to collect and process local decisions to produce a global decision. We thoroughly study and examine the performance of the proposed scheme by determining the detection error probability (DEP), efficacy, and asymptotic relative efficiency (ARE). The optimization problems that yield the reliability thresholds for the collection scheme are formulated. We show, for example, that the reliability thresholds maximizing the channel throughput are not always optimal. Because the proposed scheme orders transmissions of the local-decisions in approximately descending order of reliability but suffers collisions, it will offer better performance than a collision-free scheme with no reliability ordering when the time constraint prevents transmission of all local decisions. The transition point between the two schemes is found by deriving the ARE of the proposed scheme relative to a TDMA-based scheme.

- *Chapter 3:* We derive *collision-aware* fusion rules for time-constrained distributed detection using the reliability-based splitting algorithm. Unlike other distributed detection algorithms with random-access protocols in which packet collisions are treated as errors and ignored, a collision-aware fusion rule exploits the numbers of successful *and* collision time slots in making a global decision. The numerical results show that the collision-aware distributed detection outperforms TDMA-based distributed detection.

- *Chapter 4:* We propose an *ordered sequential detection* scheme which jointly integrates the reliability-based splitting algorithm, an ordered-transmission strategy, and a sequential probability ratio test (SPRT). The proposed scheme allows the FC to collect the local observations in descending order of their reliabilities by using the reliability-based splitting algorithm. As it receives successfully transmitted observations, the FC sequentially decides whether to make a global decision or to continue collecting more local observations. The numerical results show that the proposed scheme significantly outperforms a conventional SPRT scheme. The improvement increases as the number of sensor nodes in the network increases.

- *Chapter 5:* We propose an *ordered sequential detection* algorithm that is *aware of* packet collisions. Unlike many schemes, where packet collisions are treated as errors and ignored, the FC in the proposed scheme can *partially* retrieve the observations from collisions. As a result, the FC sequentially decides whether to make a global decision or to continue collecting more local observations by using *both* the successfully received observations and these partially retrieved observations. Numerical results show that the proposed approach significantly outperforms a conventional SPRT scheme.

- *Chapter 6:* We consider *distributed estimation* applications in which the FC has

a *limited time* to collect local estimates The reliability-based splitting algorithm is applied in a time-constrained distributed estimation application in which the FC uses a best linear unbiased estimator (BLUE) to compute a global estimate. As the performance of the schemes depends on the reliability thresholds, the number of bits representing the estimates, and the number of time slots in a frame, we formulate time-constrained optimization problems and derive methods to obtain the optimal values of these parameters. An interesting result shows that the optimal reliability thresholds do not maximize the channel's throughput.

CHAPTER II

RELIABILITY-BASED SPLITTING ALGORITHMS FOR TIME-CONSTRAINED DISTRIBUTED DETECTION

2.1 Introduction

In a common model of wireless sensor networks (WSNs) that perform distributed detection [12,79], a number of small, inexpensive, sensor-equipped nodes are dispersed over or move around a geographic area to detect events. The local decisions that they make about these events are collected over a wireless channel and processed by a fusion center (FC) to make a reliable global decision. However, when resources such as time, bandwidth, and energy are limited, it may not be possible for the FC to collect the local decisions from all nodes. A sensor-selection strategy is thus required.

Distributed detection schemes with sensor-selection strategies have been studied extensively. The *censoring-sensor* strategy introduced by [65] demonstrates that only reliable decisions should be collected and fused by the FC. Distributed detection with multiple-level censoring has been proposed in [22, 94]. As an extension of censoring strategies, [13] proposed an *ordered-transmission* strategy that combines a censoring-sensor strategy with a sequential detector and the transmission, in descending order, of the likelihood ratios (LR) computed from the nodes' observations. The principle of the ordered-transmission strategy naturally fits in the problems of distributed signal processing with resource constraints. Interesting examples of applying the ordered-transmission strategy can be found in [11, 15, 37, 52, 94]. These papers all considered distributed systems with *no transmission collisions*; they typically assume parallel access channels, not *shared channels*. They thus did not have to develop transmission scheduling algorithms or account for collisions in the channel.

Nodes in a WSN usually share a single channel and use random access protocols, such as ALOHA or CSMA/CA, or scheduling protocols, such as TDMA, to control access to the channel [7]. Distributed detection over a channel with a random access protocol has been studied in, for example, [19, 44, 92, 93, 97]. Random access protocols with adaptive collision resolution algorithms were proposed in [92, 97]. A distributed detection scheme exploiting a threshold-based slotted ALOHA protocol has been studied in [19,44], where the multiuser diversity [3,64] is applied. A slotted-ALOHA protocol with a splitting-tree algorithm for sequential distributed detection was proposed in [93].

2.1.1 Scope and Proposed Scheme

In this chapter, we design a distributed detection scheme that integrates sensor-selection, transmission and decision fusion strategies. We consider the problem of distributed detection in a *large*, shared-channel[1] WSN in which every node is within a *single-hop* of the FC. Time on the shared channel is divided into time slots and at most one node's decision can be transmitted successfully in each slot. The FC is allowed T time slots, called the collection time, to gather local decisions from the nodes and make a global decision. Each node's local decision is assumed to be available at the beginning of the collection time and is *not* updated during T. Note that this is different from the scenario considered in [19]. For a binary WSN, only *binary* decisions $\{1, -1\}$ are sent to the FC. We further assume that the number of nodes, N, is *larger* than T, in which case the FC cannot collect local decisions from all of the nodes.

In an optimal strategy for the above problem, the FC would collect the T most reliable local decisions [13] and fuse them after weighting them according to a function of their reliabilities [18, 68, 75]. This implies that each transmitting node must send

[1]We assume a collision model in which a node's transmission is successful only if it is the only one to transmit during that time.

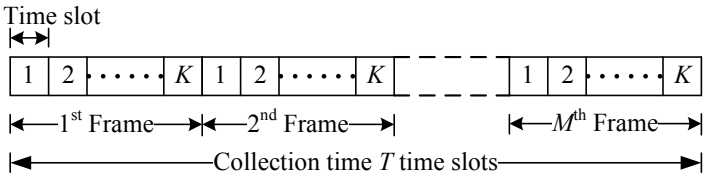

Figure 5: T time slots are available for the collection of binary local decisions. This super-frame of length T is divided into M frames, each with K time slots.

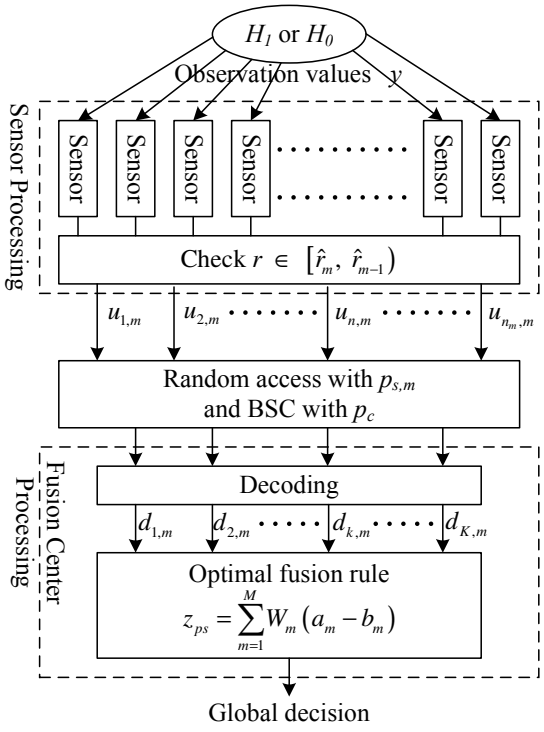

Figure 6: The proposed scheme consists of three layers: sensor processing, channel access, and fusion-center processing. The procedures in each layer are described in Section 2.1.1.

both its local decision and the reliability of that decision to the FC. If the nodes save energy by sending only their local *binary* decisions, the FC does *not* have information on the reliability of each local decision it receives. However, if the arrival times of local decisions at the FC depend on their reliabilities as in [13, 19], the FC is able to approximate the reliabilities of the received *binary* decisions. Inspired by [13,18,19,65], we devise the following time-constrained distributed-detection scheme.

Proposed Scheme: The collection time T is divided into M frames, where each

frame consists of K time slots; i.e., $T = KM$, as shown in Fig. 5. The proposed scheme shown in Fig. 6 performs the following steps. Further details are provided in Section 2.2.

1) *Reliability-based splitting strategy:* The sensor nodes are divided into $M + 1$ groups according to a set of reliability thresholds $\{\hat{r}_m\}$, for $m = 1, \ldots, M$, where $0 \leq \hat{r}_M \leq \ldots \leq \hat{r}_1 < \infty$. The mth group contains the nodes whose observations have reliabilities $r \in [\hat{r}_m, \hat{r}_{m-1})$, where the observation reliability r is defined in Section 2.2, and $\hat{r}_0 = \infty$. Note that the $(M + 1)$st group contains the nodes whose observations have reliabilities $r < \hat{r}_M$.

2) *Sensor processing:* A node collects an observation, makes a binary local decision, and computes its observation's reliability. If its observation's reliability r is such that $r \in [\hat{r}_m, \hat{r}_{m-1})$, then it schedules the transmission of its local decision within the mth frame.

3) *Channel access protocol:* We assume for simplicity that the WSN uses slotted ALOHA; CSMA could be used but would be significantly more complex to analyze. When the mth frame arrives, each node with $r \in [\hat{r}_m, \hat{r}_{m-1})$ independently and randomly chooses one of the K slots in which to transmit its local decision. After sending their decisions, these sensor nodes leave the collection process.

4) *Fusion center processing:* At the FC, the hard decision $d_{k,m}$ corresponding to the signal received at the kth time slot of the mth frame is obtained. The test statistic z_{ps} is computed from a weighted sum of $\{d_{k,m}\}$. Thereafter, a global decision U_G is made by using z_{ps}.

The reliability thresholds control a *tradeoff* between the number of successfully received local decisions at the FC and their decision reliabilities. This tradeoff will be studied in Section 2.3.2. Note that when $K = 1$, the collection-time structure of the proposed scheme is partially similar to that modeled in [19, Sec. IV]. Furthermore,

when $K = 1$, it is almost equivalent to that each sensor node uses a reliability-countdown timer [13] to know when to send its local decision.

There are three characteristics of the proposed scheme worth mentioning.

1) *Collision avoidance by use of frame-based random access:* At any given reliability value, there might be more than one node whose reliabilities are close to this value (within a particular range). If a reliability-countdown timer [13] or $K = 1$ is used, transmission collisions will certainly occur. To reduce the number of collisions among nodes with similar reliabilities, we should have $K > 1$ and these nodes should independently and randomly choose one of the K slots in which to transmit their local decisions.

2) *Header-time reduction by no retransmission:* In the proposed scheme, we are considering a case of extremely limited resources in which only one single communication channel and limited collection time are available. Unfortunately, allowing a retransmission strategy induces significant overhead, including: feedback of ACKs from the FC, back-off times to sort out collisions, and transmit-receive switching times for sensor nodes. Therefore, the proposed scheme does not use a retransmission strategy in the current scenario. Consequently, the sensor nodes operate only in the transmit mode.

3) *Complexity compared with a TDMA-based scheme:* We will compare the performance of the proposed scheme to that of a TDMA-based scheme, so a comparison of their complexities is appropriate. Both schemes require the nodes to be able to follow a specific transmission schedule that has been determined and transmitted to them by the FC or has been stored in the nodes before deployment. In our proposed scheme, we assume that the set of reliability thresholds are computed at the FC before being transmitted to the nodes at the start of the collection period. Thus, the two schemes have comparable overheads from the point of view of the sensor nodes. We do not consider how/when to update the reliability thresholds in our algorithm because we

focus in this work on optimizing the performance over one collection time.

By jointly designing the channel access scheme and the fusion rule, the proposed scheme addresses: (1) how to best transmit local decisions when resources are limited to a single communication channel and a fixed collection time, and (2) how to improve the performance of distributed detection algorithms.

2.1.2 Summary of Results

A distributed detection scheme that uses a *reliability-based splitting algorithm* in a *frame*-based random access channel is modeled, and parameters that optimize its performance are determined. As the number of reliability intervals used to split the population is increased, the performance of the scheme improves significantly. The performance of this scheme is then compared with that of a collision-free (TDMA) scheme in which information about the reliability of decisions is not available. When the time to collect decisions is less than a certain threshold, the proposed scheme offers better performance than the TDMA-based scheme, despite the presence of collisions. We determine this threshold by deriving the relative efficiency of the two schemes.

We study our proposed scheme in a *worst-case* scenario: all local decisions that arrive within a frame are *assigned* the lowest reliability allowed in that frame. We thus obtain guaranteed lower bounds on performance. The performance of the proposed scheme is measured by its detection error probability (DEP), efficacy, and asymptotic relative efficiency (ARE) with respect to a TDMA-based scheme. Approximations of the DEP, efficacy, and ARE are derived and shown in (8), (16), and (27), respectively. These reveal the roles of the proposed scheme's parameters and variables: $\{\hat{r}_m\}$, M, N, T, SNR, random access (the probability of successful transmission), and noise distribution. We, thus, use these *approximations* of the DEP, efficacy, and ARE to answer the following questions.

1) *What are the optimal and possibly suboptimal but good reliability thresholds?:*

The effects of the thresholds $\{\hat{r}_m\}$ on the DEP (8) and efficacy (16) are studied. We have formulated constrained optimization problems in (11) and (19) to find the thresholds minimizing the DEP (8) and maximizing the efficacy (16), respectively. Since solving these optimization problems is computationally complex for large M, we propose a set of possibly suboptimal reliability thresholds called the *maximum-throughput thresholds*, which maximize the channel throughput per time slot. We find that the maximum-throughput thresholds are optimal in many cases, such as high SNR or low T, but not in general. Necessary and sufficient conditions for these maximum-throughput thresholds to be optimal are shown in Sections 2.3.2 and 2.4.2. Specific numerical values are determined in Section 2.6.

2) *Can the proposed scheme achieve any required performance by increasing N for a fixed T?:* We study the efficacy of the proposed scheme to answer this question. Using the maximum-throughput thresholds and under the considered system model, the efficacy (22) reveals that if we have $\frac{f'_X(x)}{f_X(x)} \to -\infty$ as $x \to \infty$, where $f_X(x)$ and $f'_X(x)$ are the noise distribution and its first derivative, respectively, then the proposed scheme can achieve any value of efficacy by increasing the network size N. This is important because in the proposed scheme the FC collects only a *subset* of the most reliable local decisions.

3) *When does the proposed scheme outperform a TDMA-based scheme?:* We derive and study the ARE of the proposed scheme relative to a TDMA-based scheme in Section 2.5. The ARE shows a tradeoff between an intelligent collection strategy in which channel collisions are allowed and a random collection strategy in which transmission times are pre-assigned. The expression of the ARE (27) reveals the effects of the collection time, the thresholds, and the noise distribution. We use the ARE to indicate when the proposed scheme asymptotically outperforms a TDMA-based scheme for collecting local decisions from the nodes. For example, as shown in Section 2.6.5, when the observation noise is Gaussian, the numerical results show

Table 2: A summary of key variables and notation.

θ	Event strength
n_m	Number of active nodes in the mth frame
$\bar{n}_m$	Expectation of n_m
p_c	Channel cross-over probability
$p_{e,m}$	Probability of local decision error in the mth frame
$p_{s,m}$	Probability of successful transmission in the mth frame
$\bar{p}_{s,m}$	Probability of successful transmission in the mth frame when the number of active nodes is $\bar{n}_m$
$\hat{\mathbf{r}} = \{\hat{r}_m\}$	Set of reliability thresholds
$\hat{\mathbf{r}}^* = \{\hat{r}_m^*\}$	Set of optimal thresholds
$\hat{\mathbf{r}}^\star = \{\hat{r}_m^\star\}$	Set of asymptotically optimal thresholds
$\hat{\mathbf{r}}^\circ = \{\hat{r}_m^\circ\}$	Set of maximum-throughput thresholds
$\hat{\mathbf{r}}^\diamond = \{\hat{r}_m^\diamond\}$	Set of asymptotic maximum-throughput thresholds
x	Observation noise
K	Total number of time slots in a frame
K_m	Minimum value between K and n_m
$\bar{K}_m$	Minimum value between K and $\bar{n}_m$
M	Total number of frames in one collection time
N	Total number of nodes in the network
SNR	Observation signal-to-noise ratio
T	Allowed collection time
$\mathbf{W} = \{W_m\}$	Set of weights
$\mathbf{W}^* = \{W_m^*\}$	Set of optimal weights
$\mathbf{W}^\star = \{W_m^\star\}$	Set of asymptotically optimal weights
$\breve{(\cdot)}$	Variable inside divided by K
$(\cdot)$	Variable inside divided by N
$f'(z)$	First derivative of $f(z)$ w.r.t. the variable z
$f''(z)$	Second derivative of $f(z)$ w.r.t. the variable z

that the proposed scheme asymptotically outperforms the TDMA-based scheme if $\frac{T}{N} < 0.19$ for $M = 1$ and $\frac{T}{N} < 0.55$ as $M \to \infty$.

The chapter is organized as follows. Section 2.2 describes the proposed system. The DEP and its optimal parameters are developed and discussed in Section 2.3. We investigate the asymptotic performance of the proposed scheme in Section 2.4, where the efficacy and its optimal parameter values are considered, and Section 2.5, where the ARE is studied. Numerical results are shown in Sections 2.6. Conclusions are provided in Section 2.7. To assist the reader, we provide a summary of frequently used variables and notation in Table 2.

2.2 System Model

N sensor nodes are spread over an area to detect events of interest. Assume that the spatially localized and noisy observation y collected by a node is given by:[2] $H_1 : y = \theta + x$ and $H_0 : y = x$, where $\theta > 0$ and the observation noise x seen by each node is independent and identically distributed (IID) with probability density function (PDF) $f_X(x)$. Then, the conditional PDFs of y are: $f(y|H_1) = f_X(y - \theta)$ and $f(y|H_0) = f_X(y)$.

Assumption 1. *We have the following assumptions:*

1) The PDF $f_X(x)$ considered in this chapter is continuous*,* symmetric about zero*,* unimodal*, with* infinite support*, and has a* monotone likelihood ratio[3]*.*

2) The probabilities that H_1 happens and H_0 happens are equally likely: $Pr(H_1) = Pr(H_0)$. This can be relaxed but doing so leads to obscuring details. □

Note that The proposed scheme does still work without the "monotone likelihood ratio" assumption. The derivations of DEP, efficacy, and ARE do not actually require this property. The proposed scheme, the DEP, efficacy, and ARE are functions of the given reliability thresholds. However, some analytical expressions and results shown subsequently would need to be modified and computation of the reliability thresholds would be more complex.

Based on the above assumptions about $f_X(x)$, the absolute value of the log-likelihood ratio (LLR) of y, $\left|\log \frac{f_X(y-\theta)}{f_X(y)}\right|$, is an even function of y with a reflection point at $y = \frac{\theta}{2}$. Therefore, instead of the LLR value, we define an *observation reliability* by $r = |y - \frac{\theta}{2}|$, which is a difference between the observation strength and the decision's threshold $\frac{\theta}{2}$. By defining the reliability in this way, we will later have

[2] A shift-in-mean model has been extensively used in distributed detection, for example, [13, 19, 22, 44, 65, 92–94].

[3] *The monotone likelihood ratio property gives $\frac{d}{dy}\left(\frac{f_X(y-\theta)}{f_X(y)}\right) \geq 0$ or, equivalently, $\frac{f'_X(x_1)}{f_X(x_1)} \geq \frac{f'_X(x_2)}{f_X(x_2)}$ for all $x_1 \leq x_2$. It leads to a single contiguous reliability interval, $[\hat{r}_m, \hat{r}_{m-1})$, for each m, which simplifies our results.*

a clear vision of the effect of the reliability thresholds $\{\hat{r}_m\}$ on the proposed scheme. Instead of studying the performance of the proposed scheme in an average sense, we are interested in a worst-case scenario:

Assumption 2. *A* worst-case *scenario – all local decisions that arrive within a frame are assigned the smallest reliability in the range associated with that frame.* □

The worst-case scenario provides lower bounds on performance. More optimistic but less reliable results would be obtained if the *average* reliability in the interval were used instead of the minimum reliability.

2.2.1 Sensor Processing

Each node makes its own local decision u independently using its observation value y. We have $u = \mathbf{1}_{\{y \geq \frac{\theta}{2}\}} - \mathbf{1}_{\{y < \frac{\theta}{2}\}}$, where the operator $\mathbf{1}_{\{A\}}$ is 1 if A is true and 0 otherwise. We exploit a set of M reliability thresholds, $\{\hat{r}_m\}$, for $m = 1, \ldots, M$, where $0 \leq \hat{r}_M \leq \hat{r}_{M-1} \leq \ldots \leq \hat{r}_1$, to control nodes' channel access, which will be explained in Section 2.2.2. Let u_m be a binary local decision being transmitted in the mth frame. According to the assumption on the worst-case scenario, the reliability of u_m is $\hat{r}_m$. Therefore, we have

$$\Pr(u_m = 1|H_1) = \frac{f_X(\frac{\theta}{2} - \hat{r}_m)}{f_X(\frac{\theta}{2} - \hat{r}_m) + f_X(\frac{\theta}{2} + \hat{r}_m)}, \tag{1}$$

and $\Pr(u_m = -1|H_1) = 1 - \Pr(u_m = 1|H_1)$. Since $f_X(x)$ is symmetric, we also have $\Pr(u_m = -1|H_0) = \Pr(u_m = 1|H_1)$ and $\Pr(u_m = 1|H_0) = \Pr(u_m = -1|H_1)$.

2.2.2 Channel Access Protocol

In the proposed system, the thresholds $\{\hat{r}_m\}$ are used to control nodes' access to the channel. Only the nodes with $r \in [\hat{r}_m, \hat{r}_{m-1})$ are allowed to send their local decisions during the mth frame. Since we have $0 \leq \hat{r}_M \leq \hat{r}_{M-1} \leq \ldots \leq \hat{r}_1 < \infty$, the local decisions are thus sent to the FC approximately in order from the highest to lowest

observation reliabilities. Consequently, the number of nodes attempting transmission in the mth frame, n_m, is a random variable. The joint probability mass function (PMF) of $n_1, \ldots, n_M$ is a multinomial distribution:

$$f(\mathbf{n}) = \frac{N!}{n_1! \cdots n_{M+1}!} \Delta F_1^{n_1}(\theta) \cdots \Delta F_{M+1}^{n_{M+1}}(\theta), \tag{2}$$

where $\mathbf{n} = \{n_m\}$, $n_{M+1} = N - \sum_{m=1}^{M} n_m$, $\Delta F_{M+1}(\theta) = 1 - \sum_{m=1}^{M} \Delta F_m(\theta)$, $\Delta F_m(\theta) = \Delta F_m^{(+)}(\theta) + \Delta F_m^{(-)}(\theta)$, $\Delta F_m^{(+)}(\theta) = \int_{\frac{\theta}{2}+\hat{r}_m}^{\frac{\theta}{2}+\hat{r}_{m-1}} f_X(x)\, dx$, and $\Delta F_m^{(-)}(\theta) = \int_{\frac{\theta}{2}-\hat{r}_{m-1}}^{\frac{\theta}{2}-\hat{r}_m} f_X(x)\, dx$. The average number of nodes attempting transmission in the mth frame is $\bar{n}_m = N\Delta F_m(\theta)$. Note that because of our assumption about the PDF $f_X(x)$, the joint PMF $f(\mathbf{n})$ does *not* depend on the hypothesis H_i.

Since the *identities* and number of the nodes that will attempt transmission in the mth frame are unknown in advance, we assume a *slotted ALOHA* protocol enables them to share the channel. Each node active during this frame will *randomly choose a time slot* to send its local decision. Because a collision channel is assumed, a node's transmission is successful only if it is the only one to transmit in that slot. Since the active nodes use a fixed transmission probability strategy, feedback on the channel state (success, idle, collision) is not necessary. In addition, we do not consider the case of multi-packet reception in this work. Therefore, the conditional probability of successful transmission $p_{s,m}$ in *any one* of the time slots in the mth frame is expressed as: $p_{s,m} = \frac{n_m}{K}\left(1 - \frac{1}{K}\right)^{n_m - 1}$, which is a function of the random variable n_m. Note that $p_{s,m}$ is obtained from dividing the expected number of successful time slots (derived in Appendix B) by K.

The wireless channel is assumed to be a binary symmetric channel (BSC) with channel crossover probability p_c.

2.2.3 Fusion Center Processing

At the FC, the decoded bit at the kth time slot of the mth frame is denoted by $d_{k,m} \in \{1, -1, 0\}$, where 0 indicates an unrecoverable bit because of either an idle

slot or a collision, which happens with probability $1 - p_{s,m}$. The bits 1 and -1 are successfully received with the probability $p_{s,m}$. In addition to the effect of collisions, the successfully received bits might still be incorrect because of either channel errors or observation errors. Similar to many papers, we assume that any u_m sent at a time slot in the mth frame has identical PMFs: $P(u_m = 1|H_i)$ and $P(u_m = -1|H_i)$, for $i = 0, 1$, defined in (1). Therefore, supposing that u_m is sent, the conditional PMFs of the decoded bit $d_{k,m}$ can be written as, for $i = 0, 1$ and $j = 1, -1$:

$$\Pr(d_{k,m} = j|H_i) = p_{s,m}\big[p_c P(u_m = -j|H_i) + (1 - p_c)P(u_m = j|H_i)\big],$$

and $\Pr(d_{k,m} = 0|H_i) = 1 - p_{s,m}$. Note that the conditional PMFs of $d_{k,m}$ are independent of k. We can show that

$$\Pr(d_{k,m} = 1|H_1) = \Pr(d_{k,m} = -1|H_0) = p_{s,m}(1 - p_{e,m}),$$

$$\Pr(d_{k,m} = 1|H_0) = \Pr(d_{k,m} = -1|H_1) = p_{s,m}p_{e,m},$$

where $p_{e,m}$ is the probability of bit error in the mth frame:

$$p_{e,m} = \frac{p_c f_X(\frac{\theta}{2} - \hat{r}_m) + (1 - p_c)f_X(\frac{\theta}{2} + \hat{r}_m)}{f_X(\frac{\theta}{2} - \hat{r}_m) + f_X(\frac{\theta}{2} + \hat{r}_m)}. \tag{3}$$

After collecting local decisions for T time slots, the FC makes a global decision U_G from the following weighted sum of the number of successfully received/decoded local decisions:

$$z_{ps} = \sum_{m=1}^{M} W_m(a_m - b_m) \begin{cases} > 0, & \text{then } U_G = \quad 1\,(H_1), \\ < 0, & \text{then } U_G = -1\,(H_0), \\ = 0, & \text{randomly choose } U_G, \end{cases} \tag{4}$$

where a_m is the number of decoded bits equal to 1 obtained from the mth frame, b_m is the number of decoded bits equal to -1 obtained from the mth frame, $a_m + b_m \leq \min(K, n_m)$, and W_m is the weight used for local decisions received in the mth frame. Given the hypothesis H_i, for $i = 0$ and 1, the joint conditional PMF of a_m and b_m, is

$$f(a_m, b_m|n_m, H_i) = \frac{K_m!}{a_m!\, b_m!\, c_m!}(p_{s,m}p_{m|i})^{a_m}\left[p_{s,m}(1 - p_{m|i})\right]^{b_m}(1 - p_{s,m})^{c_m}, \tag{5}$$

where $K_m = \min(K, n_m)$, $c_m = K_m - a_m - b_m$, and $p_{m|0} = 1 - p_{m|1} = p_{e,m}$.

Remark 1. *The optimal fusion rule of the proposed scheme is derived in Appendix C. We have the following remarks.*

1) The optimal fusion rule of the proposed scheme is also in the form of a weighted sum of a_m and b_m, where the weights are equal to $\omega_m = \log\left(\frac{1-p_{e,m}}{p_{e,m}}\right)$. However, if we used these weights in (4)*, it would lead us to an intractable analysis since, for example, in the approximation of DEP shown in Proposition 1, no terms are canceled out. Therefore, we leave the weights in* (4) *as parameters we will optimize later.*

2) We will find the optimal weights W_m^* in the next section. The normalized weight $\frac{W_m^*}{W_M^*}$ is slightly different from the normalized weight $\frac{\omega_m}{\omega_M}$.

3) If $f(\mathbf{n})$ depended on H_i, the optimal fusion rule would be a function of c_m too; i.e., the number of collisions and idle slots in each frame *would suggest which hypothesis is happening.* □

2.3 Finite Sample-Size Performance Analysis

In this section, we study the DEP of the proposed scheme for a finite T, the optimal values of the weights $\{W_m\}$, and reliability thresholds $\{\hat{r}_m\}$. Since a closed-form expression for the exact DEP has not been found, we use Gaussian approximation to derive an approximation of the proposed scheme's DEP. We find the weights $\{W_m^*\}$ that are optimal under this approximation and formulate a constrained optimization problem to find the optimal thresholds $\{\hat{r}_m^*\}$.

2.3.1 Derivation of the DEP

The DEP of the proposed scheme is expressed

$$P_E(\mathbf{W}, \hat{\mathbf{r}}) = \sum_{n_1+\ldots+n_{M+1}=N} \cdots \sum P_E(\mathbf{W}, \hat{\mathbf{r}}, \mathbf{n}) f(\mathbf{n}),$$

where $\mathbf{n} = \{n_m\}$, $\mathbf{W} = \{W_m\}$, $\hat{\mathbf{r}} = \{\hat{r}_m\}$, for $m = 1, \ldots, M$, and $P_E(\mathbf{W}, \hat{\mathbf{r}}, \mathbf{n})$ is the DEP depending on the random variables $\mathbf{n}$, and expressed as

$$P_E(\mathbf{W}, \hat{\mathbf{r}}, \mathbf{n}) = \sum_{a_1+b_1+c_1=K_1} \cdots \sum \cdots \sum_{a_M+b_M+c_M=K_M} \cdots \sum \prod_{m=1}^{M} f(a_m, b_m | n_m, H_1) \Big(\mathbf{1}_{\{z_{ps}<0\}} + \frac{1}{2} \mathbf{1}_{\{z_{ps}=0\}} \Big),$$

We show $\mathbf{W}$ and $\hat{\mathbf{r}}$ in the above notation, which will help indicate what $\mathbf{W}$ and $\hat{\mathbf{r}}$ we are using. The number of iterations according to the summations to compute $P_E(\mathbf{W}, \hat{\mathbf{r}})$ is equal to $\left[\frac{(N+M)!}{N!\,M!}\right]\left[\frac{(K_1+2)!}{2!\,K_1!}\right]\cdots\left[\frac{(K_M+2)!}{2!\,K_M!}\right]$. Since no closed form of $P_E(\mathbf{W}, \hat{\mathbf{r}})$ has been found, an approximation of $P_E(\mathbf{W}, \hat{\mathbf{r}})$ is derived instead.

Proposition 1. *An approximation of $P_E(\mathbf{W}, \hat{\mathbf{r}})$ can be expressed as*

$$\tilde{P}_E(\mathbf{W}, \hat{\mathbf{r}}) = \Phi\left(-\sqrt{\frac{\left[\sum_{m=1}^{M} W_m \bar{K}_m \bar{p}_{s,m}(1-2p_{e,m})\right]^2}{\sum_{m=1}^{M} W_m^2 \bar{K}_m \bar{p}_{s,m}\left[1-\bar{p}_{s,m}(1-2p_{e,m})^2\right]}}\right),$$

where $\Phi(\cdot)$ is the Gaussian cumulative distribution function, $\bar{K}_m = \min(K, \bar{n}_m)$, $\bar{p}_{s,m} = \frac{\bar{n}_m}{K}\left(1-\frac{1}{K}\right)^{\bar{n}_m - 1}$, $\bar{n}_m = \mathbb{E}\{n_m\}$, and $\mathbb{E}\{\cdot\}$ is the expectation operator.

Proof. Please see Appendix D, where the conditional PDF of the test statistic z_{ps} is approximated by its asymptotic distribution, i.e., a Gaussian distribution:

$$f_Z(z_{ps}|\mathbf{n}, H_i) \overset{approx}{\sim} \mathcal{N}\big(\mu_i, \sigma_i^2\big), \tag{6}$$

where $\mu_i = \sum_{m=1}^{M} W_m K_m p_{s,m}(2p_{m|i}-1)$ and $\sigma_i^2 = \sum_{m=1}^{M} W_m^2 K_m p_{s,m}\big[1-p_{s,m}(2p_{m|i}-1)^2\big]$. Note that, to obtain the approximation of $P_E(\mathbf{W}, \hat{\mathbf{r}})$, we also applied Craig's formula [25] and Gauss-Hermite quadrature integration. □

The optimal weights $\{W_m^*\}$ minimizing $\tilde{P}_E(\mathbf{W}, \hat{\mathbf{r}})$ are

$$W_m^* = \frac{(1-2p_{e,m})}{[1-\bar{p}_{s,m}(1-2p_{e,m})^2]}, \tag{7}$$

where the proof can be found in Appendix E. Substituting these optimal weights into $\tilde{P}_E(\mathbf{W}, \hat{\mathbf{r}})$, we have

$$\tilde{P}_E(\mathbf{W}^*, \hat{\mathbf{r}}) = \Phi\left(-\sqrt{\sum_{m=1}^{M} \bar{K}_m \frac{\bar{p}_{s,m}(1-2p_{e,m})^2}{[1-\bar{p}_{s,m}(1-2p_{e,m})^2]}}\right), \tag{8}$$

where $\mathbf{W}^* = \{W_m^*\}$. We notice that $\frac{\bar{p}_{s,m}(1-2p_{e,m})^2}{[1-\bar{p}_{s,m}(1-2p_{e,m})^2]}$ in (8) is the *Deflection Coefficient* (DC) of $d_{k,m}$, DC_m, divided by 4. A higher value of DC_m indicates that the detector has a better ability to distinguish between H_1 and H_0.

2.3.2 Optimal and Suboptimal Reliability Thresholds

The reliability thresholds $\{\hat{r}_m\}$ affect the DEP (8) through the variables $\bar{K}_m$, $\bar{p}_{s,m}$, and $p_{e,m}$. The explanations are provided in Appendix F. In summary, varying the reliability thresholds $\{\hat{r}_m\}$ adjusts a tradeoff between the numbers of successfully received local decisions ($\bar{K}_m p_{s,m}$) and the local decision errors ($p_{e,m}$). To find thresholds $\{\hat{r}_m^*\}$ that minimize $\tilde{P}_E(\mathbf{W}^*, \hat{\mathbf{r}})$, we formulate a constrained optimization problem, where constraints are obtained from the following lemma indicating the feasible regions for $\{\hat{r}_m^*\}$.

Lemma 1. *The reliability thresholds $\{\hat{r}_m^*\}$ that minimize $\tilde{P}_E(\mathbf{W}^*, \hat{\mathbf{r}})$ must satisfy, for all m,*

$$\int_{\frac{\theta}{2}-\hat{r}_{m-1}^*}^{\frac{\theta}{2}-\hat{r}_m^*} f_X(x)\,dx + \int_{\frac{\theta}{2}+\hat{r}_m^*}^{\frac{\theta}{2}+\hat{r}_{m-1}^*} f_X(x)\,dx \leq \frac{K}{N}, \tag{9}$$

where $\hat{r}_0^* = \infty$.

Proof. Please see Appendix F. □

Lemma 1 implies that the *optimal average number of active nodes* in any frame must be less than or equal to K. Therefore, when the optimal thresholds are used, the average number of active nodes in the proposed scheme is independent of the size of the network N. An immediate result is the value of $\hat{r}_M^*$, which is shown below.

Corollary 1. *If the optimal reliability thresholds $\{\hat{r}_m^*\}$ are used, $\hat{r}_M^* \geq \hat{r}^\ddagger$, where $\hat{r}^\ddagger$ satisfies*

$$\int_{-\infty}^{\frac{\theta}{2}-\hat{r}^\ddagger} f_X(x)\,dx + \int_{\frac{\theta}{2}+\hat{r}^\ddagger}^{\infty} f_X(x)\,dx = \frac{T}{N}. \tag{10}$$

Proof. The result is given by Lemma 1. □

Therefore, from (8), Lemma 1, and Corollary 1, the optimal thresholds $\{\hat{r}_m^*\}$ can

be obtained by solving the following constrained optimization problem:

$$\max_{\{\hat{r}_1,\ldots,\hat{r}_M\}} \sum_{m=1}^{M} \bar{n}_m \frac{\bar{p}_{s,m}(1-2p_{e,m})^2}{[1-\bar{p}_{s,m}(1-2p_{e,m})^2]} \tag{11}$$

$$\text{s. t.} \quad \int_{\frac{\theta}{2}-\hat{r}_{m-1}}^{\frac{\theta}{2}-\hat{r}_m} f_X(x)\,dx + \int_{\frac{\theta}{2}+\hat{r}_m}^{\frac{\theta}{2}+\hat{r}_{m-1}} f_X(x)\,dx \le \frac{K}{N}, \ \forall m,$$

$$\hat{r}^{\ddagger} \le \hat{r}_M \le \hat{r}_{M-1} \le \ldots \le \hat{r}_1 < \infty,$$

where $\hat{r}_0 = \hat{r}_0^* = \infty$. Because the thresholds $\hat{r}^{\ddagger}$ depend on T in addition to the noise distribution $f_X(x)$, the collection time T affects the choices of the optimal thresholds in the proposed scheme. For any $T < N$, we can restate that, unlike a quantization process [40,58,63,78], where the optimal thresholds depend on the *whole* noise distribution, the proposed scheme's optimal thresholds are characterized by the *tails* of the noise distribution once T is specified. Recall that we assumed the noise distribution has a monotone likelihood ratio; otherwise, the optimal thresholds will be characterized by other parts of the PDF.

An analytical solution to Problem (11) has not been found. Numerical methods (for finding the optimal solution) and suboptimal solutions are studied instead [40,58, 63,78]. Greedy algorithms similar to [78, Section III.A] and [45, Algorithm 2] can be applied to find a candidate (probably, local optimum) of the set of optimal thresholds $\{\hat{r}_m^*\}$.

We now introduce a set of possibly suboptimal thresholds $\{\hat{r}_m^\circ\}$, the *maximum-throughput thresholds*.

Definition 1. *The* maximum-throughput thresholds $\{\hat{r}_m^\circ\}$ *are the thresholds satisfying, for all* $m = 1, \ldots, M$,

$$\int_{\frac{\theta}{2}-\hat{r}_{m-1}^\circ}^{\frac{\theta}{2}-\hat{r}_m^\circ} f_X(x)\,dx + \int_{\frac{\theta}{2}+\hat{r}_m^\circ}^{\frac{\theta}{2}+\hat{r}_{m-1}^\circ} f_X(x)\,dx = \frac{K}{N}, \tag{12}$$

and, $0 \le \hat{r}_M^\circ \le \hat{r}_{M-1}^\circ \le \ldots \le \hat{r}_1^\circ < \hat{r}_0^\circ = \infty$. □

By using the thresholds $\{\hat{r}_m^\circ\}$, the average number of nodes participating in each frame is equal to the number of time slots, K. According to the proposed scheme's

channel access protocol (Section 2.2.2), the active nodes in a frame will attempt to send their decisions with the optimal probability of successful transmission [7]. As a result, using the thresholds $\{\hat{r}_m^\circ\}$ maximizes the channel throughput. An important benefit of the thresholds $\{\hat{r}_m^\circ\}$ is that they are *easily* found by using (12).[4] However, in general, as shown in Lemma 1, the maximum throughput does not guarantee minimization of the DEP of the proposed scheme since the values of the probabilities $\{p_{e,m}\}$ have been compromised. From the optimization problem in (11), necessary conditions for the thresholds $\{\hat{r}_m^\circ\}$ to be optimal can be shown below.

Proposition 2. *If the thresholds* $\hat{\mathbf{r}}^\circ = \{\hat{r}_m^\circ\}$ *are optimal, then* $\lambda_m(\hat{\mathbf{r}}^\circ) \geq 0$*, for all* m*, where*

$$\lambda_m(\hat{\mathbf{r}}^\circ) = -\sum_{i=m}^{M} \frac{\nabla_i^{(\theta)}(\hat{\mathbf{r}}^\circ)}{\left[f_X\left(\frac{\theta}{2} - \hat{r}_i^\circ\right) + f_X\left(\frac{\theta}{2} + \hat{r}_i^\circ\right)\right]}, \tag{13}$$

$$\nabla_i^{(\theta)}(\hat{\mathbf{r}}^\circ) = \Big[\tfrac{4K}{N}\tfrac{(W_i^*)^2}{(1-2p_{e,i})}U_{1,i} - W_i^* U_{2,i}U_{3,i} + W_{i+1}^* U_{2,i}U_{3,i+1}\Big] N\left(1-\tfrac{1}{K}\right)^{K-1},$$

$$U_{1,i} = \frac{(p_c - p_{e,i})f_X'\left(\frac{\theta}{2}-\hat{r}_i^\circ\right) + (p_c + p_{e,i} - 1)f_X'\left(\frac{\theta}{2}+\hat{r}_i^\circ\right)}{f_X\left(\frac{\theta}{2}-\hat{r}_i^\circ\right) + f_X\left(\frac{\theta}{2}+\hat{r}_i^\circ\right)},$$

$$U_{2,i} = f_X\left(\tfrac{\theta}{2} - \hat{r}_i^\circ\right) + f_X\left(\tfrac{\theta}{2} + \hat{r}_i^\circ\right),$$

$$U_{3,i} = (1-2p_{e,i}) + W_i^*\left[1 + K\ln\left(1-\tfrac{1}{K}\right)\right],$$

$$U_{3,M+1} = W_{M+1}^* = 0,\ f_X'(x) = \tfrac{d}{dx}f_X(x).$$

Proof. We briefly outline the proof. The Lagrange multipliers that arise when solving (11) are the variables $\{\lambda_m(\hat{\mathbf{r}}^\circ)\}$ shown in (13), where

$$\nabla_i^{(\theta)}(\hat{\mathbf{r}}^\circ) = \frac{\partial}{\partial \hat{r}_i}\sum_{m=1}^{M} \bar{n}_m \frac{\bar{p}_{s,m}(1-2p_{e,m})^2}{[1-\bar{p}_{s,m}(1-2p_{e,m})^2]}\Big|_{\hat{r}_i=\hat{r}_i^\circ}.$$

From the Karush-Kuhn-Tucker (KKT) conditions, when $\lambda_m(\hat{\mathbf{r}}^\circ) \geq 0$, for all m, the thresholds $\{\hat{r}_m^\circ\}$ are KKT points. The derivation of Proposition 2 is straight forward but tedious and requires a large number of equations. We therefore omit the details. □

[4] The thresholds $\{\hat{r}_m^\circ\}$ can be computed iteratively; for a given $\hat{r}_{m-1}^\circ$, we find $\hat{r}_m^\circ$.

Proposition 2 is a tool for the finite sample-size regime to verify whether the thresholds $\{\hat{r}_m^\circ\}$ under considered scenarios make the DEP $\tilde{P}_E(\mathbf{W}^*, \hat{\mathbf{r}}^\circ)$ a candidate for the optimum. The optimal thresholds $\{\hat{r}_m^*\}$ for *Gaussian noise* are studied in Section 2.6.2. The numerical results show that the conditions in Proposition 2 are also *sufficient*; i.e., the maximum-throughput thresholds $\{\hat{r}_m^\circ\}$ are optimal when these conditions are true.

The conditions in Proposition 2 are also useful in finding the region of T that the thresholds $\{\hat{r}_m^\circ\}$ are optimal. When the thresholds $\{\hat{r}_m^\circ\}$ are not optimal, the DEP $\tilde{P}_E(\mathbf{W}^*, \hat{\mathbf{r}}^\circ)$ they yield is still very close to the minimum DEP $\tilde{P}_E(\mathbf{W}^*, \hat{\mathbf{r}}^*)$. Therefore, when it is not possible to find the optimal thresholds $\{\hat{r}_m^*\}$ because of computational complexity (e.g., when M is large), a system designer might choose the thresholds $\{\hat{r}_m^\circ\}$, suffering only a slight performance degradation.

A sufficient condition on of the optimality of the maximum-throughput thresholds $\{\hat{r}_m^\circ\}$ is stated in the proposition below, which is very intuitive.

Proposition 3. *If we have $p_{e,1} = \ldots = p_{e,M}$ (i.e., all local decisions have the same reliability), the maximum-throughput thresholds $\{\hat{r}_m^\circ\}$ are optimal.*

Proof. It is obvious from the DEP (8) that if we have $p_{e,1} = \ldots = p_{e,M}$ (i.e., all local decisions have the same reliability), the maximum-throughput thresholds $\{\hat{r}_m^\circ\}$ are optimal since they maximize $\bar{K}_m$ and $p_{s,m}$ for all m. □

Actually, this condition can be relaxed to $p_{e,1} \approx \ldots \approx p_{e,M}$, which is very likely to happen when $\frac{T}{N}$ is small. As shown in Section 2.6.2, the maximum-throughput thresholds $\{\hat{r}_m^\circ\}$ are optimal for small $\frac{T}{N}$. Note that if the condition $p_{e,1} = \ldots = p_{e,M}$ is true, there is no benefit to using $M > 1$.

2.4 Asymptotic Performance Analysis - Efficacy

In this section and the next section, we consider the asymptotic performance of the proposed scheme when the size of the network is large ($N \to \infty$) and the event

strength is low ($\theta \to 0$). The setup here is different from a traditional asymptotic analysis in the sense that only a *subset* of local decisions are collected. Note that the asymptotic performance as $N \to \infty$ when *only* the best observation is collected – called a single-transmission scheme – is studied in [15, 52].

Asymptotic analysis has also been used extensively in the study of quantization for signal detection [40, 63], whose optimal quantization thresholds are designed from the *efficacy* and overall performance is evaluated based on *asymptotic relative efficiency* (ARE). One of the main advantages of asymptotic analysis in this case was that the absence of θ leads to *analytical expressions linking the noise distribution* $f_X(x)$ *and the parameter values*: the optimal weights, optimal thresholds, and suboptimal thresholds.

In this section, we derive the efficacy of the proposed scheme and use it to find optimal weights and thresholds. Furthermore, we will use efficacy to determine whether the proposed scheme can achieve any efficacy value as $N \to \infty$.

For our asymptotic analysis to be meaningful, we must determine how several variables should behave as a function of N:

1) We set $\theta = \frac{\gamma}{\sqrt{N}}$, where γ is a constant [41]. Therefore, we have $\theta \to 0$ as $N \to \infty$.

2) As $N \to \infty$, we keep the following ratios constant: $\frac{T}{N} = \check{T}$ and $\frac{T}{K} = M$, where $0 < \check{T} \leq 1$. Note that, as $N \to \infty$, T and K must also approach ∞.

Any variables with the notation $\check{(\cdot)}$ and $\breve{(\cdot)}$ have been normalized by N and K, respectively. Since $\theta \to 0$, we will be able to clearly see the effect of the noise distribution.

2.4.1 Derivation of the Efficacy

As discusses above, as $N \to \infty$ we will also have $T \to \infty$, and $K \to \infty$. The test statistic z_{ps} in (4) is asymptotically a Gaussian random variable with the PDF shown

in (6). Let $\xi(\mathbf{W}, \hat{\mathbf{r}}, \mathbf{n})$ denote the efficacy of the proposed scheme, which can be expressed as [41]

$$\begin{aligned}\xi(\mathbf{W}, \hat{\mathbf{r}}, \mathbf{n}) &= \lim_{N\to\infty} \frac{1}{T} \frac{\left[\frac{\partial}{\partial\theta}\mathbb{E}\{z_{ps}|H_1\}\big|_{\theta=0}\right]^2}{\mathbb{V}ar\{z_{ps}|H_0\}|_{\theta=0}} \\ &= \lim_{N\to\infty} \frac{1}{4M} \frac{\left\{\sum_{m=1}^{M} W_m \breve{K}_m p_{s,m} \left[(1-2p_c)\frac{f'_X(\hat{r}_m)}{f_X(\hat{r}_m)}\right]\right\}^2}{\sum_{m=1}^{M} W_m^2 \breve{K}_m p_{s,m}},\end{aligned} \tag{14}$$

where $\mathbb{V}ar\{z_{ps}|H_0\}$ is the variance of z_{ps} given H_0, and $\breve{K}_m = \min\left(1, \frac{n_m}{K}\right)$. In the derivation of (14), since the PDF $f_X(x)$ is symmetric about zero (Assumption 1), we have $f_X(-\hat{r}_m) = f_X(\hat{r}_m)$ and $f'_X(-\hat{r}_m) = -f'_X(\hat{r}_m)$. Note that $\xi(\mathbf{W}, \hat{\mathbf{r}}, \mathbf{n})$ is a function of random variables $\{n_m\}$. Applying similar steps in Appendix E, we can show that the *asymptotically optimal weights* $\mathbf{W}^\star = \{W_m^\star\}$, which maximize $\xi(\mathbf{W}, \hat{\mathbf{r}}, \mathbf{n})$, are $W_m^\star = -\frac{f'_X(\hat{r}_m)}{f_X(\hat{r}_m)}$. With $\{W_m^\star\}$, we find the efficacy $\xi(\mathbf{W}^\star, \hat{\mathbf{r}}, \mathbf{n})$, as shown in the lemma below.

Lemma 2. *With the asymptotically optimal weights $\{W_m^\star\}$, the efficacy of the proposed scheme can be expressed as*

$$\xi(\mathbf{W}^\star, \hat{\mathbf{r}}, \check{\mathbf{n}}) = \frac{M}{4\check{T}^2} \sum_{m=1}^{M} \min\left(\frac{\check{T}}{M}, \check{n}_m\right) \check{n}_m e^{-\frac{M}{\check{T}}\check{n}_m} \left[(1-2p_c)\frac{f'_X(\hat{r}_m)}{f_X(\hat{r}_m)}\right]^2. \tag{15}$$

Note that $\xi(\mathbf{W}^\star, \hat{\mathbf{r}}, \check{\mathbf{n}})$ is a function of random variables $\{\check{n}_m\}$, where $\check{n}_m = \frac{n_m}{N}$.

Proof. Substituting $\{W_m^\star\}$ into (14), we have

$$\xi(\mathbf{W}^\star, \hat{\mathbf{r}}, \check{\mathbf{n}}) = \lim_{N\to\infty} \frac{1}{4M} \sum_{m=1}^{M} \breve{K}_m p_{s,m} \left[(1-2p_c)\frac{f'_X(\hat{r}_m)}{f_X(\hat{r}_m)}\right]^2.$$

Let $\check{n}_m = \frac{n_m}{N}$. We have $\breve{K}_m = \min\left(1, \frac{\check{n}_m N}{T/M}\right) = \min\left(1, \frac{\check{n}M}{\check{T}}\right) = \frac{M}{\check{T}}\min\left(\frac{\check{T}}{M}, \check{n}_m\right)$, where $\frac{\check{T}}{M}$ is the normalized (by N) frame length. Similarly, we have $p_{s,m} = \frac{\check{n}_m N}{T/M}\left[\left(1-\frac{1}{K}\right)^K\right]^{\frac{\check{n}_m N}{T/M} - \frac{1}{K}}$. As $N \to \infty$, we have $K \to \infty$ and, then, $p_{s,m} \to \frac{M}{\check{T}}\check{n}_m e^{-\frac{M}{\check{T}}\check{n}_m}$. Consequently, we rewrite $\xi(\mathbf{W}^\star, \hat{\mathbf{r}}, \check{\mathbf{n}})$ as (15). □

Since no closed form of $\mathbb{E}_{\check{\mathbf{n}}}\{\xi(\mathbf{W}^\star, \hat{\mathbf{r}}, \check{\mathbf{n}})\}$ has been found, we derive an approximation:

Proposition 4. *An approximation of* $\mathbb{E}_{\check{\mathbf{n}}}\{\xi(\mathbf{W}^\star, \hat{\mathbf{r}}, \check{\mathbf{n}})\}$ *can be expressed as*

$$\tilde{\xi}(\mathbf{W}^\star, \hat{\mathbf{r}}) = \frac{1}{4\check{T}} \sum_{m=1}^{M} \min\left(\frac{\check{T}}{M}, 2\Delta F_m^{(+)}(0)\right) \times \frac{M}{\check{T}} 2\Delta F_m^{(+)}(0) e^{-\frac{M}{\check{T}} 2\Delta F_m^{(+)}(0)} \left[(1-2p_c)\frac{f_X'(\hat{r}_m)}{f_X(\hat{r}_m)}\right]^2. \tag{16}$$

Proof. We briefly outline the proof. By using the Demoivre-Laplace theorem [61], the joint PDF of the random variables $\{\check{n}_m\}$ can be approximated as

$$f(\check{n}_1, \ldots, \check{n}_M) \approx \prod_{m=1}^{M} \frac{1}{\sqrt{2\pi}\check{\sigma}_m} e^{-\frac{(\check{n}_m - \check{\mu}_m)^2}{2\check{\sigma}_m^2}}, \tag{17}$$

where $\check{\sigma}_m^2 = 2\Delta F_m^{(+)}(0)\left(1 - 2\Delta F_m^{(+)}(0)\right)$ and $\check{\mu}_m = 2\Delta F_m^{(+)}(0)$. We then use Gauss-Hermite quadrature integration along with (17) and apply the same steps shown in [44, Appendix A]. □

Notice that: the term $2\Delta F_m^{(+)}(0)$ represents the normalized (by N) number of active nodes in a frame; the term $\frac{M}{\check{T}} 2\Delta F_m^{(+)}(0) e^{-\frac{M}{\check{T}} 2\Delta F_m^{(+)}(0)}$ represents the successful transmission probability when using slotted ALOHA; and the term $\left[(1-2p_c)\frac{f_X'(\hat{r}_m)}{f_X(\hat{r}_m)}\right]^2$ is obtained from $\left[\frac{d}{d\theta}(2p_{e,m}-1)\big|_{\theta=0}\right]^2$.

2.4.2 Optimal and Suboptimal Reliability Thresholds

Similar to Section 2.3, to find the *asymptotically optimal thresholds* $\{\hat{r}_m^\star\}$ maximizing $\tilde{\xi}(\mathbf{W}^\star, \hat{\mathbf{r}})$, we formulate a constrained optimization problem, where the constraints are obtained from the following lemma indicating the feasible region of $\{\hat{r}_m^\star\}$.

Lemma 3. *The thresholds* $\{\hat{r}_m^\star\}$ *maximizing* $\tilde{\xi}(\mathbf{W}^\star, \hat{\mathbf{r}})$ *must satisfy, for all* m*,*

$$\int_{\hat{r}_m^\star}^{\hat{r}_{m-1}^\star} f_X(x)\, dx = F_X(\hat{r}_{m-1}^\star) - F_X(\hat{r}_m^\star) \leq \frac{1}{2}\frac{\check{T}}{M}, \tag{18}$$

where $F_X(x)$ *is the cumulative distribution function (CDF).*

Proof. The proof is similar to that of Lemma 1. □

From Lemma 3, we have $\sum_{m=1}^{M}\left[F_X(\hat{r}_{m-1}^{\star})-F_X(\hat{r}_m^{\star})\right]=1-F_X(\hat{r}_M^{\star})\leq\frac{1}{2}\check{T}$, where $F_X(\hat{r}_0^{\star})=1$. Therefore, the corollary below is obtained.

Corollary 2. *If the thresholds* $\{\hat{r}_m^{\star}\}$ *maximizing* $\tilde{\xi}(\mathbf{W}^{\star},\hat{\mathbf{r}})$*, are used, we have* $\hat{r}_M^{\star}\geq F_X^{-1}\left(1-\frac{1}{2}\check{T}\right)$*, where* $F_X^{-1}(\cdot)$ *denotes the inverse CDF.* □

Therefore, from (16), Lemma 3, and Corollary 2, asymptotically optimal thresholds $\{\hat{r}_m^{\star}\}$ can be obtained by solving the following constrained optimization problem:

$$\begin{aligned}\max_{\{\hat{r}_1,\ldots,\hat{r}_M\}}\ &\sum_{m=1}^{M}e^{-\frac{2M}{T}\Delta F_m^{(+)}(0)}\left[\Delta F_m^{(+)}(0)\frac{f_X'(\hat{r}_m)}{f_X(\hat{r}_m)}\right]^2 \\ \text{s. t.}\quad &F_X(\hat{r}_{m-1})-F_X(\hat{r}_m)\leq\frac{1}{2}\frac{\check{T}}{M}, \\ &F_X^{-1}\Big(1-\frac{1}{2}\check{T}\Big)\leq\hat{r}_M\leq\hat{r}_{M-1}\leq\ldots\leq\hat{r}_1<\infty.\end{aligned}\tag{19}$$

The objective function is obtained from the fact that, under these constraints, we have $\min\left(\frac{\check{T}}{M},\,2\Delta F_m^{(+)}(0)\right)=2\Delta F_m^{(+)}(0)$, and, then, $\tilde{\xi}(\mathbf{W}^{\star},\hat{\mathbf{r}})=(1-2p_c)^2\frac{M}{T^2}\sum_{m=1}^{M}e^{-\frac{2M}{T}\Delta F_m^{(+)}(0)}\left[\Delta F_m^{(+)}(0)\frac{f_X'(\hat{r}_m)}{f_X(\hat{r}_m)}\right]^2$. Since $(1-2p_c)^2\frac{M}{T^2}$ does not depend on $\{\hat{r}_m\}$, we omit it in the expression of the objective function. Note that, according to Corollary 2, the value of the efficacy is characterized by the tails of the noise distribution $f_X(x)$.

We might apply Greedy algorithms similar to [78, Section III.A] and [45, Algorithm 2] to find the asymptotically optimal thresholds $\{\hat{r}_m^{\star}\}$. However, these algorithms might return a set of locally optimal thresholds. In addition, we consider a set of possibly suboptimal thresholds $\{\hat{r}_m^{\diamond}\}$ called the *asymptotic maximum-throughput thresholds*.

Definition 2. *Under the low observation SNR regime, the* asymptotic maximum-throughput thresholds $\{\hat{r}_m^{\diamond}\}$ *are the thresholds satisfying, for* $m=1,\ldots,M$*,*

$$F_X(\hat{r}_{m-1}^{\diamond})-F_X(\hat{r}_m^{\diamond})=\frac{1}{2}\frac{\check{T}}{M},\tag{20}$$

and, $0\leq\hat{r}_M^{\diamond}\leq\hat{r}_{M-1}^{\diamond}\leq\ldots\leq\hat{r}_1^{\diamond}<\hat{r}_0^{\diamond}=\infty$. □

When the thresholds $\{\hat{r}_m^\diamond\}$ are used, the areas of the CDF between the two consecutive thresholds are equal to half of the normalized frame length. On the other hand, the expected normalized number of active nodes is equal to the normalized frame length. From (19), for the low SNR observation, necessary conditions for the thresholds $\{\hat{r}_m^\diamond\}$ to be optimal can be shown below.

Proposition 5. *For the low SNR observation, if the asymptotic maximum-throughput thresholds* $\hat{\mathbf{r}}^\diamond = \{\hat{r}_m^\diamond\}$ *are optimal,* $\nu_m(\hat{\mathbf{r}}^\diamond) \geq 0$*, for all* m*, where*

$$\nu_m(\hat{\mathbf{r}}^\diamond) = -\sum_{i=m}^{M} \frac{\nabla_i^{(0)}(\hat{\mathbf{r}}^\diamond)}{f_X(\hat{r}_i^\diamond)}, \tag{21}$$

$$\nabla_i^{(0)}(\hat{\mathbf{r}}^\diamond) = \tfrac{1}{2}\tfrac{\check{T}}{M} e^{-1} \left(\tfrac{\check{T}}{M} \tfrac{f_X'(\hat{r}_i^\diamond)}{f_X(\hat{r}_i^\diamond)} V_{1,i} - f_X(\hat{r}_i^\diamond) V_{2,i} \right),$$

$$V_{1,i} = \tfrac{f_X''(\hat{r}_i^\diamond)}{f_X(\hat{r}_i^\diamond)} - \left[\tfrac{f_X'(\hat{r}_i^\diamond)}{f_X(\hat{r}_i^\diamond)} \right]^2,$$

$$V_{2,i} = \left[\tfrac{f_X'(\hat{r}_i^\diamond)}{f_X(\hat{r}_i^\diamond)} \right]^2 - \left[\tfrac{f_X'(\hat{r}_{i+1}^\diamond)}{f_X(\hat{r}_{i+1}^\diamond)} \right]^2, \quad \tfrac{f_X'(\hat{r}_{M+1}^\diamond)}{f_X(\hat{r}_{M+1}^\diamond)} = 0.$$

Proof. The proof is similar to that of Proposition 2. The Lagrange multipliers are $\{\nu_m(\hat{\mathbf{r}}^\diamond)\}$, where $\nabla_m^{(0)}(\hat{\mathbf{r}}^\diamond) = \frac{\partial}{\partial \hat{r}_m} \sum_{m=1}^{M} e^{-\frac{2M}{\check{T}} \Delta F_m^{(+)}(0)} \left[\Delta F_m^{(+)}(0) \frac{f_X'(\hat{r}_m^\diamond)}{f_X(\hat{r}_m^\diamond)} \right]^2 \Big|_{\hat{r}_m = \hat{r}_m^\diamond}$. The above conditions are from the KKT conditions. Similarly, since the derivation of Proposition 5 is straight forward but tedious, we omit the details. □

As shown in Section 2.6.4, for Gaussian noise, the thresholds $\{\hat{r}_m^\diamond\}$ are optimal for a small $\check{T}$ and the conditions in Proposition 5 are sufficient. A sufficient condition for the optimality of the asymptotic maximum-throughput thresholds $\{\hat{r}_m^\diamond\}$ can be stated as below.

Proposition 6. *If* $\frac{f_X'(x)}{f_X(x)}$ *is a constant for* $x \geq F_X^{-1}\big(1 - \frac{1}{2}\check{T}\big)$*, the asymptotic maximum-throughput thresholds* $\{\hat{r}_m^\diamond\}$ *are optimal.*

Proof. When $\frac{f_X'(x)}{f_X(x)}$ is a constant, the efficacy (16) is a function of $\min\big(\frac{\check{T}}{M}, 2\Delta F_m^{(+)}(0)\big)$ and $\frac{M}{\check{T}} 2\Delta F_m^{(+)}(0) e^{-\frac{M}{\check{T}} 2\Delta F_m^{(+)}(0)}$, which are maximized at the thresholds $\{\hat{r}_m^\diamond\}$. Note that this condition is required only for $x \geq F_X^{-1}\big(1 - \frac{1}{2}\check{T}\big)$, i.e., a tail of the noise distribution. □

Corollary 3. *For $\frac{T}{N} \to 0$, the maximum-throughput thresholds $\{\hat{r}_m^\diamond\}$ are optimal.*

Proof. It is a direct result from Proposition 6. For $\frac{T}{N} \to 0$, we have $x \to \infty$. The term $\frac{f_X'(x)}{f_X(x)}$ is a constant or approaches $-\infty$ as $x \to \infty$. □

2.4.3 Properties of the Efficacy

In distributed detection using the censoring-sensor or ordered-transmission strategy, there is an interesting question: Can the proposed scheme achieve any desired performance measure by increasing N for a fixed T, and under what conditions? For comparison, in a typical distributed detection scheme, N is also the number of local decisions received at the FC. Therefore, there is no problem achieving a desired performance measure as $N \to \infty$. On the other hand, what we are considering here is a case in which the number of local decisions received at the FC is fixed (according to a fixed T). We can study this behavior in the proposed scheme by letting $\check{T}$ get smaller:

Proposition 7.

1) Assume that the maximum-throughput thresholds $\{\hat{r}_m^\diamond\}$ are used. The efficacy is a nonincreasing function of $\check{T}$.

2) Assume that the optimal thresholds $\{\hat{r}_m^\star\}$ or the maximum-throughput thresholds $\{\hat{r}_m^\diamond\}$ are used. If we have $\frac{f_X'(x)}{f_X(x)} \to -\infty$ as $x \to \infty$, the proposed scheme can achieve any efficacy value as $N \to \infty$.

Proof. By substituting the maximum-throughput thresholds $\{\hat{r}_m^\diamond\}$ into (16), we have a nice form:

$$\tilde{\xi}(\mathbf{W}^\star, \hat{\mathbf{r}}^\diamond) = \frac{(1-2p_c)^2 e^{-1}}{4M} \sum_{m=1}^{M} \left[\frac{f_X'(\hat{r}_m^\diamond)}{f_X(\hat{r}_m^\diamond)}\right]^2. \tag{22}$$

The thresholds $\hat{r}_m^\diamond$ depend on $\check{T}$ as shown in Definition 2. Consider $\check{T}_1$ and $\check{T}_2$, where $\check{T}_1 \le \check{T}_2$. Let $\{\hat{r}_{1,m}^\diamond\}$ and $\{\hat{r}_{2,m}^\diamond\}$ be the corresponding maximum-throughput thresholds obtained from $\check{T}_1$ and $\check{T}_2$, respectively. Therefore, we have $\hat{r}_{1,1}^\diamond \ge \hat{r}_{2,1}^\diamond$,

$\hat{r}^{\diamond}_{1,2} \geq \hat{r}^{\diamond}_{2,2}$, ..., and $\hat{r}^{\diamond}_{1,M} \geq \hat{r}^{\diamond}_{2,M}$. Because of the assumption that the PDF $f_X(x)$ has the monotone likelihood ratio: $\frac{f'_X(x)}{f_X(x)} \leq 0$ and $\frac{f'_X(\hat{r}^{\diamond}_{1,m})}{f_X(\hat{r}^{\diamond}_{1,m})} \leq \frac{f'_X(\hat{r}^{\diamond}_{2,m})}{f_X(\hat{r}^{\diamond}_{2,m})}$ for all m, we have $\left[\frac{f'_X(\hat{r}^{\diamond}_{1,m})}{f_X(\hat{r}^{\diamond}_{1,m})}\right]^2 \geq \left[\frac{f'_X(\hat{r}^{\diamond}_{2,m})}{f_X(\hat{r}^{\diamond}_{2,m})}\right]^2$ for all m. Therefore, we have proved the first statement.

When we let $\check{T}$ get smaller, $\hat{r}^{\diamond}_M$ will get larger. Therefore, if the considered PDF has the property $\frac{f'_X(x)}{f_X(x)} \to -\infty$ as $x \to \infty$, we have $\tilde{\xi}(\mathbf{W}^{\star}, \hat{\mathbf{r}}^{\diamond}) \to \infty$. Since $\tilde{\xi}(\mathbf{W}^{\star}, \hat{\mathbf{r}}^{\star}) \geq \tilde{\xi}(\mathbf{W}^{\star}, \hat{\mathbf{r}}^{\diamond})$, the condition is also applicable to the optimal thresholds $\{\hat{r}^{\star}_m\}$. In other words, whether the efficacy of the proposed scheme is bounded can be seen from the value of $\frac{f'_X(x)}{f_X(x)}$ as $x \to \infty$. Therefore, we have proved the second statement. □

Recall that, in the proposed scheme, increasing $\check{T}$ means that the scheme collects additional local decisions with lower reliabilities. As shown in the first statement in the proposition (which considers $\theta \to 0$), increasing $\check{T}$ does not improve the efficacy. Instead, the efficacy is maximized as $\check{T} \to 0$, or $\hat{r}^{\diamond}_M \to \infty$. This conclusion is similar to the problem considered in [15], where the global decision is made based only on the most reliable local observation.

2.5 Asymptotic Performance Analysis - ARE

In addition to the DEP and efficacy, we are also interested in the relative efficiency of the proposed scheme; specifically, the *Pittman asymptotic relative efficiency* (ARE). The relative efficiency has been used extensively for performance comparisons between two schemes. Examples can be found in classic signal detection [63,73] and distributed signal processing [16, 32, 78]. In this section, we derive the ARE of the proposed scheme relative to a TDMA-based scheme. For a shared channel, TDMA is a popular channel access protocol because it completely *avoids* collisions and can thus achieve full channel utilization. However, when $N > T$, without any advance information on the nodes' observation reliabilities, a distributed detection scheme based on TDMA must blindly collect T local decisions out of the N available. The question that immediately arises is: When is the TDMA scheme outperformed by our proposed

modification to slotted ALOHA that orders the transmission of decisions by their reliabilities? The ARE will give this answer by indicating the range of $\frac{T}{N}$ that the proposed scheme asymptotically outperforms the TDMA-based scheme. In addition, the ARE allows us to study the effect of different noise distributions $f_X(x)$, as shown in Section 2.6.5.

2.5.1 Derivation of the ARE

The ARE is defined as

$$ARE(\mathbf{W}, \hat{\mathbf{r}}, \mathbf{n}) = \lim_{N\to\infty} \frac{T_{ts}(\alpha, \beta, \theta)}{T_{ps}(\alpha, \beta, \theta, \mathbf{W}, \hat{\mathbf{r}}, \mathbf{n})}, \tag{23}$$

where $T_{ts}(\alpha, \beta, \theta)$ and $T_{ps}(\alpha, \beta, \theta, \mathbf{W}, \hat{\mathbf{r}}, \mathbf{n})$ are the collection time for the TDMA-based scheme and the proposed scheme, respectively, to achieve the same probabilities of false alarm α and detection β for a given θ. An ARE larger than one indicates that the proposed scheme requires a smaller collection time than the TDMA-based scheme to achieve the same probabilities, and, as a result, the proposed scheme offers better performance. The expressions of $T_{ts}(\alpha, \beta, \theta)$ and $T_{ps}(\alpha, \beta, \theta, \mathbf{W}, \hat{\mathbf{r}}, \mathbf{n})$ are derived in the lemmas below. The proofs of Lemmas 4 and 5 can be executed in a manner similar to that shown in [29].

Lemma 4. *Consider distributed detection using TDMA with N identical nodes in the network. The noisy observation is defined in Section 2.2, and the local decision rule is $u = \mathbf{1}_{\{y\geq\theta/2\}} - \mathbf{1}_{\{y<\theta/2\}}$. The local decisions are sent to the FC according to a pre-assigned order to avoid collisions. The FC's test statistic is a sum of the local decisions. The asymptotic distribution given H_i of the test statistic is a Gaussian distribution with mean $\mu_{tdma,i} = Tp_i$ and variance $\sigma^2_{tdma,i} = Tp_i(1-p_i)$, where $p_0 = 1 - p_1 = \bar{p}_e$ and $\bar{p}_e = p_c F_X(\frac{\theta}{2}) + (1-p_c)\big[1 - F_X(\frac{\theta}{2})\big]$. Asymptotically, the collection time to achieve a probability of false alarm α and a probability of detection β is*

$$T_{ts}(\alpha, \beta, \theta) = \frac{\bar{p}_e(1-\bar{p}_e)}{(1-2\bar{p}_e)^2}[\Phi^{-1}(1-\alpha) - \Phi^{-1}(1-\beta)]^2, \tag{24}$$

where $\Phi(\cdot)$ is the Gaussian CDF. □

Lemma 5. *With the optimal weights $\mathbf{W}^* = \{W_m^*\}$ (shown in Section 2.3) and thresholds $\hat{\mathbf{r}} = \{\hat{r}_m\}$, asymptotically, the collection time that the proposed scheme needs to achieve a probability of false alarm α and a probability of detection β is expressed as*

$$T_{ps}(\alpha, \beta, \theta, \mathbf{W}^*, \hat{\mathbf{r}}, \mathbf{n}) = \frac{M}{4}\left[\Phi^{-1}(1-\alpha) - \Phi^{-1}(1-\beta)\right]^2 \times \left[\sum_{m=1}^{M} \breve{K}_m \frac{p_{s,m}(1-2p_{e,m})}{[1-p_{s,m}(1-2p_{e,m})^2]}\right]^{-1}, \quad (25)$$

where $\breve{K}_m = \min\left(1, \frac{n_m}{K}\right)$. Note that $T_{ps}(\alpha, \beta, \theta, \mathbf{W}^*, \hat{\mathbf{r}}, \mathbf{n})$ is a function of random variables $\{n_m\}$. □

From (24) and (25), $ARE(\mathbf{W}^*, \hat{\mathbf{r}}, \mathbf{n})$ can be shown below.

Proposition 8. *With the optimal weights $\{W_m^*\}$, the ARE of the proposed scheme relative to the distributed detection using TDMA is expressed as*

$$ARE(\mathbf{W}^*, \hat{\mathbf{r}}, \breve{\mathbf{n}}) = \frac{M}{4\breve{T}^2}\left[\frac{1}{f_X(0)}\right]^2 \sum_{m=1}^{M} \min\left(\frac{\breve{T}}{M}, \breve{n}_m\right) \breve{n}_m e^{-\frac{M}{\breve{T}}\breve{n}_m} \left[\frac{f_X'(\hat{r}_m)}{f_X(\hat{r}_m)}\right]^2, \quad (26)$$

where $\breve{T} = \frac{T}{N}$ and $\breve{n}_m = \frac{n_m}{N}$.

Proof. Please see Appendix G. □

There is no p_c in (26), since the channel error affects both schemes equally. Furthermore, unlike conventional ARE values [27,29], which are constants, $ARE(\mathbf{W}^*, \hat{\mathbf{r}}, \breve{\mathbf{n}})$ is a function of the normalized collection time $\breve{T}$ of the proposed scheme. The effect of $\breve{T}$ on the ARE will be discussed at the end of this section and shown in Section 2.6.5. Since there is no closed form of $\mathbb{E}_{\breve{\mathbf{n}}}\{ARE(\mathbf{W}^*, \hat{\mathbf{r}}, \breve{\mathbf{n}})\}$ has been found, we derive an approximation, which is shown below.

Proposition 9. *An approximation of $\mathbb{E}_{\breve{\mathbf{n}}}\{ARE(\mathbf{W}^*, \hat{\mathbf{r}}, \breve{\mathbf{n}})\}$ can be expressed as*

$$\tilde{ARE}(\mathbf{W}^*, \hat{\mathbf{r}}) = \frac{M}{2\breve{T}^2}\left[\frac{1}{f_X(0)}\right]^2 \sum_{m=1}^{M} \min\left(\frac{\breve{T}}{M}, 2\Delta F_m^{(+)}(0)\right) \times e^{-\frac{2M}{\breve{T}}\Delta F_m^{(+)}(0)} \Delta F_m^{(+)}(0) \left[\frac{f_X'(\hat{r}_m)}{f_X(\hat{r}_m)}\right]^2. \quad (27)$$

Proof. The proof is similar to that of Proposition 4. □

We see that $A\tilde{R}E(\mathbf{W}^*, \hat{\mathbf{r}})$ is a function of $\tilde{\xi}(\mathbf{W}^*, \hat{\mathbf{r}})$ shown in (16). The optimal thresholds of $A\tilde{R}E(\mathbf{W}^*, \hat{\mathbf{r}})$ are the thresholds $\{\hat{r}_m^\star\}$ discussed in Section 2.4.2. The necessary and sufficient conditions provided in Propositions 5 and 6 for the thresholds $\{\hat{r}_m^\diamond\}$ optimizing $A\tilde{R}E(\mathbf{W}^*, \hat{\mathbf{r}})$ hold.

Similar to the efficacy, $A\tilde{R}E(\mathbf{W}^*, \hat{\mathbf{r}})$ with the thresholds $\hat{\mathbf{r}}^\diamond = \{\hat{r}_m^\diamond\}$ has a nice form:

$$A\tilde{R}E(\mathbf{W}^*, \hat{\mathbf{r}}^\diamond) = \frac{e^{-1}}{4}\left[\frac{1}{f_X(0)}\right]^2 \frac{1}{M}\sum_{m=1}^{M}\left\{\frac{f_X'(\hat{r}_m^\diamond)}{f_X(\hat{r}_m^\diamond)}\right\}^2. \tag{28}$$

As $M \to \infty$, we have

$$A\tilde{R}E^\infty(\mathbf{W}^*, \hat{\mathbf{r}}^\diamond) = \frac{e^{-1}}{4}\left[\frac{1}{f_X(0)}\right]^2 \mathbb{E}_X\left\{\left[\frac{f_X'(x)}{f_X(x)}\right]^2 \middle| x \geq \hat{r}_M^\diamond\right\},$$

which is an upper bound of $A\tilde{R}E(\mathbf{W}^*, \hat{\mathbf{r}}^\diamond)$. We see that $A\tilde{R}E(\mathbf{W}^*, \hat{\mathbf{r}}^\diamond)$ consists of three terms. The term e^{-1} is the optimal throughput per time slot (of slotted ALOHA) obtained from use of the thresholds $\{\hat{r}_m^\diamond\}$. The term $\left[\frac{1}{f_X(0)}\right]^2$ is obtained from the TDMA-based scheme. Finally, the term $\frac{1}{M}\sum_{m=1}^{M}\left\{\frac{f_X'(\hat{r}_m^\diamond)}{f_X(\hat{r}_m^\diamond)}\right\}^2$ is obtained from the proposed scheme. Since the ARE is a function of the efficacy, Proposition 7 is applicable to the ARE, too. Specifically, $A\tilde{R}E(\mathbf{W}^*, \hat{\mathbf{r}}^\diamond)$ is a nonincreasing function of $\check{T}$ (equivalently, a nondecreasing function of $\hat{r}_M^\diamond$), and unbounded as $\check{T} \to \infty$ if $\frac{f_X'(x)}{f_X(x)} \to -\infty$ as $x \to \infty$. These will be shown in Section 2.6.5.

2.5.2 Preferred Collection Time

Our main objective in deriving the ARE is to find the largest normalized collection time $\check{T} = \frac{T}{N}$ for which the proposed scheme outperforms the TDMA-based scheme. The proposition below provides such a $\check{T}$.

Proposition 10. *Assume that the optimal threshold $\{\hat{r}_m^\star\}$ or the maximum-throughput*

thresholds $\{\hat{r}_m^{\diamond}\}$ *are used. The proposed scheme asymptotically outperforms the TDMA-based scheme for any* $\check{T}$ *satisfying the following condition:*

$$-\left.\frac{f_X'(x)}{f_X(x)}\right|_{x=F_X^{-1}(1-0.5\check{T})} > 2e^{\frac{1}{2}} f_X(0). \tag{29}$$

Proof. Condition (29) is directly obtained from (28) with $M = 1$, and $\hat{r}_1^{\diamond} = F_X^{-1}(1 - 0.5\check{T})$. Recall that $\frac{f_X'(x)}{f_X(x)}$ is a negative value. During the derivation, when we take a square root, the minus sign has to be added in front of $\frac{f_X'(x)}{f_X(x)}$. Since we derive Condition (29) based on $M = 1$, the proposed scheme with any M will asymptotically outperform the TDMA-based scheme for any $\check{T}$ satisfying Condition (29). □

We see that $\check{T}$ satisfying Condition (29) depends on the noise distribution $f_X(x)$. The effect of the noise distribution will be studied in Section 2.6.5.

2.6 Numerical Results and Discussions

2.6.1 Validation of the DEP Approximation; Comparisons

We investigate the validity of the DEP approximation expressed in (8) and compare the DEPs of the proposed scheme with a TDMA-based scheme in Fig. 7. The observation noise x is a Gaussian random variable with zero mean and unit variance. The maximum-throughput thresholds $\{\hat{r}_m^{\circ}\}$ are used. The number of frames M is equal to 5. The other parameter values are shown in the figure's caption. In this figure, we show the DEPs versus the collection time T, where those DEPs are from Monte Carlo simulations of the TDMA-based scheme (TS-SIM), Monte Carlo simulations of the proposed scheme (PS-SIM), and the analytical expressions (8) of the proposed scheme (PS-ANA). The number of Monte Carlo trials is 10^6 for SNR $= -3$ and 0 dB, and 10^7 for SNR $= 3$ dB. The simulation results PS-SIM are also obtained from the worst-case assumption, where the error probabilities of local decisions are equal to (3), and the FC makes a global decision from (4) with the optimal weights $\{W_m^*\}$ defined in (7).

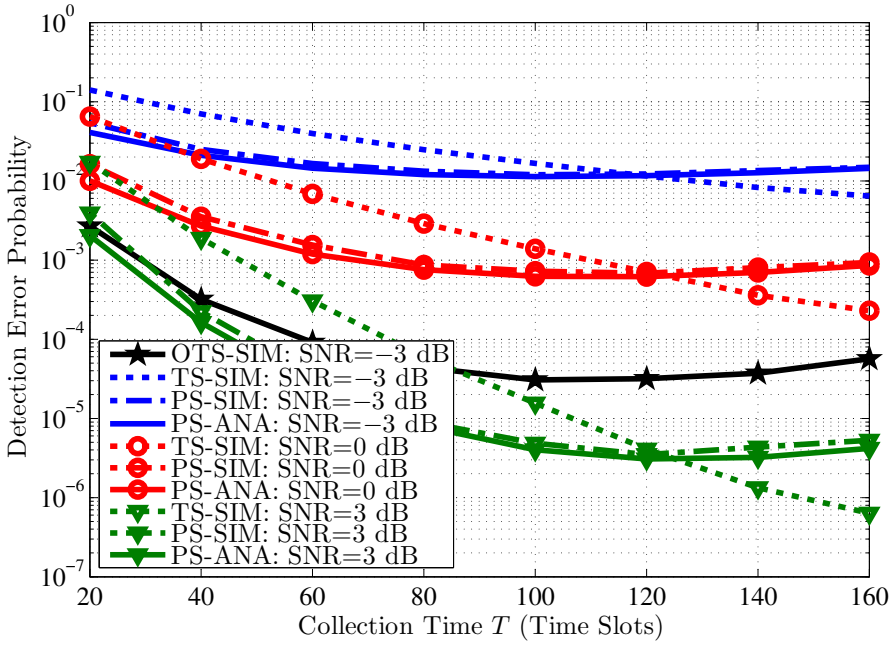

Figure 7: We compare the DEPs of the proposed scheme (PS-SIM) with the TDMA-based scheme (TS-SIM), where both are obtained from simulations. We also validate the approximation of the proposed scheme's DEP expressed in (8) by comparing the DEPs from (8) (PS-ANA) with the proposed scheme's DEP obtained from simulations (PS-SIM). The DEP of the oracle TDMA-based scheme (OTS-SIM) for SNR= -3 dB is show as a benchmark. The observation noise is Gaussian with zero mean and unit variance. The other parameters are set as follows for both the simulations and analytical results: $N = 200$, $p_c = 0.05$, $\{W_m^*\}$, $\{\hat{r}_m^\circ\}$, and $M = 5$. The DEPs are shown for SNR $= -3$, 0, 3 dB.

In addition, we show the DEP of an *oracle* TDMA-based scheme (OTS-SIM) for SNR= -3 dB in Fig. 7. Note that OTS-SIM is obtained from Monte Carlo simulations with 10^6 trials. In the oracle TDMA-based scheme, the FC knows the reliabilities of the nodes' observations, and perfectly schedules the local-decision transmissions in descending order of the reliabilities with the collision-free TDMA. Indeed, the oracle TDMA-based scheme is not practical in our scenario (or, generally, in any scenarios with large N). However, we use it here as a benchmark where the DEP of a supreme scheme is. Note that the DEPs of the oracle TDMA-based scheme for SNR= 0 dB and SNR= 3 dB are omitted since their values are out of the considered range.

As shown in Fig. 7, PS-SIM and PS-ANA from the approximation (8) match quite

well under the given ranges of the parameter values. Therefore, the DEP approximation (8), $\tilde{P}_E(\mathbf{W}^*, \hat{\mathbf{r}})$, will be used to investigate the optimal thresholds in the next subsection.

Comparisons between the DEPs from TS-SIM and PS-SIM demonstrate a significant DEP improvement by use of the proposed scheme over the TDMA-based scheme when T is small. For the TDMA-based scheme, since the reliabilities of the nodes' observations are not known in advance, the FC must collect T local decisions *blindly* from the N deployed nodes ($T < N$). Consequently, the FC makes a global decision from a composite of *diverse* local decision reliabilities using the *unweighted* version of the sum of local decisions in (4). In contrast, the proposed scheme's FC is able to collect the local decisions in approximately descending order of their reliabilities and makes a global decision from a weighted sum of the received local decisions. Statistically, since the maximum-throughput thresholds $\{\hat{r}_m^\circ\}$ are used here, the proposed scheme's FC receives e^{-1} of the T most reliable local decisions. However, the advantage of *ordered* collection of local decisions decreases when T is large, because most of the collected local decisions at the end are unreliable and some reliable decisions have been lost in collisions in earlier frames.

As shown in Fig. 7, we have the following interesting results. First, in the proposed scheme, there exists an optimal collection time $T^*(\theta)$ such that spending more time collecting local decisions does not improve the DEP any further. This is also true when the optimal thresholds $\{\hat{r}_m^*\}$ are used, as shown in the next section. Similar results are also shown in [65, 81]. In Fig. 7, we notice that $T^*(\theta)$ gets smaller as θ decreases. Second, let $\mathcal{T}(\theta)$ be the collection time such that the DEPs of the proposed scheme and the TDMA-based scheme are equal. We see that the proposed scheme outperforms the TDMA-based scheme for all $T < \mathcal{T}(\theta)$. From Fig. 7, $\mathcal{T}(\theta)$ is a non decreasing function of the observation SNR. The results here are consistent with the ARE shown in Section 2.6.5. Asymptotically, as $\theta \to 0$, from the ARE results in

Table 3: For $M = 5$ and SNR= 5 dB: optimal thresholds, maximum throughput thresholds, and the necessary conditions (13). The other parameters are $N = 100$, $p_c = 0.05$, and $\{W_m^*\}$.

	Optimal Thresholds					
T	$\hat{r}_1^*$	$\hat{r}_2^*$	$\hat{r}_3^*$	$\hat{r}_4^*$	$\hat{r}_5^*$	$\tilde{P}_E(\mathbf{W}^*, \hat{\mathbf{r}}^*)$
20	2.64	2.30	2.07	1.90	1.75	1.42×10^{-3}
40	2.30	1.90	1.62	1.39	1.19	1.23×10^{-4}
60	2.07	1.62	1.29	1.01	0.76	4.14×10^{-5}
80	1.93	1.44	1.08	0.78	0.49	3.97×10^{-5}

	Maximum Throughput Thresholds						Conditions (13)
T	$\hat{r}_1^\circ$	$\hat{r}_2^\circ$	$\hat{r}_3^\circ$	$\hat{r}_4^\circ$	$\hat{r}_5^\circ$	$\tilde{P}_E(\mathbf{W}^*, \hat{\mathbf{r}}^\circ)$	$\min\{\lambda_m(\hat{\mathbf{r}}^\circ)\}$
20	2.64	2.30	2.07	1.90	1.75	1.42×10^{-3}	26.6
40	2.30	1.90	1.62	1.39	1.19	1.23×10^{-4}	15.9
60	2.07	1.62	1.29	1.01	0.76	4.14×10^{-5}	3.8
80	1.89	1.39	1.01	0.68	0.37	4.35×10^{-5}	-4.6

Section 2.6.5, we have $0.19N \leq \mathcal{T}(0) \leq 0.55N$, depending on M.

2.6.2 Optimal Thresholds

We show the optimal thresholds $\{\hat{r}_m^*\}$ and the DEP $\tilde{P}_E(\mathbf{W}^*, \hat{\mathbf{r}}^*)$ in Table 3 for $M = 5$ and SNR= 5 dB. The optimal thresholds are obtained from the constrained optimization problem (11), where we search all feasible sets of thresholds $\{\hat{r}_m\}$ for the set of optimal thresholds. Note that we use $\hat{r}_0 = 5$ instead of ∞ and discretize the reliability value r into discrete values with a resolution of 0.01. For a comparison, we also show the maximum-throughput thresholds $\{\hat{r}_m^\circ\}$, the DEP $\tilde{P}_E(\mathbf{W}^*, \hat{\mathbf{r}}^\circ)$, and the values of $\min\{\lambda_m(\hat{\mathbf{r}}^\circ)\}$ of the necessary conditions in Proposition 2 in those tables. The rows with $\min\{\lambda_m(\hat{\mathbf{r}}^\circ)\} < 0$ are highlighted. The observation noise x is assumed to be Gaussian with zero mean and unit variance. The other parameters used are: $N = 100$, $p_c = 0.05$.

From Table 3, for a small T, we see that not only the thresholds $\{\hat{r}_m^\circ\}$ satisfy the conditions (13), where $\lambda_m(\hat{\mathbf{r}}^\circ) \geq 0$ for all m, but they are also optimal. These results indicate that the conditions (13) are *sufficient* for *Gaussian* noise. Therefore, by using the conditions (13), we can also find the optimal thresholds for Gaussian noise in other scenarios. Even though the thresholds $\{\hat{r}_m^\circ\}$ are not optimal for a

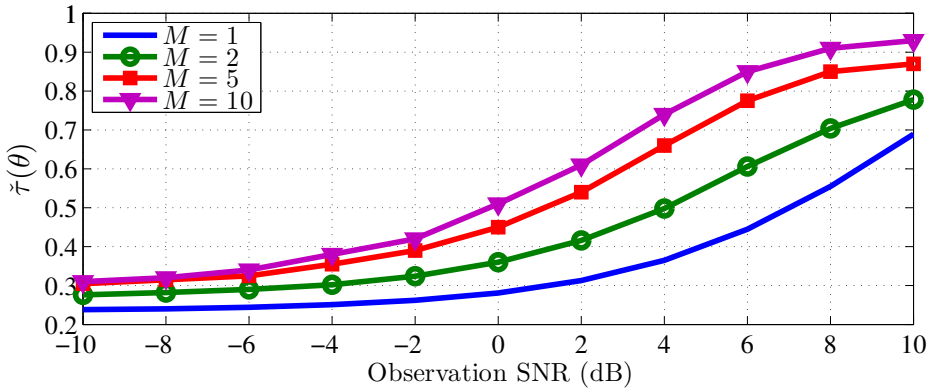

Figure 8: $\check{\tau}(\theta)$ versus SNR for various M when the observation noise is Gaussian, $N = 1000$, and $p_c = 0.05$. The thresholds $\{\hat{r}_m^\circ\}$ are optimal when $\check{T} \leq \check{\tau}(\theta)$.

large T, the DEP $\tilde{P}_E(\mathbf{W}^*, \hat{\mathbf{r}}^\circ)$ they yield is only slightly higher than the minimum DEP $\tilde{P}_E(\mathbf{W}^*, \hat{\mathbf{r}}^*)$. For a large T, we notice that the optimal thresholds $\{\hat{r}_m^*\}$ favor an expected number of active nodes in some frames that is less than K.

Furthermore, the maximum-throughput thresholds are optimal in a larger range of T as SNR or M increases. This is studied as follows. Let $\tau(\theta) = \max\{T : \lambda_m(\hat{\mathbf{r}}^\circ) \geq 0, \forall m\}$, $\check{\tau}(\theta) = \frac{\tau(\theta)}{N}$, and $\check{T} = \frac{T}{N}$. The variable $\tau(\theta)$ is the maximum T for which the conditions (13) are still true and $\check{\tau}(\theta)$ is its normalized version. In other words, for Gaussian noise, the thresholds $\{\hat{r}_m^\circ\}$ are optimal when $\check{T} \leq \check{\tau}(\theta)$. By using the conditions (13), we show the relationship among $\check{\tau}(\theta)$, M, and SNR in Fig. 8 for Gaussian noise and $N = 1000$. It is clear that $\check{\tau}(\theta)$ is a nondecreasing function of M and SNR. On the other hand, at SNR $= -10$ dB, we obtain $\check{\tau}(\theta) = 0.238$, 0.276, 0.305, and 0.310 for $M = 1$, 2, 5, and 10, respectively. Therefore, for Gaussian noise and $N = 1000$, we can say that the maximum-throughput thresholds $\{\hat{r}_m^\circ\}$ are optimal for all $\check{T} \leq 0.238$ when SNR ≥ -10 dB regardless of M.

2.6.3 Effects of M and N

In the proposed scheme, the parameters M and N are choices that a system designer must specify before deploying the network. The effects of these parameters on $\tilde{P}_E(\mathbf{W}^*, \hat{\mathbf{r}}^\circ)$ are shown in Fig. 9. The thresholds $\{\hat{r}_m^\circ\}$ are optimal for these scenarios.

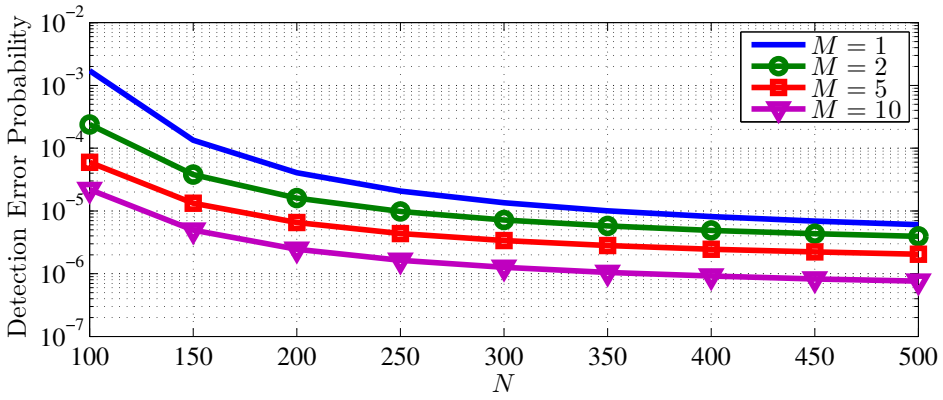

Figure 9: We show the effects of M and N on the DEP of the proposed scheme $\tilde{P}_E(\mathbf{W}^*, \hat{\mathbf{r}}^\circ)$. The maximum-throughput thresholds $\{\hat{r}_m^\circ\}$, which are optimal in this case, are used. The other parameters are Gaussian noise, $T = 50$, SNR $= 5$ dB, and $p_c = 0.05$.

Table 4: For $M = 5$: asymptotically optimal thresholds, asymptotic maximum-throughput thresholds, and the necessary conditions (21).

$\check{T}$	Asymptotically Optimal Thresholds					
	$\hat{r}_1^\star$	$\hat{r}_2^\star$	$\hat{r}_3^\star$	$\hat{r}_4^\star$	$\hat{r}_5^\star$	$\xi(\mathbf{W}^\star, \hat{\mathbf{r}}^\star)$
0.2	2.05	1.75	1.55	1.41	1.28	0.1958
0.4	1.80	1.44	1.20	1.02	0.86	0.1207
0.6	1.80	1.35	1.04	0.81	0.61	0.0808
0.8	1.67	1.23	0.94	0.68	0.44	0.0585

$\check{T}$	Asymptotic Maximum Throughput Thresholds						Conditions (21)
	$\hat{r}_1^\diamond$	$\hat{r}_2^\diamond$	$\hat{r}_3^\diamond$	$\hat{r}_4^\diamond$	$\hat{r}_5^\diamond$	$\xi(\mathbf{W}^\star, \hat{\mathbf{r}}^\circ)$	$\min\{\nu_m(\hat{\mathbf{r}}^\diamond)\}$
0.2	2.05	1.75	1.55	1.41	1.28	0.1958	0.0038
0.4	1.75	1.41	1.17	0.99	0.84	0.1200	−0.0052
0.6	1.55	1.18	0.92	0.71	0.53	0.0802	−0.0160
0.8	1.41	1.00	0.71	0.47	0.26	0.0559	−0.0256

The parameter values are set as follows: $T = 50$, SNR$= 5$ dB, and $p_c = 0.05$. Clearly, increasing M improves $\tilde{P}_E(\mathbf{W}^*, \hat{\mathbf{r}}^\circ)$ by ensuring that the received local decisions are weighted properly by $\{W_m^*\}$. A large DEP improvement is noticeable when increasing $M = 1$ to $M = 2$ for a low N. This makes it clear that using multiple frames ($M > 1$) is beneficial. The proposed scheme exploits an advantage of multi-user diversity: as N increases, more nodes will experience better observation reliabilities, which leads to reliability thresholds that yield an improved DEP.

2.6.4 Asymptotically Optimal Thresholds

We show the asymptotically optimal thresholds $\{\hat{r}_m^\star\}$ and the efficacy $\xi(\mathbf{W}^\star, \hat{\mathbf{r}}^\star)$ in Table 4 for $M = 5$. The optimal thresholds $\{\hat{r}_m^\star\}$ are obtained by searching all feasible sets of reliability thresholds for the set of optimal thresholds, where r is discretized with a resolution of 0.01 and $\hat{r}_0 = 5$. In addition, we show the asymptotic maximum-throughput thresholds $\{\hat{r}_m^\diamond\}$, the efficacy $\xi(\mathbf{W}^\star, \hat{\mathbf{r}}^\diamond)$, and $\min\{\nu_m(\hat{\mathbf{r}}^\diamond)\}$, where $\nu_m(\hat{\mathbf{r}}^\diamond)$ is from (21), for a comparison. The observation noise is Gaussian with zero mean and unit variance. The rows with $\min\{\nu_m(\hat{\mathbf{r}}^\diamond)\} < 0$ are highlighted. The results show that, for Gaussian noise, the thresholds $\{\hat{r}_m^\diamond\}$ are asymptotically optimal for small $\check{T}$, which is consistent with the results in Fig. 8. Similarly, the conditions (21) are sufficient for Gaussian noise. When the thresholds $\{\hat{r}_m^\diamond\}$ are suboptimal, the efficacy $\xi(\mathbf{W}^\star, \hat{\mathbf{r}}^\diamond)$ is slightly lower than the maximum efficacy $\xi(\mathbf{W}^\star, \hat{\mathbf{r}}^\star)$.

2.6.5 Asymptotic Relative Efficiency

As shown in Section 2.6.4, using the thresholds $\{\hat{r}_m^\diamond\}$ gives a slightly lower efficacy than the maximum. Therefore, for convenience, we will use the asymptotic maximum-throughput thresholds $\{\hat{r}_m^\diamond\}$ in studying the ARE. We show the *relative efficiency* of the proposed scheme relative to the TDMA-based scheme in Table 5. The relative efficiency here is a ratio of the collection time required by the TDMA-based scheme to the collection time required by the proposed scheme, when both achieve the same DEP. These collection times, which are from Monte Carlo simulations, are obtained from an average of 10^2 collection times that achieve the specified DEP. The number of trials to compute a DEP is 10^4. Note that long simulation running times prohibit us from showing relative efficiencies at a very low SNRs. The parameters are defined in the table's caption. For a comparison, the ARE obtained from the analytical expression (28) are also shown in the table. We see that the AREs obtained from (28) are slightly lower than the relative efficiencies from the simulations.

Table 5: Relative efficiencies from simulations. The parameters are: the desired DEP $\approx 0.005, 0.01$, $\check{T} = 0.05, 0.1, 0.5$, $M = 5$, and Gaussian noise with zero mean and unit variance. Note that the asymptotic maximum-throughput thresholds are used.

SNR	$\check{T} = 0.05$		$\check{T} = 0.1$		$\check{T} = 0.5$	
	0.005	0.01	0.005	0.01	0.005	0.01
-10 dB	3.022	3.032	2.353	2.328	0.824	0.812
-15 dB	3.016	3.021	2.316	2.284	0.817	0.797
ARE	2.867		2.188		0.761	

Next, we use (28) to study the AREs of two types of noise distributions: General Gaussian and General Logistic distributions. A General Gaussian distribution is classified as a light-tailed distribution with exponential decay, with zero mean and unit variance: $f_{GG}(x) = \frac{\kappa}{2A_G(\kappa)\Gamma(1/\kappa)} e^{-\left[\frac{|x|}{A_G(\kappa)}\right]^{\kappa}}$, where $A_G(\kappa) = \sqrt{\frac{\Gamma(1/\kappa)}{\Gamma(3/\kappa)}}$, $\Gamma(t) = \int_0^{\infty} y^{t-1} e^{-y}\, dy$ is the gamma function, and κ is the decay rate. Note that, since $\frac{f'_{GG}(x)}{f_{GG}(x)} = -\frac{\kappa}{A_G(\kappa)} x^{\kappa-1}$, we have $\frac{f'_{GG}(x)}{f_{GG}(x)} = -\frac{1}{\sqrt{2}}$ for all x when $\kappa = 1$, and $\frac{f'_{GG}(x)}{f_{GG}(x)} \to -\infty$ as $x \to \infty$ when $\kappa \geq 2$.

A General Logistic distribution is a heavy-tailed distribution, with zero mean and unit variance: $f_{GL}(x) = \frac{\kappa e^{-\kappa x}}{(1+e^{-\kappa x})^2}$, where κ is the decay rate. Note that since $\frac{f'_{GL}(x)}{f_{GL}(x)} = -\kappa \frac{(1-e^{-\kappa x})}{(1+e^{-\kappa x})}$, we have $\frac{f'_{GL}(x)}{f_{GL}(x)} \to -\kappa$ as $x \to \infty$. Recall that an ARE larger than one indicates that the proposed scheme outperforms the TDMA-based scheme. We denote the ARE for $M = 1$ by $A\tilde{R}E^{1}(\mathbf{W}^*, \hat{\mathbf{r}}^{\diamond})$ and for $M \to \infty$ by $A\tilde{R}E^{\infty}(\mathbf{W}^*, \hat{\mathbf{r}}^{\diamond})$, which are the lower and upper bounds of $A\tilde{R}E(\mathbf{W}^*, \hat{\mathbf{r}}^{\diamond})$ for any M, respectively.

We show $A\tilde{R}E^{1}(\mathbf{W}^*, \hat{\mathbf{r}}^{\diamond})$ and $A\tilde{R}E^{\infty}(\mathbf{W}^*, \hat{\mathbf{r}}^{\diamond})$ versus the normalized collection time $\check{T} = \frac{T}{N}$ for a General Gaussian distribution in Fig. 10(a). Note that the Y-axis is shown in log-scale. Fig. 10(a) shows that there is no advantage of using the proposed scheme over the TDMA-based scheme when $\kappa = 1$ (Laplacian distribution) because we have $\frac{f'_{GG}(x)}{f_{GG}(x)} = -\frac{1}{\sqrt{2}}$ for all x. Thus, the ordered collection strategy does not work in this case. As a result, $A\tilde{R}E^{1}(\mathbf{W}^*, \hat{\mathbf{r}}^{\diamond})$ and $A\tilde{R}E^{\infty}(\mathbf{W}^*, \hat{\mathbf{r}}^{\diamond})$ are equal to e^{-1} for all $\check{T}$.

On the other hand, increasing the decay rate ($\kappa = 2$, 3) significantly favors the

performance of the proposed scheme. These results are consistent with those shown in Section 2.6.1 that, as $\check{T}$ decreases, the proposed scheme requires a smaller number of local decisions than the TDMA-based scheme does to achieve the same probability of error. Since the ARE is obtained under the assumption of a low SNR, slight improvement is obtained when $M \to \infty$.

We also see that, for $\kappa = 2$ and 3, as $\check{T} \to 0$, both $A\tilde{R}E^{1}(\mathbf{W}^*, \hat{\mathbf{r}}^{\diamond})$ and $A\tilde{R}E^{\infty}(\mathbf{W}^*, \hat{\mathbf{r}}^{\diamond})$ approach infinity, while both $A\tilde{R}E^{1}(\mathbf{W}^*, \hat{\mathbf{r}}^{\diamond})$ and $A\tilde{R}E^{\infty}(\mathbf{W}^*, \hat{\mathbf{r}}^{\diamond})$ decrease to some values less than one as $\check{T} \to 1$. The ARE shown in Fig. 10(a) gives a criterion, asymptotically, whether to use the proposed scheme over the TDMA-based scheme. For example, as shown in Fig. 10(a), for $\kappa = 2$ (Gaussian distribution), a system designer would choose the proposed scheme regardless of M when $\frac{T}{N} < 0.19$ since $A\tilde{R}E^{1}(\mathbf{W}^*, \hat{\mathbf{r}}^{\diamond}) > 1$.

We show $A\tilde{R}E^{1}(\mathbf{W}^*, \hat{\mathbf{r}}^{\diamond})$ and $A\tilde{R}E^{\infty}(\mathbf{W}^*, \hat{\mathbf{r}}^{\diamond})$ versus $\check{T}$ for a General Logistic distribution in Fig. 10(b). Unlike the ARE for a light-tailed distribution, the ARE for a heavy-tailed distribution is bounded as $\check{T} \to 0$. Therefore, there exists a finite number such that increasing N beyond this number only slightly improves the proposed scheme's performance. We notice that, for the General Logistic distributions, the ARE values are identical for the considered values of κ. As shown in Fig. 10(b), a system designer would use the proposed scheme instead of the TDMA-based scheme regardless of M when $\frac{T}{N} < 0.18$ since $A\tilde{R}E^{1}(\mathbf{W}^*, \hat{\mathbf{r}}^{\diamond}) > 1$.

2.7 Conclusion

We proposed a reliability-based splitting algorithm using slotted ALOHA for time-constrained distributed detection. The scheme enables the FC to collect the binary local decisions in descending order of reliability and then optimally weight the successfully received local decisions when fusing them to create the global decision. We derived the DEP, efficacy and ARE (relative to a TDMA-based scheme), and used them

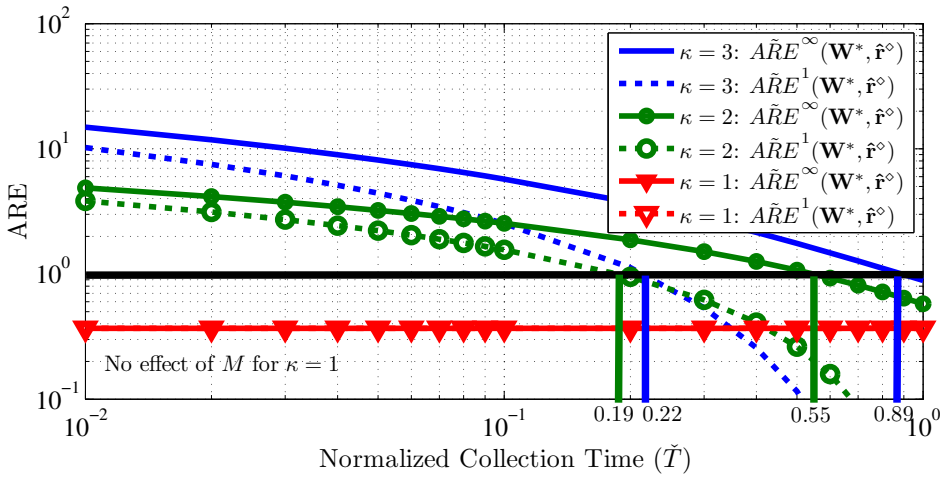

(a) General Gaussian distribution. If, for example, the decay rate κ is 2, the proposed scheme is better than the TDMA-based scheme when $\check{T} < 0.19$ for $M = 1$ and $\check{T} < 0.55$ for $M \to \infty$. Note that the AREs of $M = 1$ and $M \to \infty$ when $\kappa = 1$ are identical.

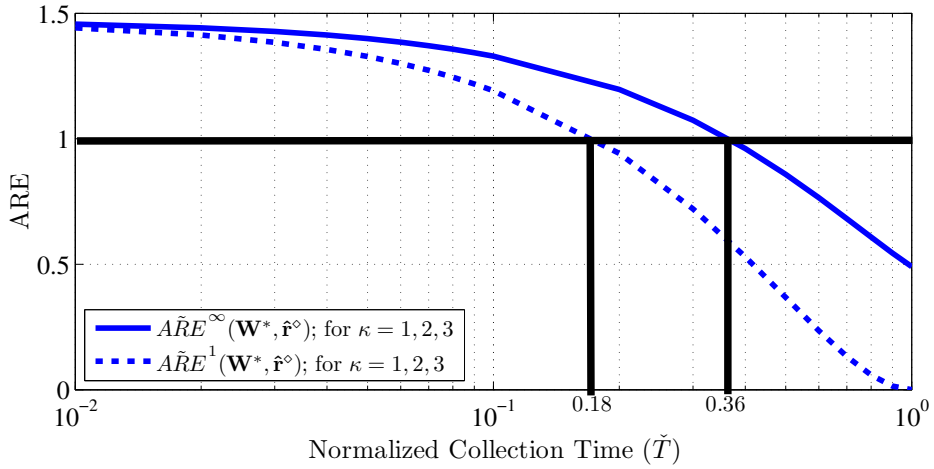

(b) General Logistic distribution. For all considered decay rates, κ (1, 2, and 3), the proposed scheme is better than the TDMA-based scheme when $\check{T} < 0.18$ for $M = 1$ and $\check{T} < 0.36$ for $M \to \infty$. Note that the decay rate κ has *no effect* on the ARE.

Figure 10: We show the ARE $A\tilde{R}E^{1}(\mathbf{W}^*, \hat{\mathbf{r}}^\diamond)$ in (28) and $A\tilde{R}E^{\infty}(\mathbf{W}^*, \hat{\mathbf{r}}^\diamond)$ versus the normalized collection time $\check{T}$ of the proposed scheme for two distributions. An ARE above one indicates that, asymptotically, the proposed scheme outperforms the TDMA-based scheme.

to determine the following variables: 1) the optimal thresholds and the maximum-throughput thresholds; 2) the performance bound as N increases; and, 3) asymptotically preferred collection times. The results are summarized in Section 2.1.2.

CHAPTER III

COLLISION-AWARE DECISION FUSION IN DISTRIBUTED DETECTION USING RELIABILITY-BASED SPLITTING ALGORITHMS

3.1 Introduction

In distributed detection [12, 79], a number of sensor nodes are deployed in an area to monitor the events of interest. The local decisions on these events made by the sensor nodes are collected by the fusion center (FC) over wireless channels. The FC applies a decision fusion rule on the received local decisions to make a global decision. The optimal fusion rules have been derived extensively in many scenarios, for example, classic optimal fusion rule [18], channel-aware fusion rules [20, 57], topology-aware fusion rules [4, 68, 75], etc. Most of the work has assumed that the FC is able to collect all local decisions. However, under limited resources, such as bandwidth, time, and energy, a *sensor-selection* strategy must be applied.

Two significant sensor-selection strategies have been proposed: censoring sensor [65] and ordered transmissions [13], which optimize energy and number of transmission efficiency. Applying these strategies in a finite-bandwidth system requires a proper channel access method. Many transmission protocols based on *random access* have been introduced for distributed detection that incorporates censoring-sensor/ordered-transmission strategies [19,44,92,93]. However, in these papers, the FC makes a global decision based on only successfully received local decisions, while considering packet collisions to be transmission errors. In fact, these collisions might provide useful information about the events of interest.

In this chapter, we consider a large, single-hop, wireless sensor network (WSN)

performing distributed detection with a limited collection time and a shared transmission channel. In this scenario, the FC has a limited time to collect the *binary* local decisions, which are sent through a shared transmission channel. Since the FC is not allowed to collect all local decisions, we apply a sensor-selection strategy called the reliability-based splitting algorithm [44] to the considered distributed detection. By applying this algorithm, the sensor nodes are divided into groups according to their observation reliabilities. The sensor nodes in a group will send their binary decisions in the same assigned frame by using slotted ALOHA. We derive both optimal and suboptimal *collision-aware* fusion rules, where the FC computes a global decision from not only the successfully received local decisions but also the *numbers of successful transmission slots and collision slots*.[1] In addition, we proposed a two-level reliability-based splitting algorithm, where the sensor nodes are divided into groups based on both observation reliabilities and local decisions they have made. As a result, the received local decisions are *subframe-dependent* and *invulnerable* to channel errors. The optimal and suboptimal collision-aware fusion rules are derived as a function of the numbers of successful and collision time slots. The probabilities of false alarm and miss detection for these collision-aware fusion rules are derived and evaluated.

The remainder of this chapter is organized as follows. The system model is provided in Section 3.2. We derive the collision-aware fusion rules and performance measures of the distributed detection using the reliability-based splitting algorithm in Section 3.3. The two-level reliability-based splitting algorithm, its collision-aware fusion rules, and the performance measures are explained and derived in Section 3.4. The numerical results are shown in Section 3.5. Finally, conclusions are given in Section 3.6.

[1] In the proposed schemes, if we know the numbers of successful and collision time slots, we also know the number of idle time slots.

3.2 System Model

We consider a distributed detection system with the following assumptions.

3.2.1 Centralized Fusion System

There are N sensor nodes deployed in an area to monitor events. The FC will broadcast an inquiry about an event of interest to start the local-decision collection process. Each node will make an observation of this event, make a local *binary* decision, and send it to the FC via a single-hop wireless channel.[2]

3.2.2 Transmission Channel

We assume that the sensor nodes share a transmission channel when sending their binary decisions to the FC. The channel is divided into time slots, where the FC and sensor nodes know when a time slot begins and ends (i.e., synchronous time). A local decision will be successfully sent to the FC in a time slot if it is the only one transmitted in that slot; otherwise, the slot is idle or a collision occurs. We assume that the collisions are solely from the transmissions of the nodes in the considered network. The length of each time slot is equal to the packet containing a local decision.

3.2.3 Time Constraint

The FC is allocated T time slots to collect local decisions. We assume that $T < N$; i.e., the FC is not able to collect all local decisions.

3.2.4 Binary Hypothesis Testing Model

We assume that the noisy observation at a sensor node, x, is governed by the following binary hypothesis model:

$$H_0 : \ x \sim f_X(x|H_0) \quad \text{and} \quad H_1 : \ x \sim f_X(x|H_1),$$

[2]Specifically, each node has made one observation on the event of interest.

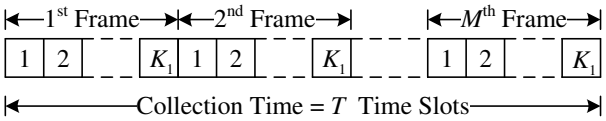

Figure 11: The proposed scheme divides the allocated collection time T into M frames, where each frame consists of K_1 time slots.

where $f_X(x|H_i)$ is the conditional probability density function (PDF) of x. The observations are assumed to be *independent and identically distributed* (IID) given H_i, for $i = 0, 1$. The prior probability that H_0 happens, $\Pr(H_0)$, is equal to P_0, and, the prior probability that H_1 happens is equal to P_1.

3.3 Decision Fusion in Reliability-Based Splitting Algorithm

3.3.1 Scheme's Outline

The collection time T is divided into M frames, where each frame consists of K_1 time slots; i.e., $T = K_1 M$, as shown in Fig. 11. The proposed scheme performs the following steps. At the beginning of the collection time, the FC broadcasts a set of reliability thresholds $\{\hat{r}_m\}$, for $m = 1, \ldots, M$, where $0 \leq \hat{r}_M \leq \ldots \leq \hat{r}_1 < \hat{r}_0$, where $\hat{r}_0 = \infty$.[3] Each node makes its own local binary decision and computes the observation reliability r as shown in Section 3.3.2. The nodes with the observation reliabilities $r \in [\hat{r}_m, \hat{r}_{m-1})$ will send their local decisions in the mth frame, and, then, *leave* the decision collection process (i.e., no retransmissions).[4] More details on the channel access protocol are shown in Section 3.3.3. Therefore, the sensor nodes are divided into $M+1$ groups, where the nodes whose $r < \hat{r}_M$ do not send their decisions to the FC. At the end of the collection time, the FC makes a global decision based on the fusion rules presented in Section 3.3.4. The probabilities of false alarm and miss detection are derived in Section 3.3.5.

[3]Since we have a fixed collection time, other arrangements are possible. However, those might introduce a difficult mathematical formulation.

[4]The nodes whose $\hat{r}_M \leq r < \hat{r}_m$ is waiting for their frames.

3.3.2 Sensor Processing and Observation Reliability

Each node will make a local *binary* decision u from its observation x by using the following local decision rule:

$$\log \frac{f_X(x|H_1)}{f_X(x|H_0)} \underset{u=-1}{\overset{u=1}{\gtrless}} \tau. \tag{30}$$

where τ is a threshold. Note that all nodes use this decision rule. The reliability of a local decision is equivalent to the observation reliability, which is defined as follows.

Definition 3 (**Observation Reliability**). *Let x be a local observation. The reliability of the observation x, which is denoted by r, is equal to*

$$r = \left| \log \frac{f_X(x|H_1)}{f_X(x|H_0)} - \tau \right|. \tag{31}$$

Given the reliabilities r_A and r_B, where $r_A \leq r_B$, let $\mathcal{X}^{(-)}(r_A, r_B)$ be the set of observations x whose $\log \frac{f_X(x|H_1)}{f_X(x|H_0)} \in (-r_B, -r_A]$, and let $\mathcal{X}^{(+)}(r_A, r_B)$ be the set of observations x whose $\log \frac{f_X(x|H_1)}{f_X(x|H_0)} \in [r_A, r_B)$. Mathematically, we have

$$\mathcal{X}^{(-)}(r_A, r_B) = \left\{ x : -r_B < \log \frac{f_X(x|H_1)}{f_X(x|H_0)} - \tau \leq -r_A \right\},$$
$$\mathcal{X}^{(+)}(r_A, r_B) = \left\{ x : r_A \leq \log \frac{f_X(x|H_1)}{f_X(x|H_0)} - \tau < r_B \right\},$$

and $\mathcal{X}(r_A, r_B) = \mathcal{X}^{(-)}(r_A, r_B) \cup \mathcal{X}^{(+)}(r_A, r_B)$. □

According to the proposed scheme's channel access protocol, explained in Section 3.3.3, the nodes whose observation reliabilities $r \in [\hat{r}_m, \hat{r}_{m-1})$ will send their decisions to the FC in the mth frame. Let u_m be a local decision sent to the FC in the mth frame. We have the following probabilities of false alarm and miss detection for the local decisions:

$$\alpha_m = \Pr(u_m = 1|H_0) = \frac{\int_{x \in \mathcal{X}^{(+)}(\hat{r}_m, \hat{r}_{m-1})} f_X(x|H_0)\, dx}{\int_{x \in \mathcal{X}(\hat{r}_m, \hat{r}_{m-1})} f_X(x|H_0)\, dx},$$
$$\beta_m = \Pr(u_m = -1|H_1) = \frac{\int_{x \in \mathcal{X}^{(-)}(\hat{r}_m, \hat{r}_{m-1})} f_X(x|H_1)\, dx}{\int_{x \in \mathcal{X}(\hat{r}_m, \hat{r}_{m-1})} f_X(x|H_1)\, dx}.$$

3.3.3 Channel Access Protocol

The reliability thresholds $\{\hat{r}_m\}$ are used to control nodes' access to the channel. Only the nodes with $r \in [\hat{r}_m, \hat{r}_{m-1})$ are allowed to send their local decisions during the mth frame. In other words, the nodes with almost the same reliability will compete for the channel with each other. For convenience, we have $0 \leq \hat{r}_M \leq \hat{r}_{M-1} \leq \ldots \leq \hat{r}_1 < \infty$. As a result, the local decisions are thus sent to the FC approximately in order from the highest to lowest observation reliabilities. Consequently, the number of nodes attempting transmission in the mth frame, n_m, is a random variable. The joint probability mass function (PMF) of $\mathbf{n} = (n_1, \ldots, n_M)$ is a multinomial distribution:

$$f(\mathbf{n}|H_i) = \frac{N!}{n_1! \cdots n_{M+1}!} q_{1|i}^{n_1} \cdots q_{(M+1)|i}^{n_{M+1}}, \tag{32}$$

where $q_{m|i} = \int_{x \in \mathcal{X}(\hat{r}_m, \hat{r}_{m-1})} f_X(x|H_i)\, dx$, $q_{(M+1)|i} = 1 - \sum_{m=1}^{M} q_{m|i}$, and $n_{M+1} = N - \sum_{m=1}^{M} n_m$. The average number of nodes attempting transmissions in the mth frame, $\bar{n}_{m|i}$, is equal to $N q_{m|i}$.

Since the *identities* and number of the nodes that will attempt transmission in the mth frame are unknown in advance, we assume a *slotted ALOHA* protocol enables them to share the channel. Each node active during this frame will send its decision in a time slot with the probability $\frac{1}{K_1}$. Because a collision channel is assumed, a node's transmission is successful only if it is the only one to transmit in that slot. Since the active nodes use a fixed transmission probability strategy, feedback on the channel state (success, idle, collision) is not necessary. In addition, we do not consider the case of multi-packet reception in this work. Therefore, in any one of the time slots in the mth frame, the conditional probabilities of successful transmission $p_{S|n_m}$, idle time slot $p_{I|n_m}$, and collision $p_{C|n_m}$ can be expressed as: $p_{S|n_m} = \frac{n_m}{K_1}\left(1 - \frac{1}{K_1}\right)^{n_m - 1}$, $p_{I|n_m} = \left(1 - \frac{1}{K_1}\right)^{n_m}$, and $p_{C|n_m} = 1 - p_{S|n_m} - p_{I|n_m}$. Note that the probabilities $p_{S|n_m}$, $p_{I|n_m}$ and $p_{C|n_m}$ depend on H_i through the random variable n_m as shown in (32). We assume K_1 is large enough such that the probability that two or more successful transmissions

are from the same node is negligible. Furthermore, the wireless channel is assumed to be a binary symmetric channel (BSC) with the channel-crossover probability ρ.

3.3.4 Optimal and Suboptimal Fusion Rules

Let $d_{k,m}$ be a bit decoded by the FC at the kth time slot in the mth frame. We have $d_{k,m} \in \{1, -1, e, 0\}$. The decoded bits $d_{k,m} = e$ and $d_{k,m} = 0$ indicate *unrecoverable* bits because of a collision time slot and an idle time slot, respectively. Therefore, we have

$$\begin{aligned} \Pr(d_{k,m} = e|n_m, H_i) &= \Pr(d_{k,m} = e|n_m) = p_{C|n_m}, \\ \Pr(d_{k,m} = 0|n_m, H_i) &= \Pr(d_{k,m} = 0|n_m) = p_{I|n_m}. \end{aligned} \tag{33}$$

The decoded bit $d_{k,m} \in \{1, -1\}$ indicates a *successfully* decoded bit with probability $p_{S|n_m}$. However, the successfully decoded bits might still be incorrect because of either channel errors or observation errors. Therefore, we have

$$\begin{aligned} \Pr(d_{k,m} = -1|n_m, H_0) &= p_{S^{(-|0)}|n_m} = p_{S|n_m}(1 - p_{E|0,m}), \\ \Pr(d_{k,m} = 1|n_m, H_0) &= p_{S^{(+|0)}|n_m} = p_{S|n_m} p_{E|0,m}, \\ \Pr(d_{k,m} = -1|n_m, H_1) &= p_{S^{(-|1)}|n_m} = p_{S|n_m} p_{E|1,m}, \\ \Pr(d_{k,m} = 1|n_m, H_1) &= p_{S^{(+|1)}|n_m} = p_{S|n_m}(1 - p_{E|1,m}), \end{aligned} \tag{34}$$

where $p_{E|0,m} = \rho(1 - \alpha_m) + (1 - \rho)\alpha_m$ and $p_{E|1,m} = \rho(1 - \beta_m) + (1 - \rho)\beta_m$. Note that the probabilities above do not depend on k.

Let $z_{S,m}^{(+)}$, $z_{S,m}^{(-)}$, $z_{C,m}$, and $z_{I,m}$ be the numbers of $d_{k,m} = 1$, $d_{k,m} = -1$, $d_{k,m} = e$, and $d_{k,m} = 0$, respectively, in the mth frame. Note that $z_{S,m}^{(+)} + z_{S,m}^{(-)} + z_{C,m} + z_{I,m} = K_1$. Equivalently, $z_{S,m}^{(+)} + z_{S,m}^{(-)}$, $z_{C,m}$, and $z_{I,m}$ are the numbers of successful, collision, and idle time slots, respectively, in the mth frame. We denote $\mathbf{z}_m = \left(z_{S,m}^{(+)}, z_{S,m}^{(-)}, z_{C,m}, z_{I,m}\right)$. The joint probability $f(\mathbf{z}_m|n_m, H_i)$ is, for $i = 0, 1$,

$$f(\mathbf{z}_m|n_m, H_i) = \frac{K_1!}{z_{S,m}^{(+)}!\, z_{S,m}^{(-)}!\, z_{C,m}!\, z_{I,m}!} p_{S^{(+|i)}|n_m}^{z_{S,m}^{(+)}} p_{S^{(-|i)}|n_m}^{z_{S,m}^{(-)}} p_{C|n_m}^{z_{C,m}} p_{I|n_m}^{z_{I,m}}, \tag{35}$$

where $p_{S^{(+|i)}|n_m} + p_{S^{(-|i)}|n_m} + p_{C|n_m} + p_{I|n_m} = 1$. The optimal fusion rule can be expressed as follows.

Proposition 11 (**Optimal Collision-Aware Fusion Rule**). *Consider the proposed scheme described in Section 3.3.1. At the end of the collection time T, the FC receives the decoded bits $\{d_{k,m}\}$ for $k = 1, \ldots, K_1$ and $m = 1, \ldots, M$, which result in $\mathbf{z}_1, \ldots, \mathbf{z}_M$. The optimal fusion rule is a function of both* successfully *decoded bits and the* numbers *of successful and collision time slots:*

$$\Lambda\big(\mathbf{z}_1, \ldots, \mathbf{z}_M\big) = \sum_{m=1}^{M} \left[z_{S,m}^{(+)} \log\left(\frac{1 - p_{E|1,m}}{p_{E|0,m}}\right) + z_{S,m}^{(-)} \log\left(\frac{p_{E|1,m}}{1 - p_{E|0,m}}\right)\right] + \log\left[\frac{\sum \cdots \sum_{n_1+\ldots+n_{M+1}=N} \prod_{m=1}^{M} p_{S|n_m}^{z_{S,m}} p_{I|n_m}^{z_{I,m}} p_{C|n_m}^{z_{C,m}} f(\mathbf{n}|H_1)}{\sum \cdots \sum_{n_1+\ldots+n_{M+1}=N} \prod_{m=1}^{M} p_{S|n_m}^{z_{S,m}} p_{I|n_m}^{z_{I,m}} p_{C|n_m}^{z_{C,m}} f(\mathbf{n}|H_0)}\right] \underset{H_0}{\overset{H_1}{\gtrless}} \log\frac{P_0}{P_1}, \quad (36)$$

where $z_{S,m} = z_{S,m}^{(+)} + z_{S,m}^{(-)}$ and $z_{I,m} = K_1 - z_{S,m} - z_{C,m}$.

Proof. From Bayes' rule, we have

$$\log\frac{f\big(\mathbf{z}_1, \ldots, \mathbf{z}_M|H_1\big)}{f\big(\mathbf{z}_1, \ldots, \mathbf{z}_M|H_0\big)} \underset{H_0}{\overset{H_1}{\gtrless}} \log\frac{P_0}{P_1}. \quad (37)$$

The conditional probability $f(\mathbf{z}_1, \ldots, \mathbf{z}_M|H_i)$ is equal to

$$f(\mathbf{z}_1, \ldots, \mathbf{z}_M|H_i) = \sum \cdots \sum_{n_1+\ldots+n_{M+1}=N} \prod_{m=1}^{M} f(\mathbf{z}_m|n_m, H_i) f(\mathbf{n}|H_i). \quad (38)$$

By substituting (32), (35) and (38) into (37), and after some mathematical manipulation, we obtain (36). □

We see that the optimal fusion rule is aware of the collisions through the term on the second line in (36). The numerator and denominator of this term are proportional to the *likelihood functions* of $(\mathbf{z}_1, \ldots, \mathbf{z}_M)$ given H_1 and H_0, respectively. Specifically, given $(\mathbf{z}_1, \ldots, \mathbf{z}_M)$, which are those the FC has observed, this term will be positive if H_1 is likely to happen, and negative, otherwise. However, there is a case where the optimal fusion rule cannot exploit $(z_{C,1}, \ldots, z_{C,M})$ or $(z_{I,1}, \ldots, z_{I,M})$ to differentiate between H_0 and H_1.

Corollary 4 (**Special Case**). *Assume that the conditional PDF $f_X(x|H_0)$ is a shift-in-mean version of $f_X(x|H_1)$. Furthermore, the conditional PDF $f_X(x|H_0)$ is symmetric about its mean. The optimal fusion rule is a function of successfully decoded bits, which can be written as the following weighted sum:*

$$\sum_{m=1}^{M}\left[\left(z_{S,m}^{(+)}-z_{S,m}^{(-)}\right)\log\left(\frac{1-p_{E|1,m}}{p_{E|0,m}}\right)\right]\underset{H_0}{\overset{H_1}{\gtrless}}\log\frac{P_0}{P_1}. \tag{39}$$

Proof. From the assumption, we have $\sum\cdots\sum_{n_1+\ldots+n_{M+1}=N}\prod_{m=1}^{M}p_{S|n_m}^{z_{S,m}}p_{I|n_m}^{z_{I,m}}p_{C|n_m}^{z_{C,m}}f(\mathbf{n}|H_i)$ are identical for both H_0 and H_1. Specifically, there is *no* difference between $f(\mathbf{n}|H_0)$ and $f(\mathbf{n}|H_1)$. Therefore, the term on the third line in (36) is equal to zero. In addition, we have $\log\left(\frac{1-p_{E|1,m}}{p_{E|0,m}}\right)=-\log\left(\frac{p_{E|1,m}}{1-p_{E|0,m}}\right)$. □

When N or M is large, the computation of the optimal fusion rule in (36) is quite complicated, and, then, problematic to the FC. A simple fusion rule that is still aware of the collisions can be shown below.

Corollary 5 (**Suboptimal Collision-Aware Fusion Rule**). *Consider the distributed detection using the reliability-based splitting algorithm with a set of reliability thresholds $\{\hat{r}_m\}$. Assume that the numbers of active nodes are* deterministic. *Let $n_{m|i}$ denote the numbers of active nodes in the mth frame given H_i. The optimal fusion rule shown in* (36) *can be expressed as a* weighted *sum of $z_{S,m}^{(+)}$, $z_{S,m}^{(-)}$, and $z_{C,m}$:*

$$\sum_{m=1}^{M}\left[W_{S^{(+)},m}z_{S,m}^{(+)}+W_{S^{(-)},m}z_{S,m}^{(-)}+W_{C,m}z_{C,m}\right]\underset{H_0}{\overset{H_1}{\gtrless}}\Gamma_1, \tag{40}$$

where

$$\begin{aligned}
W_{S^{(+)},m}&=\log\left[\left(\frac{1-p_{E|1,m}}{p_{E|0,m}}\right)\left(\frac{p_{S|n_{m|1}}}{p_{S|n_{m|0}}}\right)\left(\frac{p_{I|n_{m|0}}}{p_{I|n_{m|1}}}\right)\right],\\
W_{S^{(-)},m}&=\log\left[\left(\frac{p_{E|1,m}}{1-p_{E|0,m}}\right)\left(\frac{p_{S|n_{m|1}}}{p_{S|n_{m|0}}}\right)\left(\frac{p_{I|n_{m|0}}}{p_{I|n_{m|1}}}\right)\right],\\
W_{C,m}&=\log\left[\left(\frac{p_{C|n_{m|1}}}{p_{C|n_{m|0}}}\right)\left(\frac{p_{I|n_{m|0}}}{p_{I|n_{m|1}}}\right)\right],\\
\Gamma_1&=\log\frac{P_0}{P_1}+K_1\sum_{m=1}^{M}\log\left(\frac{p_{I|n_{m|0}}}{p_{I|n_{m|1}}}\right).
\end{aligned}$$

Proof. The fusion rule in (40) is a direct result from (36) when the numbers of active nodes $\{n_m\}$ are deterministic. □

To compute the weights $W_{S^{(+)},m}$, $W_{S^{(-)},m}$, and $W_{C,m}$, we need to choose $n_{m|i}$. As shown in Section 3.5, an intuitive choice is the average number of active nodes, $\bar{n}_{m|i} = Nq_{m|i}$.

3.3.5 Performance Measures

The probability of false alarm, α, and the probability of missed detection, β, for the optimal fusion rule (36) are

$$\alpha = \sum_{\sum \mathbf{n}=N} \cdots \sum \sum_{\sum \mathbf{z}_1=K_1} \cdots \sum \cdots \sum_{\sum \mathbf{z}_M=K_1} \cdots \sum \prod_{m=1}^{M} f(\mathbf{z}_m|n_m, H_0) f(\mathbf{n}|H_0) \times \left[\mathbb{1}_{\left\{\Lambda(\mathbf{z}) > \log \frac{P_0}{P_1}\right\}} + \frac{1}{2} \mathbb{1}_{\left\{\Lambda(\mathbf{z}) = \log \frac{P_0}{P_1}\right\}} \right], \quad (41)$$

$$\beta = \sum_{\sum \mathbf{n}=N} \cdots \sum \sum_{\sum \mathbf{z}_1=K_1} \cdots \sum \cdots \sum_{\sum \mathbf{z}_M=K_1} \cdots \sum \prod_{m=1}^{M} f(\mathbf{z}_m|n_m, H_1) f(\mathbf{n}|H_1) \times \left[\mathbb{1}_{\left\{\Lambda(\mathbf{z}) < \log \frac{P_0}{P_1}\right\}} + \frac{1}{2} \mathbb{1}_{\left\{\Lambda(\mathbf{z}) = \log \frac{P_0}{P_1}\right\}} \right], \quad (42)$$

where $\sum \mathbf{n} = n_1 + \ldots + n_{M+1} = N$, $\sum \mathbf{z}_m = z_{S,m}^{(+)} + z_{S,m}^{(-)} + z_{I,m} + z_{C,m} = K_1$, $\mathbf{z}_m = \left(z_{S,m}^{(+)}, z_{S,m}^{(-)}, z_{I,m}, z_{C,m}\right)$, $\mathbf{z} = (\mathbf{z}_1, \ldots, \mathbf{z}_M)$, $f(\mathbf{z}_m|n_m, H_i)$ is shown in (35), $f(\mathbf{n}|H_i)$ is shown in (32), and $\mathbb{1}_{\{.\}}$ is the indicator function. Note that the numbers of iterations according to the summations in (41) and (42) are equal to $\left[\frac{(N+M)!}{N!\,M!}\right]\left[\frac{(K_1+3)!}{3!\,K_1!}\right]^M$, which is highly complicated for a large N, K_1, or M.

The probability of false alarm, α_{Sub}, and the probability of miss detection, β_{Sub}, for the suboptimal fusion rule (40) can be computed in the same way as shown above. Because the suboptimal fusion rule (40) is a weighted sum of $z_{S,m}^{(+)}$, $z_{S,m}^{(-)}$, and $z_{C,m}$, we can derive asymptotical approximations of α_{Sub} and β_{Sub} as shown below. The computations of these approximations are very affordable.

Proposition 12 (**Approximated Performance Measures**). *The probability of false alarm, α_{Sub}, and the probability of miss detection, β_{Sub} for the suboptimal fusion*

$$\mathbf{C}_{m|i} = \begin{bmatrix} K_1 p_{S^{(+|i)}|a_m}(1 - p_{S^{(+|i)}|a_m}) & -K_1 p_{S^{(+|i)}|a_m} p_{S^{(-|i)}|a_m} & -K_1 p_{S^{(+|i)}|a_m} p_{C|a_m} \\ -K_1 p_{S^{(+|i)}|a_m} p_{S^{(-|i)}|a_m} & K_1 p_{S^{(-|i)}|a_m}(1 - p_{S^{(-|i)}|a_m}) & -K_1 p_{S^{(-|i)}|a_m} p_{C|a_m} \\ -K_1 p_{S^{(+|i)}|a_m} p_{C|a_m} & -K_1 p_{S^{(-|i)}|a_m} p_{C|a_m} & K_1 p_{C|a_m}(1 - p_{C|a_m}) \end{bmatrix}. \tag{45}$$

---

rule (40) *can be asymptotically (i.e., when* K_1 *is large) approximated as*

$$\alpha_{Sub} \approx 1 - \left(\frac{1}{\sqrt{\pi}}\right)^M \sum_{j_1=1}^{J_1} \cdots \sum_{j_M=1}^{J_M} \omega_{j_1} \cdots \omega_{j_M} \times \Phi\Big(G_0\big(\bar{n}_{1|0} + \sqrt{2}\sigma_{1|0}\nu_{j_1}, \ \ldots, \ \bar{n}_{M|0} + \sqrt{2}\sigma_{M|0}\nu_{j_M}\big)\Big), \tag{43}$$

$$\beta_{Sub} \approx \left(\frac{1}{\sqrt{\pi}}\right)^M \sum_{j_1=1}^{J_1} \cdots \sum_{j_M=1}^{J_M} \omega_{j_1} \cdots \omega_{j_M} \times \Phi\Big(G_1\big(\bar{n}_{1|1} + \sqrt{2}\sigma_{1|1}\nu_{j_1}, \ \ldots, \ \bar{n}_{M|1} + \sqrt{2}\sigma_{M|1}\nu_{j_M}\big)\Big), \tag{44}$$

where $\Phi(\cdot)$ *is the Gaussian cumulative distribution function,* $\bar{n}_{m|i} = Nq_{m|i}$ *from* (32), $\sigma_{m|i} = \sqrt{Nq_{m|i}\big(1 - q_{m|i}\big)}$ *from* (32). *The values of* J_m, ν_{j_m} *and* ω_{j_m} *are obtained from Gauss-Hermite quadrature integration, where* J_m *is the number of sample points,* ν_{j_m} *is the root from Hermite polynomial, and* ω_{j_m} *is the associated weight. The function* $G_i(a_1, \ldots, a_M)$ *is*

$$G_i(a_1, \ldots, a_M) = \frac{\Gamma_1 - \sum_{m=1}^M \boldsymbol{\mu}_{m|i} \mathbf{W}_m^T}{\sqrt{\sum_{m=1}^M \mathbf{W}_m \mathbf{C}_{m|i} \mathbf{W}_m^T}},$$

where Γ_1 *is defined in Corollary 5,* $\boldsymbol{\mu}_{m|i}$ *is the mean vector given* H_i, $\mathbf{C}_{m|i}$ *is the covariance matrix given* H_i, *and* $\mathbf{W}_m$ *is the weight vector. We have*

$$\boldsymbol{\mu}_{m|i} = \big(K_1 p_{S^{(+|i)}|a_m}, \ K_1 p_{S^{(-|i)}|a_m}, \ K_1 p_{C|a_m}\big),$$

$\mathbf{C}_{m|i}$ *shown in* (45), *and* $\mathbf{W}_m = \big(W_{S^{(+)},m}, \ W_{S^{(-)},m}, \ W_{C,m}\big)$ *defined in Corollary 5.*

Proof. Similar to that in Appendix D, the proof applies the limiting distributions of (32) and (35), which are Gaussian distributions, Craig's formula [25], and Gauss-Hermite quadrature integration. □

3.4 Decision Fusion in Two-Level Reliability-Based Splitting Algorithm

In this section, we modify the reliability-based splitting algorithm in such a way that the sensor nodes are divided into groups based on both observation reliabilities and local decisions. We call this scheme as the *two-level* reliability-based splitting algorithm. The details are explained as follows.

3.4.1 Scheme's Details

The collection time T is divided into M frames; each frame is divided further into 2 subframes; and each subframe consists of K_2 time slots. The structure of the collection T is shown in Fig. 12, where $T = 2K_2M$. Note that for a given T, we have $K_2 = \frac{K_1}{2}$. The proposed scheme performs the following steps. At the beginning of the collection time, the FC broadcasts a set of reliability thresholds $\{\hat{r}_m\}$, for $m = 1, \ldots, M$, where $0 \leq \hat{r}_M \leq \ldots \leq \hat{r}_1 < \hat{r}_0$, where $\hat{r}_0 = \infty$. Each node makes its own local binary decision and computes the observation reliability r similar to those explained in Section 3.3.2. The nodes with the observation reliabilities $r \in [\hat{r}_m, \hat{r}_{m-1})$ and the observations $x \in \mathcal{X}^{(-)}(\hat{r}_m, \hat{r}_{m-1})$ will send their local decisions in the $(2m-1)$st subframe, and, then, leave the decision collection process (i.e., no retransmissions). On the other hand, the nodes with the observation reliabilities $r \in [\hat{r}_m, \hat{r}_{m-1})$ and the observations $x \in \mathcal{X}^{(+)}(\hat{r}_m, \hat{r}_{m-1})$ will send their local decisions in the $2m$th subframe, and, then, leave the decision collection process. Note that the nodes with $x \in \mathcal{X}^{(-)}(\hat{r}_m, \hat{r}_{m-1})$ will make negative local decisions, while the nodes with $x \in \mathcal{X}^{(+)}(\hat{r}_m, \hat{r}_{m-1})$ will make positive local decisions. Therefore, the sensor nodes are divided into $2M + 1$ groups, where the nodes whose $r < \hat{r}_M$ do not send their decisions to the FC.

Let n_l be the number of nodes that will send their decisions in the lth subframe, where $1 \leq l \leq 2M$. Note that the lth subframe is in the $\lceil \frac{l}{2} \rceil$nd frame. We have the

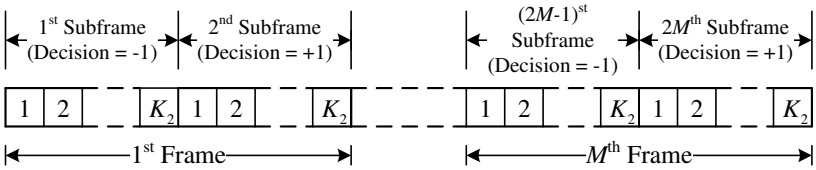

Figure 12: The proposed scheme divides the allocated collection time T into M frames; each frame consists of 2 subframes; and each subframe consists of K_2 time slots. The negative local decisions with the reliabilities $r \in [\hat{r}_m, \hat{r}_{m-1})$ will be sent during the $(2m-1)$st subframe, while the positive local decisions with the reliabilities $r \in [\hat{r}_m, \hat{r}_{m-1})$ will be sent during the $2m$th subframe.

joint PMF of $\mathbf{n} = (n_1, \ldots, n_{2M})$ as a multinomial distribution:

$$f(\mathbf{n}|H_i) = \frac{N!}{n_1! \cdots n_{2M+1}!} q_{1|i}^{n_1} \cdots q_{(2M+1)|i}^{n_{2M+1}}, \tag{46}$$

where $q_{(2m-1)|i} = \int_{x \in \mathcal{X}^{(-)}(\hat{r}_m, \hat{r}_{m-1})} f_X(x|H_i)\, dx$ and $q_{2m|i} = \int_{x \in \mathcal{X}^{(+)}(\hat{r}_m, \hat{r}_{m-1})} f_X(x|H_i)\, dx$, for $1 \leq m \leq M$. In addition, $q_{(2M+1)|i} = 1 - \sum_{l=1}^{2M} q_{l|i}$, and $n_{2M+1} = N - \sum_{l=1}^{2M} n_l$. The average number of nodes attempting transmissions in the lth subframe, $\bar{n}_{l|i}$, is equal to $N q_{l|i}$. The nodes attempting transmissions in each subframe will use slotted ALOHA with the transmission probability $\frac{1}{K_2}$ to send their decisions; specifically, these nodes will send their decisions at a time slot with the probability $\frac{1}{K_2}$. Therefore, in any one of the time slots in the lth subframe, the conditional probabilities of successful transmission $p_{S|n_l}$, idle time slot $p_{I|n_l}$, and collision $p_{C|n_l}$ are $p_{S|n_l} = \frac{n_l}{K_2}\left(1 - \frac{1}{K_2}\right)^{n_l - 1}$, $p_{I|n_l} = \left(1 - \frac{1}{K_2}\right)^{n_l}$, and $p_{C|n_l} = 1 - p_{S|n_l} - p_{I|n_l}$. At the end of the collection time, the FC makes a global decision based on the fusion rules presented in Section 3.4.2. The probabilities of false alarm and miss detection are also derived in Section 3.4.2.

This algorithm exploits the *channel activity* to differentiate between H_0 and H_1. Specifically, as will be shown in the next section, the FC will exploit the numbers of busy time slots (i.e., successful and collision time slots) in subframes to make a global decision. For a *well-behaved* distribution, there are two properties that make this work. First, if H_0 happens, we expect that there are more busy time slots in the $(2m-1)$st subframe than $2m$th subframe since more nodes have made negative local decisions than positive local decisions. Similarly, if H_1 happens, we expect that there

are more busy time slots in the $2m$th subframe than $(2m-1)$st subframe. Second, for a set of reliability thresholds $\{\hat{r}_m\}$ such that $0 \leq \hat{r}_M \leq \ldots \leq \hat{r}_1 < \infty$, we will have $\frac{\bar{n}_{1|0}}{\bar{n}_{2|0}} \geq \cdots \geq \frac{\bar{n}_{(2M-1)|0}}{\bar{n}_{2M|0}}$ if H_0 happens, and $\frac{\bar{n}_{2|1}}{\bar{n}_{1|1}} \geq \cdots \geq \frac{\bar{n}_{2M|1}}{\bar{n}_{(2M-1)|1}}$ if H_1 happens.

3.4.2 Optimal Fusion Rule, Suboptimal Fusion Rule, and Performance Measures

Let $d_{k,l}$ be a bit decoded by the FC at the kth time slot in the lth subframe. Similar to Section 3.3.4, the FC will decode the received local decisions as 1, -1, 0, and e. However, since the FC knows that the negative local decisions will be sent during the odd-number subframe, it will treat all successfully received local decisions as -1. Similarly, since the FC knows that the positive local decisions will be sent during the even-number subframe, it will treat all successfully received local decisions as 1. We can see that the successfully decoded bits are *subframe-dependent* and *invulnerable* to the channel errors. As a result, we have the decoded bit $d_{k,l} = \{s, 0, e\}$, where $d_{k,l} = s$ denotes that $d_{k,l}$ is successfully decoded (no matter it is equal to 1 or -1). Therefore, we have the following probabilities: $\Pr(d_{k,l} = s|n_l, H_i) = p_{S|n_l}$, $\Pr(d_{k,l} = 0|n_l, H_i) = p_{I|n_l}$, and $\Pr(d_{k,l} = e|n_l, H_i) = p_{C|n_l}$.

Let $z_{S,l}$, $z_{I,l}$, and $z_{C,l}$ be the numbers of $d_{k,l} = s$, $d_{k,l} = 0$, and $d_{k,l} = e$, respectively, in the lth subframe. Note that $z_{S,l} + z_{C,l} + z_{I,l} = K_2$. We denote $\mathbf{z}_l = \big(z_{S,l}, z_{C,l}, z_{I,l}\big)$. The joint probability $f(\mathbf{z}_l|n_l, H_i)$ can be expressed as, for $i = 0, 1$,

$$f(\mathbf{z}_l|n_l, H_i) = \frac{K_2!}{z_{S,l}!\, z_{C,l}!\, z_{I,l}!} p_{S|n_l}^{z_{S,l}}\, p_{C|n_l}^{z_{C,l}}\, p_{I|n_l}^{z_{I,l}}, \tag{47}$$

where $p_{S|n_l} + p_{C|n_l} + p_{I|n_l} = 1$. The optimal fusion rule can be expressed as follows.

Proposition 13 (**Optimal Collision-Aware Fusion Rule**). *Consider the proposed scheme described in Section 3.4.1. At the end of the collection time T, the FC receives the decoded bits $\{d_{k,l}\}$ for $k = 1, \ldots, K_2$ and $l = 1, \ldots, 2M$, which result in $\mathbf{z}_1, \ldots, \mathbf{z}_{2M}$. The optimal fusion rule is a function of the numbers of successful time*

slots, idle time slots, and collision time slots:

$$\log\left[\frac{\sum\cdots\sum_{n_1+\ldots+n_{2M+1}=N}\prod_{l=1}^{2M}p_{S|n_l}^{z_{S,l}}p_{I|n_l}^{z_{I,l}}p_{C|n_l}^{z_{C,l}}f(\mathbf{n}|H_1)}{\sum\cdots\sum_{n_1+\ldots+n_{2M+1}=N}\prod_{l=1}^{2M}p_{S|n_l}^{z_{S,l}}p_{I|n_l}^{z_{I,l}}p_{C|n_l}^{z_{C,l}}f(\mathbf{n}|H_0)}\right]\underset{H_0}{\overset{H_1}{\gtrless}}\log\frac{P_0}{P_1}. \tag{48}$$

Proof. The optimal fusion rule (48) is obtained by applying the same steps in the proof of Proposition 11. □

Since the optimal fusion rule (48) has high computational complexity for a large N or M, we propose a suboptimal but effective fusion rule shown in the corollary below. To compute the weights $W_{S,l}$ and $W_{C,l}$ in the suboptimal rule (49), we need to choose $n_{l|i}$. As shown in Section 3.5, an intuitive choice is the average number of active nodes, $\bar{n}_{l|i} = Nq_{l|i}$.

Corollary 6 (**Suboptimal Collision-Aware Fusion Rule**). *Consider the distributed detection described in Section 3.4.1. Assume that the numbers of active nodes are deterministic. Let $n_{l|i}$ denote the numbers of active nodes in the lth subframe given H_i. The optimal fusion rule shown in* (48) *can be expressed as a* weighted *sum of $z_{S,l}$ and $z_{C,l}$:*

$$\sum_{l=1}^{2M}\Big[W_{S,l}\,z_{S,l}+W_{C,l}\,z_{C,l}\Big]\underset{H_0}{\overset{H_1}{\gtrless}}\Gamma_2, \tag{49}$$

where $W_{S,l}=\log\left[\left(\frac{p_{S|n_{l|1}}}{p_{S|n_{l|0}}}\right)\left(\frac{p_{I|n_{l|0}}}{p_{I|n_{l|1}}}\right)\right]$, $W_{C,l}=\log\left[\left(\frac{p_{C|n_{l|1}}}{p_{C|n_{l|0}}}\right)\left(\frac{p_{I|n_{l|0}}}{p_{I|n_{l|1}}}\right)\right]$, *and* $\Gamma_2=\log\frac{P_0}{P_1}+K_2\sum_{l=1}^{2M}\log\left(\frac{P_{I|n_{l|0}}}{P_{I|n_{l|1}}}\right)$. □

The probabilities of false alarm and the probabilities of missed detection for the optimal fusion rule (48) and the suboptimal fusion rule (49) can be derived in a similar manner shown in Section 3.3.5. Again, we will face a computation complexity problem when N, K_2, or M is large. It will be shown in Section 3.5 that, under the considered scenario, the performances of the optimal fusion rule (48) and the suboptimal fusion rule (49) are very close. Asymptotic approximations of the probabilities of false alarm and miss detection for the suboptimal fusion rule (49) are shown in the

proposition below, which has a reasonable computational complexity. The derivation of Proposition 14 is similar to that in Proposition 12.

Proposition 14 (**Approximated Performance Measures**). *The probability of false alarm, α_{Sub}, and the probability of miss detection, β_{Sub} according to the suboptimal rule defined in* (49) *can be asymptotically (i.e., when K_2 is large) approximated as*

$$\alpha_{Sub} \approx 1 - \left(\frac{1}{\sqrt{\pi}}\right)^{2M} \sum_{j_1=1}^{J_1} \cdots \sum_{j_{2M}=1}^{J_{2M}} \omega_{j_1} \cdots \omega_{j_{2M}} \times \Phi\Big(G_0\big(\bar{n}_{1|0} + \sqrt{2}\sigma_{1|0}\nu_{j_1}, \ \ldots, \ \bar{n}_{2M|0} + \sqrt{2}\sigma_{2M|i}\nu_{j_{2M}}\big)\Big), \quad (50)$$

$$\beta_{Sub} \approx \left(\frac{1}{\sqrt{\pi}}\right)^{2M} \sum_{j_1=1}^{J_1} \cdots \sum_{j_{2M}=1}^{J_{2M}} \omega_{j_1} \cdots \omega_{j_{2M}} \times \Phi\Big(G_1\big(\bar{n}_{1|1} + \sqrt{2}\sigma_{1|1}\nu_{j_1}, \ \ldots, \ \bar{n}_{2M|1} + \sqrt{2}\sigma_{2M|1}\nu_{j_{2M}}\big)\Big), \quad (51)$$

where $\Phi(\cdot)$, $\bar{n}_{l|i}$, $\sigma_{l|i}$, J_l, ν_{j_l} and ω_{j_l} are defined similarly to those in Proposition 12. The function $G_i(a_1, \ldots, a_{2M})$ is

$$G_i(a_1, \ldots, a_{2M}) = \frac{\Gamma_2 - \sum_{l=1}^{2M} \boldsymbol{\mu}_{l|i} \mathbf{W}_l^T}{\sqrt{\sum_{l=1}^{2M} \mathbf{W}_l \mathbf{C}_{l|i} \mathbf{W}_l^T}},$$

where Γ_2 is defined in Corollary 6, $\boldsymbol{\mu}_{l|i}$ is the mean vector given H_i, $\mathbf{C}_{l|i}$ is the covariance matrix given H_i, and $\mathbf{W}_l$ is the weight vector. We have $\boldsymbol{\mu}_{l|i} = \big(K_2 p_{S|a_l}, \ K_2 p_{C|a_l}\big)$,

$$\mathbf{C}_{l|i} = \begin{bmatrix} K_2 p_{S|a_l}(1 - p_{S|a_l}) & -K_2 p_{S|a_l} p_{C|a_l} \\ -K_2 p_{S|a_l} p_{C|a_l} & K_2 p_{C|a_l}(1 - p_{C|a_l}) \end{bmatrix},$$

and $\mathbf{W}_l = \big(W_{S,l}, \ W_{C,l}\big)$ defined in Corollary 6. □

3.5 Numerical Results

We use the following shift-in-mean model to evaluate the detection error probability (DEP) of the proposed schemes: $H_0 : x = \eta$, and $H_1 : x = \mu + \eta$, where μ is a constant, and η is a Gaussian random variable with mean and variance

equal to zero and σ^2, respectively. The prior probabilities $\Pr(H_0)$ and $\Pr(H_1)$ are set to $\frac{1}{2}$. The local decision threshold τ in (30) is set to 0. The reliability of the observation x is $\left|\log \frac{f_X(x|H_1)}{f_X(x|H_0)}\right| = \frac{\mu}{\sigma^2}\left|x - \frac{\mu}{2}\right|$. Without loss of generality, in this case, we define the reliability of the observation x as $r = \left|x - \frac{\mu}{2}\right|$; i.e., we omit the scaling factor. Therefore, we have $\mathcal{X}^{(-)}(\hat{r}_m, \hat{r}_{m-1}) = \left(\frac{\mu}{2} - \hat{r}_{m-1},\, \frac{\mu}{2} - \hat{r}_m\right]$ and $\mathcal{X}^{(+)}(\hat{r}_m, \hat{r}_{m-1}) = \left[\frac{\mu}{2} + \hat{r}_m,\, \frac{\mu}{2} + \hat{r}_{m-1}\right)$, where $m = 1, \ldots, M$. Hence, the DEP of the distributed detection is *equal to* the probability of false alarm (or the probability of miss detection). For convenience, we will call the proposed scheme using the reliability-based splitting algorithm in Section 3.3 *Scheme I*, and the proposed scheme using the two-level reliability-based splitting algorithm in Section 3.4 *Scheme II*. We have $K_1 = \frac{T}{M}$ and $K_2 = \frac{T}{2M}$. Throughout this performance evaluation, the reliability thresholds $\{\hat{r}_m\}$ are selected such that the expected number of nodes whose $r \in [\hat{r}_m, \hat{r}_{m-1})$ is equal to K_1, for all m (if we do not specify otherwise). This set of reliability thresholds maximizes the throughput in Scheme I [44]. Mathematically, under this scenario, we choose the reliability thresholds $\{\hat{r}_m\}$ such that, for all m, $\int_{\frac{\mu}{2}-\hat{r}_{m-1}}^{\frac{\mu}{2}-\hat{r}_m} f_X(x|H_0)\,dx + \int_{\frac{\mu}{2}+\hat{r}_m}^{\frac{\mu}{2}+\hat{r}_{m-1}} f_X(x|H_0)\,dx = \frac{K_1}{N}$ [44].

In Fig. 13, we compare the DEPs of a TDMA-based scheme, Scheme I, Scheme II (using the optimal fusion rule and the suboptimal fusion rule), and the oracle-TDMA scheme for various observation signal-to-noise ratio (SNR), which is defined as $10\log_{10}\left(\frac{\mu^2}{\sigma^2}\right)$. The other parameters are specified in the figure's caption. Note that under this scenario, the optimal fusion rule and the suboptimal fusion rule of Scheme I are identical and equal to the fusion rule (39), which makes a global decision based only on the successfully received local decisions. For Scheme II using the suboptimal fusion rule (49), we use $\bar{n}_{l|i} = Nq_{l|i}$ to compute the weights in (49). In the TDMA-based scheme, the local decisions are sent to the FC in *random* order of the reliabilities, while, in the oracle-TDMA scheme, the local decisions are sent to the FC in *descending* order of the reliabilities. There are no packet collisions in

these two schemes. We see that, under this scenario, the DEPs of Scheme II using the optimal fusion rule and the suboptimal fusion rule are almost identical. Both Schemes I and II outperform the TDMA-based scheme. However, the performance of Scheme II is far better than that of Scheme I when the SNR is high. The DEP gap between Schemes I and II can be interpreted as a *value of collision information* when we handle it properly.

We also compare the exact DEPs and the approximated DEPs of Scheme I using the optimal fusion rule and Scheme II using the suboptimal fusion rule in Fig. 13. Recall that the optimal fusion rule and the suboptimal fusion rule of Scheme I are identical. The exact DEPs of Schemes I and II are computed from (41), while the approximated DEPs of Schemes I and II are obtained from (43) and (50), respectively. For Scheme I, the parameters J_m, ν_{j_m}, and ω_{j_m} from Gauss-Hermite quadrature integration are set as follows: $J_m = 4$ for all m, and $(\nu_{j_m}, \omega_{j_m})$ are $(0.525, 0.805)$, $(-0.525, 0.805)$, $(1.651, 0.081)$, and $(-1.651, 0.081)$. These values are also used in Scheme II for J_l, ν_{j_l}, and ω_{j_l}. The exact DEP and the approximated DEP of Scheme I are almost identical. On the other hand, the approximated DEP of Scheme II is a little bit optimistic when the SNR is large.

In Fig. 14, we show the DEPs of the TDMA-based scheme, Scheme I using the optimal fusion rule (39) for $M = 1$ and 2, Scheme II using the suboptimal fusion rule (49) for $M = 1$ and 2, and the oracle-TDMA scheme for various N. The parameter values are shown in the figure's caption. The DEPs of Schemes I and II are obtained from the approximations (43) and (50), respectively. Scheme I, Scheme II, and the oracle-TDMA scheme significantly get a benefit from increasing N since more nodes have highly reliable observations. Increasing M helps to improve the DEPs of Schemes I and II especially for low N. Note that the improvement gained by increasing M depends on the shape of the distributions $f_X(x|H_i)$.

We study the optimal reliability threshold $\hat{r}_1^*$ when $M = 1$ and $T = 40$ in Fig. 15,

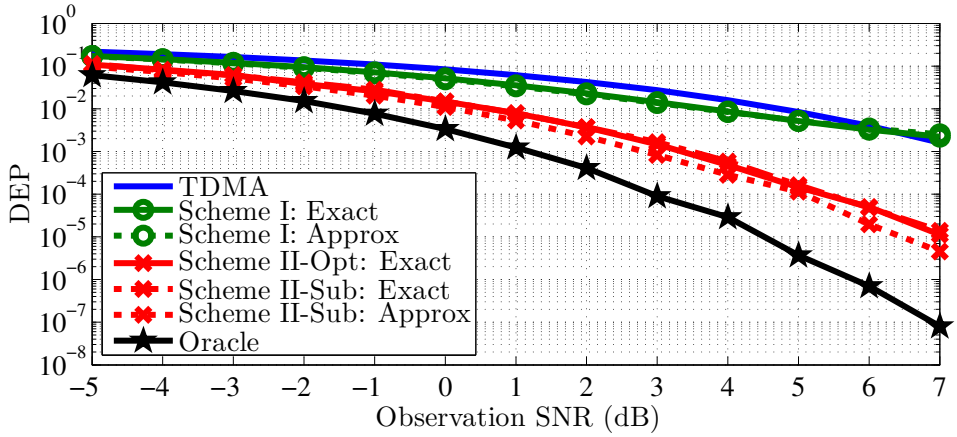

Figure 13: The detection error probabilities (DEPs) of the TDMA-based scheme, the proposed scheme I, the proposed scheme II (for both optimal and suboptimal fusion rules), and the oracle-TDMA scheme for various SNR. The other parameters are $N = 50$, $T = 20$, $M = 1$, $\rho = 0.05$.

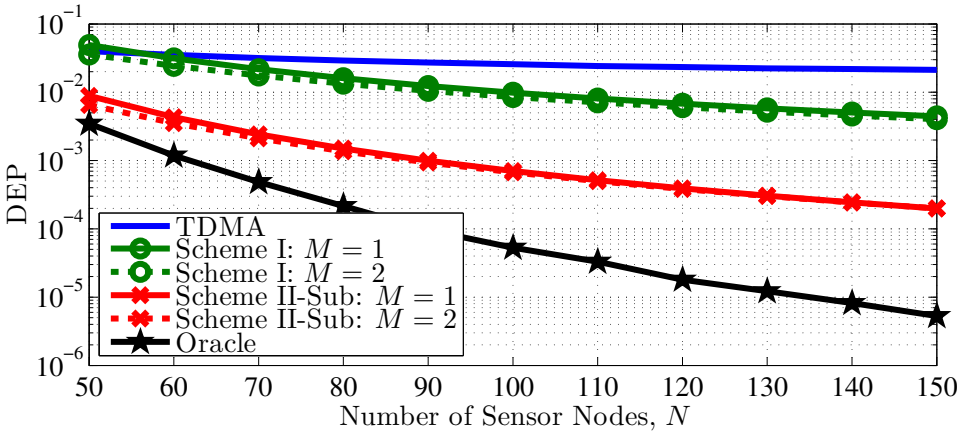

Figure 14: The detection error probabilities (DEPs) of the TDMA-based scheme, the proposed scheme I ($M = 1$ and 2), the proposed scheme II ($M = 1$ and 2), and the oracle-TDMA scheme for various N. The other parameters are $T = 40$, SNR= 0dB, $\rho = 0.05$. The DEPs of Schemes I and II are from the approximations.

where we show the DEPs of Scheme I using the optimal fusion rule (39) and Scheme II using the suboptimal fusion rule (49) versus the expected number of nodes whose $r \in [\hat{r}_1, \infty)$. The parameter values are shown in the figure's caption. As result, we have $K_1 = 40$ and $K_2 = 20$. Recall that in Figs. 13 and 14, we select $\{\hat{r}_m\}$ such that the expected number of nodes whose $r \in [\hat{r}_m, \hat{r}_{m-1})$ is equal to K_1, for all m, which maximize the throughput of Scheme I. We see that the optimal DEP of Scheme I is

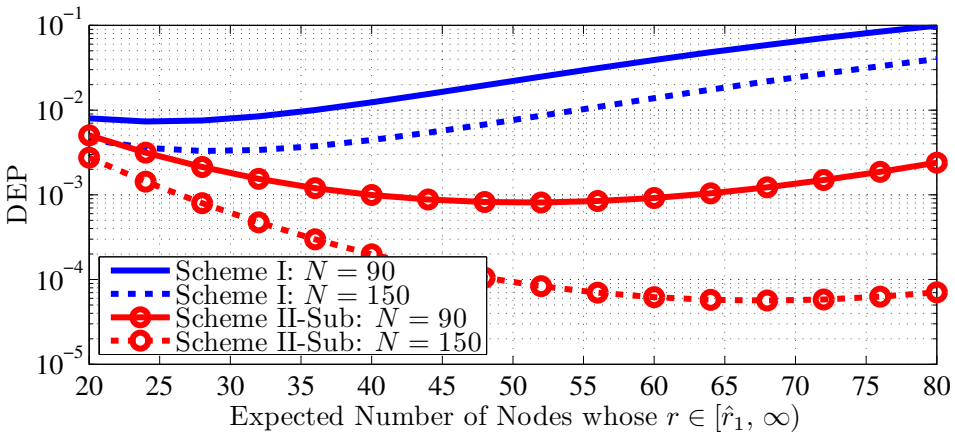

Figure 15: The detection error probabilities (DEPs) of Scheme I ($N = 90$ and 150) and Scheme II ($N = 90$ and 150) versus the expected numbers of nodes whose $r \in [\hat{r}_1, \infty)$. The other parameters are $T = 40$, $M = 1$, SNR= 0dB, $\rho = 0.05$. The DEPs of Schemes I and II are from the approximations.

located where the expected number of nodes whose $r \in [\hat{r}_1, \infty)$ is less than 40. As a result, Scheme I prefers more idle time slots than collisions. On the other hand, since Scheme II exploits the number of busy time slots (i.e., successful and collision time slots) in making a global decision, the optimal DEP of Scheme II is located where the expected number of nodes whose $r \in [\hat{r}_1, \infty)$ is larger than 40 (i.e., there are a lot of busy time slots in Scheme II).

3.6 Conclusion

We proposed two reliability-based splitting algorithms for distributed detection and derived the optimal and suboptimal collision-aware fusion rules. In these fusion rules, the FC will also exploit the numbers of the successful and collision time slots in making a global decision. Under the considered scenarios, the numerical results showed that the proposed schemes outperform the TDMA-based scheme. The DEPs gained from using the optimal and suboptimal fusion rules are almost identical. Therefore, a system designer might prefer using the suboptimal fusion rules, which are in the form of a weighted sum, because of their low computation complexity.

CHAPTER IV

ADAPTIVE RELIABILITY-BASED SPLITTING ALGORITHMS FOR ORDERED SEQUENTIAL DETECTION

4.1 Introduction

A popular application of wireless sensor networks (WSNs) is distributed detection [12, 79], where a fusion center (FC) collects the nodes' local observations on the state of an event and processes them to make a global decision. Distributed detection schemes can generally be classified into fixed-sample-size (FSS) detection and the sequential detection. In FSS detection, the FC will not make a global decision until after collecting a predefined number of local observations. On the other hand, in sequential detection, the FC will sequentially compare a test statistic with a stopping rule, and decide whether to make a global decision or continue the collection process.

It is well known that a class of sequential detection strategies called *sequential probability ratio test* (SPRT) [80] requires, on average, a smaller number of observations than the FSS strategy does to achieve the same probabilities of false alarm and miss. The average number of observations required by the SPRT can be further reduced by incorporating an ordered-transmission strategy [13], where the FC collects the local observations in descending order of their reliabilities. This strategy has been applied in many scenarios [37, 94], where a transmission protocol to achieve the ordered-transmission strategy is not considered. However, under a bandwidth constraint (for example, a shared transmission channel), implementing an ordered-transmission strategy requires a proper channel access protocol.

One way to achieve an ordered-transmission strategy in a finite-bandwidth system

is to exploit a random access protocol. Many transmission protocols based on random access have been introduced for distributed detection that incorporates an ordered-transmission strategy [19, 44, 92, 93] . In [19, 92], the sensor nodes send their observations to the FC by using slotted ALOHA. A reliability-based splitting algorithm for time constrained distributed detection was proposed in [44]. A slotted-ALOHA protocol with a splitting-tree algorithm for ordering transmissions was introduced in [93].

In this chapter, we propose an ordered sequential detection based on a joint design of a reliability-based splitting algorithm [44], an ordered-transmission strategy [13], and an SPRT [80]. The proposed scheme divides the transmission channel into frames, where each frame consists of K time slots. At the beginning of each frame, the FC will sequentially update and announce a *reliability threshold*, which is used as an admission control. The reliability threshold will be updated in descending order such that the observations with the highest reliabilities would be collected earlier. Only nodes that have observation reliabilities larger than or equal to this reliability threshold and have not yet successfully sent their observations will attempt transmissions in this frame by using framed slotted ALOHA. At the end of each frame, the FC will decide whether to stop the collection process and make a global decision or to continue collecting more local observations. In addition, a set of suboptimal reliability thresholds is derived, and the proposed scheme's performance is evaluated.

The remainder of this chapter is organized as follows. The system model is provided in Section 4.2. We describe the proposed scheme in Section 4.3, where an algorithm to compute the reliability thresholds is derived in Section 4.4. The performance of the proposed scheme is shown and compared to other related schemes in Section 4.5. Finally, conclusions are given in Section 4.6.

4.2 System Model

We consider a distributed detection system with the following assumptions.

4.2.1 Centralized Fusion System

There are N sensor nodes deployed in an area to monitor events. The FC will broadcast an inquiry about an event of interest to start the data collection process. Each node will make an observation of this event; encapsulate it into a data packet; send it to the FC via a single-hop wireless channel; and, then, leave the collection process when its packet is sent successfully.[1] Note that we assume that the packet length is long enough that the effect of the observation quantization can be omitted. Furthermore, we do not consider the effect of channel errors here.

4.2.2 Transmission Channel

We assume that the sensor nodes share a transmission channel when sending their data packets to the FC. The channel is divided into time slots, where the FC and sensor nodes know when a time slot begins and ends (i.e., synchronous time). A data packet will be successfully sent to the FC in a time slot if it is the only packet transmitted in that slot; otherwise the slot is idle or a collision occurs. We assume that the collisions are solely from the transmissions of the nodes in the considered network. At the end of each transmission, the FC will send an acknowledgement packet to indicate whether a data packet was sent successfully or has collided with others. The length of each time slot is equal to the data packet length plus the acknowledgement packet length. Therefore, the FC and the nodes are able to monitor the activity on the channel.

[1] Specifically, each node has made one observation on the event of interest.

4.2.3 Binary Hypothesis Testing Model

We assume that the noisy observation at a sensor node, x, is governed by the following binary hypothesis model:

$$H_0 : \ x \sim f_X(x|H_0) \quad \text{and} \quad H_1 : \ x \sim f_X(x|H_1),$$

where $f_X(x|H_i)$ is the conditional probability density function (PDF) of x. The observations are assumed to be *independent and identically distributed* (IID) given H_i, for $i = 0, 1$. The prior probability that H_0 happens, $\Pr(H_0)$, is equal to ν.

4.2.4 Observation Reliability

In detection, the reliability of an observation x can be defined as the magnitude of the log-likelihood ratio (LLR) of x. Therefore, the observation reliability r of the observation x is equal to $\left|\log \frac{f_X(x|H_1)}{f_X(x|H_0)}\right|$. Given the reliabilities r_A and r_B, where $r_A \leq r_B$, let $\mathcal{X}(r_A, r_B)$ be the set of observations x whose reliabilities $r \in [r_A, r_B)$. Mathematically, we have

$$\mathcal{X}(r_A, r_B) = \left\{ x : r_A \leq \left| \log \frac{f_X(x|H_1)}{f_X(x|H_0)} \right| < r_B \right\}. \tag{52}$$

4.3 Ordered Sequential Detection Using a Reliability-Based Splitting Algorithm

In this section, we explain the details of the proposed scheme, which is a joint design of a reliability-based splitting algorithm [44], an ordered-transmission strategy [13], and an SPRT [80] to achieve ordered sequential detection in a random-access WSN. The reliability-based splitting algorithm allows the FC to collect the local observations in descending order of their reliabilities. As a result, the collection process will reach its stopping condition early. Since the reliability-based splitting algorithm is a random-access protocol, we apply a retransmission strategy to retrieve collided packets.

In the proposed scheme, the transmission channel that the sensor nodes will use to send their observations to the FC (as explained in Section 4.2.2) is divided into frames

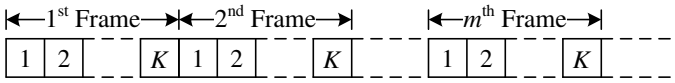

Figure 16: The transmission channel of the proposed scheme is divided into frames. Each frame consists of K time slots.

as shown in Fig. 16. Each frame consists of K time slots. At the beginning of each frame, the FC will decide to either stop the collection process and, then, make a global decision, or to continue the collection process with a new reliability threshold. If the FC continues the collection process, the nodes will follow the channel access protocol described in Section 4.3.1 to send their observations. The FC will decide whether to continue or stop the collection process based on the stopping rule in Section 4.3.2.

4.3.1 Channel Access Protocol - Reliability-Based Splitting Algorithm with Retransmissions

Assume that, at the beginning of the mth frame, that the FC decides to continue the data collection process, and then selects a reliability threshold $\hat{r}_m$, where $\hat{r}_m \leq \hat{r}_{m-1}$ and $\hat{r}_0 = \infty$. An algorithm to find a suitable reliability threshold $\hat{r}_m$ will be introduced in Section 4.4.2. The reliability threshold $\hat{r}_m$ is used as an admission control. Note that, after each node obtains its observation, it will compute the observation reliability as explained in Section 4.2.4. The nodes that have reliabilities $r \geq \hat{r}_m$, and have *not* yet successfully sent their data packets will attempt transmissions. These nodes will randomly choose one of K time slots in the mth frame to send their packets. As a result, the nodes that have successfully sent their packets to the FC will leave the collection process. On the other hand, the nodes that have experienced packet collisions will attempt retransmissions again in the next frame. Since we have $\ldots \leq \hat{r}_m \leq \ldots \leq \hat{r}_1 < \infty$, the FC almost receives the data packets in descending order of the observation reliabilities. Similar to many papers [92], [93], the reliability threshold $\hat{r}_m$ will be sent to the sensor nodes through an *additional* control channel.

4.3.2 Stopping Rule - Sequential Probability Ratio Test

Assume that the $(m-1)$st frame contains of $z_{S,m-1}$ successful time slots; equivalently, the FC has successfully received $z_{S,m-1}$ data packets. Let $\mathbf{x}_{z_{S,m-1}} = (x_{m-1,1}, x_{m-1,2}, \ldots, x_{m-1,z_{S,m-1}})$ be the corresponding observations in these packets. At the beginning of the mth frame, the FC will update the value of the LLR as

$$L_m = L_{m-1} + \sum_{j=1}^{z_{S,m-1}} \log \frac{f_X(x_{m-1,j}|H_1)}{f_X(x_{m-1,j}|H_0)}, \tag{53}$$

where L_{m-1} is the value of LLR at the beginning of the $(m-1)$st frame, and the summation in (53) is from the IID assumption on the observations in Section 4.2.3. Thereafter, the FC will make a decision by following the SPRT rule: if $L_m \leq A$, the FC announces H_0; if $L_m \geq B$, the FC announces H_1; and if $A < L_m < B$, the FC selects a reliability threshold $\hat{r}_m$, and continues collecting the data packets in the mth frame. The values of A and B are obtained from Wald's approximations [80]: $A \approx \log\left(\frac{P_{\text{Miss}}}{1-P_{\text{FA}}}\right)$ and $B \approx \log\left(\frac{1-P_{\text{Miss}}}{P_{\text{FA}}}\right)$, where P_{Miss} and P_{FA} are the desired probabilities of miss and false alarm, respectively. Assume that the FC terminates the collection process at the beginning of the Mth frame. The *collection time* is equal to $K(M-1)$ time slots, where $M = \min\{m \geq 1 : L_m \notin (A, B)\}$. The value M is an unknown random variable.

4.3.3 Lower Bound of the Average Collection Time

The following proposition provides a lower bound of the proposed scheme's average collection time (ACT).

Proposition 15. *Let r_{N_0} and r_{N_1} be the observation reliability values such that*

$$N \int_{x \in \mathcal{X}(r_{N_0}, \infty)} f_X(x|H_0) \log \frac{f_X(x|H_1)}{f_X(x|H_0)}\, dx \approx A, \tag{54}$$

$$N \int_{x \in \mathcal{X}(r_{N_1}, \infty)} f_X(x|H_1) \log \frac{f_X(x|H_1)}{f_X(x|H_0)}\, dx \approx B. \tag{55}$$

Let $N_0 = N\int_{x\in\mathcal{X}(r_{N_0},\infty)} f_X(x|H_0)\,dx$ *and* $N_1 = N\int_{x\in\mathcal{X}(r_{N_1},\infty)} f_X(x|H_1)\,dx$. *A lower bound of the proposed scheme's ACT is*

$$ACT_{LO,\ PS} = \frac{N_0 Pr(H_0) + N_1 Pr(H_1)}{\left(1-\frac{1}{K}\right)^{K-1}}. \tag{56}$$

Proof. A lower bound of the proposed scheme's ACT is obtained from the fact that the lowest ACT of the proposed scheme occurs when the FC collects the *smallest* number of observations such that $L_m \notin (A,\, B)$ with the *optimal* probability of successful transmission per time slot. As a result, this lower bound is obtained from the ACT of the oracle sequential detection divided by $\left(1-\frac{1}{K}\right)^{(K-1)}$. In the oracle sequential detection, the FC collects the observations in descending order of reliabilities. From *Wald's identity*, the average LLR given H_0 of the oracle sequential detection can be written as

$$\begin{aligned}
&\mathbb{E}\left\{\sum_{j=1}^{N_0}\log\frac{f_X(x_j|H_1)}{f_X(x_j|H_0)}\middle| x_j\in\mathcal{X}(r_{N_0},\infty), H_0\right\}\\
&\qquad= \mathbb{E}\left\{N_0\middle| x\in\mathcal{X}(r_{N_0},\infty), H_0\right\}\mathbb{E}\left\{\log\frac{f_X(x|H_1)}{f_X(x|H_0)}\middle| x\in\mathcal{X}(r_{N_0},\infty), H_0\right\},\\
&\qquad= N\int_{x\in\mathcal{X}(r_{N_0},\infty)} f_X(x|H_0)\,\log\frac{f_X(x|H_1)}{f_X(x|H_0)}\,dx.
\end{aligned} \tag{57}$$

Let r_{N_0} be the observation value such that (57) is approximately equal to A. We have N_0 defined in the proposition is the average number of observations required to obtain the average of LLR approximately equal to A when H_0 happens. The average number N_1 can be derived in a similar way. Therefore, a lower bound of the oracle sequential detection' ACT is equal to $N_0\mathrm{Pr}(H_0) + N_1\mathrm{Pr}(H_1)$, and, as a result, a lower bound of the proposed scheme's ACT can be shown as (56). □

4.4 Adaptive Reliability Threshold

The performance of the proposed scheme – i.e., the collection time – depends on the set of reliability thresholds used in the system. The set of optimal reliability thresholds can be derived from a dynamic programming algorithm, which will map

the system state to the optimal reliability threshold. However, since the system state of the proposed scheme (shown in Section 4.4.1) consists of many variables which are continuous or hidden, the computation of the optimal thresholds is highly complicated. Therefore, we propose a simple but efficient algorithm to derive suboptimal reliability thresholds instead. This algorithm, which is shown in Section 4.4.2, is based on the one-step look-ahead (1-SLA) rule. It will be shown in Section 4.5 that the collection time obtained by using the reliability thresholds from the 1-SLA rule is very close to the proposed scheme's optimal collection time.

4.4.1 System State and Evolution

In this section, we introduce the system state at the beginning of the mth frame, $\mathbf{s}_m$, of the proposed scheme, and study its evolution when a reliability threshold $\hat{r}_m$ is used. This relationship will be used to derive the suboptimal reliability threshold based on the 1-SLA rule in the next section. We define the system state at the beginning of the mth frame as $\mathbf{s}_m = (\tilde{b}_m, Y_m, \gamma_m, \nu_m)$. The entries of $\mathbf{s}_m$ are defined as follows: The variable $\tilde{b}_m$ is an estimate of the number of *backlogged* nodes[2] at the beginning of the mth frame. Note that the number of backlogged nodes is partially observable. The variable Y_m is the total number of *successful* nodes[3] up to the beginning of the mth frame. Specifically, $Y_m = \sum_{i=1}^{m-1} z_{S,i}$. The variable γ_m is the reliability threshold used in the previous frame, i.e., $\gamma_m = \hat{r}_{m-1}$. The variable ν_m is the posterior probability that H_0 happens given all previous successfully received observations. Note that, for $m = 1$, we have $\tilde{b}_1 = 0$, $Y_1 = 0$, $\gamma_1 = \infty$, and $\nu_1 = \nu$. In the rest of the chapter, for clarity, we will write a probability of random variables given the system state and reliability threshold in the conditional form. This will also be applied to the expectation.

[2]A backlogged node is the node who has attempted packet transmissions previously but experienced collisions.

[3]A successful node is the node who has the successful transmission.

At the beginning of the mth frame, assume that the system state is $\mathbf{s}_m = (\tilde{b}_m, Y_m, \gamma_m, \nu_m)$, and the FC continues the collection process using the reliability threshold $\hat{r}_m$. The system state evolution can be tracked as follows. In the mth frame, there will be $\tilde{b}_m + n_m$ nodes attempting transmissions, where n_m is the number of *new* active nodes[4]. Given the system state $\mathbf{s}_m$, the probability of n_m new active nodes when the reliability threshold $\hat{r}_m$ is used can be expressed as

$$f(n_m|\mathbf{s}_m, \hat{r}_m) = \nu_m\, f(n_m|\mathbf{s}_m^{(0)}, \hat{r}_m) + (1-\nu_m)\, f(n_m|\mathbf{s}_m^{(1)}, \hat{r}_m), \tag{58}$$

for $0 \le n_m \le N - \tilde{b}_m - Y_m$, where $\mathbf{s}_m^{(i)} = (\tilde{b}_m, Y_m, \gamma_m, H_i)$, for $i = 0, 1$, and the conditional probability of the number of new active nodes is equal to

$$f(n_m|\mathbf{s}_m^{(i)}, \hat{r}_m) = \binom{N - \tilde{b}_m - Y_m}{n_m} q^{n_m} (1-q)^{(N-\tilde{b}_m - Y_m - n_m)}, \tag{59}$$

where $q = \int_{x \in \mathcal{X}(\hat{r}_m, \gamma_m)} f_X(x|H_i)\, dx$ and $\mathcal{X}(\hat{r}_m, \gamma_m)$ is defined in (52).

These $\tilde{b}_m + n_m$ nodes will randomly choose one of K time slots to send their data packets. Because of the random access scheme, a frame will consist of successful time slots, idle time slots, and collision time slots. Let $z_{S,m}$, $z_{I,m}$, and $z_{C,m}$ be the numbers of successful time slots, idle time slots, and collision time slots, respectively, in the mth frame, where $z_{S,m} + z_{I,m} + z_{C,m} = K$. Note that the number of successful nodes (or packets) in this frame is also equal to $z_{S,m}$. The joint probability that there are $z_{S,m}$ successful time slots and $z_{I,m}$ idle time slots given the number of active nodes $\tilde{b}_m + n_m$ is equal to

$$f(z_{S,m}, z_{I,m}|\tilde{b}_m + n_m) = f(z_{I,m}|z_{S,m}, \tilde{b}_m + n_m)\, f(z_{S,m}|\tilde{b}_m + n_m), \tag{60}$$

for $0 \le z_{S,m} + z_{I,m} \le K$, $0 \le z_{S,m} \le \min\big(K, \tilde{b}_m + n_m\big)$, $0 \le z_{I,m} \le K$, and we

[4]A new active node is the node who will send its packet for the first time or, specifically, a node who has reliability $r \in [\hat{r}_m, \gamma_m)$, where, $\hat{r}_m \le \gamma_m$.

have [31, p. 102 and p. 112]

$$f(z_{S,m}|\tilde{b}_m+n_m)=\frac{(-1)^{z_{S,m}}K!(\tilde{b}_m+n_m)!}{z_{S,m}!K^{(\tilde{b}_m+n_m)}}\sum_{i\geq z_{S,m}}^{\min(K,\tilde{b}_m+n_m)}\frac{(-1)^i(K-i)^{(\tilde{b}_m+n_m-i)}}{(i-z_{S,m})!(K-i)!(\tilde{b}_m+n_m-i)!},\tag{61}$$

$$f(z_{I,m}|z_{S,m},\tilde{b}_m+n_m)=\binom{K-z_{S,m}}{z_{I,m}}\sum_{i=0}^{z_{C,m}}(-1)^i\binom{z_{C,m}}{i}\Big(1-\frac{z_{I,m}+i}{K-z_{S,m}}\Big)^{(\tilde{b}_m+n_m)},\tag{62}$$

where $z_{C,m}=K-z_{S,m}-z_{I,m}$. We use $z_{C,m}$ in (62) for brevity.

Assume that we have $z_{S,m}$ successful time slots and $z_{I,m}$ idle time slots during the mth frame. Furthermore, let the vector $\mathbf{x}_{z_{S,m}}=(x_{m,1},x_{m,2},\ldots,x_{m,z_{S,m}})$ be the corresponding observations in the successfully received packets. At the beginning of the $(m+1)$st frame, the FC will update the system state $\mathbf{s}_{m+1}=(\tilde{b}_{m+1},Y_{m+1},\gamma_{m+1},\nu_{m+1})$ as follows. The total number of successful nodes is $Y_{m+1}=Y_m+z_{S,m}$. The value of γ_{m+1} is equal to $\hat{r}_m$, by the definition. The posterior probability ν_{m+1}, which is defined as $\Pr(H_0|\mathbf{x}_{z_{S,1}},\ldots,\mathbf{x}_{z_{S,m}})$, can be computed recursively as [9, p. 266]

$$\nu_{m+1}=\frac{\nu_m f_X(\mathbf{x}_{z_{S,m}}|H_0)}{\nu_m f_X(\mathbf{x}_{z_{S,m}}|H_0)+(1-\nu_m)f_X(\mathbf{x}_{z_{S,m}}|H_1)},\tag{63}$$

where $f_X(\mathbf{x}_{z_{S,m}}|H_i)=f_X(x_{m,1}|H_i)\cdots f_X(x_{m,z_{S,m}}|H_i)$, for $i=0,1$, because of the IID assumption in Section 4.2.3.

To compute an estimate of the number of backlogged nodes, $\tilde{b}_{m+1}$, we have to update the belief vector $\boldsymbol{\beta}_{m+1}$, which consists of $\beta_{m+1}(b)$, where $b\in\mathcal{B}_{m+1}$ and $\mathcal{B}_{m+1}=\{2z_{C,m},\,2z_{C,m}+1,\ldots,N-Y_m-z_{S,m}\}$, i.e., $\boldsymbol{\beta}_{m+1}=\big(\beta_{m+1}(2z_{C,m}),\beta_{m+1}(2z_{C,m}+1),\ldots,\beta_{m+1}(N-Y_m-z_{S,m})\big)$. The support of b starts from $2z_{C,m}$ because a collision time slot is from at least two nodes sending their packets in this time slot. The value $\beta_{m+1}(b)$ is the posterior probability that the number of backlogged nodes is equal to b at the beginning of the $(m+1)$st frame given the previous $\mathbf{z}_i=(z_{S,i},z_{I,i})$, for $i=1,\ldots,m$. The value of $\beta_{m+1}(b)$ is computed sequentially as [28]

$$\beta_{m+1}(b)=\frac{\sum_{j\in\mathcal{B}_m}\Pr\big(b_{m+1}=b,\mathbf{z}_m=(z_{S,m},z_{I,m})|b_m=j,Y_m,\gamma_m,\nu_{m+1},\hat{r}_m\big)\beta_m(j)}{\sum_{b\in\mathcal{B}_{m+1}}\sum_{j\in\mathcal{B}_m}\Pr\big(b_{m+1}=b,\mathbf{z}_m=(z_{S,m},z_{I,m})|b_m=j,Y_m,\gamma_m,\nu_{m+1},\hat{r}_m\big)\beta_m(j)},\tag{64}$$

where

$$\begin{aligned}
&\Pr\big(b_{m+1}=b, \mathbf{z}_m=(z_{S,m},z_{I,m})|b_m=j, Y_m, \gamma_m, \nu_{m+1}, \hat{r}_m\big)\\
&\quad=\Pr\big(n_m+j-z_{S,m}=b, \mathbf{z}_m=(z_{S,m},z_{I,m})|b_m=j, Y_m, \gamma_m, \nu_{m+1}, \hat{r}_m\big),\\
&\quad=f(z_{S,m},z_{I,m}|b+z_{S,m})\Pr(n_m=b+z_{S,m}-j|b_m=j, Y_m, \gamma_m, \nu_{m+1}, \hat{r}_m). \qquad (65)
\end{aligned}$$

The probability (65) is derived from the evolution of the number of backlogged nodes: $b_{m+1}=b_m+n_m-z_{S,m}$. The probability $\Pr(n_m=b+z_{S,m}-j|b_m=j, Y_m, \gamma_m, \nu_{m+1}, \hat{r}_m)$ can be obtained from (58), where ν_{m+1} is used instead of ν_m. Therefore, we can estimate the number of backlogged nodes at the beginning of the $(m+1)$th frame as $\tilde{b}_{m+1}=\big\lceil \sum_{b\in\mathcal{B}_{m+1}} b\,\beta_{m+1}(b)\big\rceil$, where $\lceil\cdot\rceil$ is the ceiling function.

4.4.2 One-Step Look-Ahead Rule

In this section, we will find the reliability threshold $\hat{r}_m$ by using a simple strategy based on the 1-SLA rule. Assume that, at the beginning of the mth frame, where the system state is $\mathbf{s}_m$, the FC decides to continue the collection process, i.e., $L_m\in(A,\,B)$. From the 1-SLA perspective, the FC will sequentially select the reliability threshold $\hat{r}_m$ that maximizes the expectation of the difference $\big|L_{m+1}-L_m\big|$. Therefore, given the system state $\mathbf{s}_m$, the reliability threshold $\hat{r}_m$ can be obtained from

$$\begin{aligned}
&\max_{\hat{r}_m\le\gamma_m}\mathbb{E}\left\{\left|\sum_{j=1}^{z_{S,m}}\log\frac{f_X(x_{m,j}|H_1)}{f_X(x_{m,j}|H_0)}\right|\,\middle|\,\mathbf{s}_m,\hat{r}_m\right\}\\
&\qquad=\max_{\hat{r}_m\le\gamma_m}\left[(1-\nu_m)\,\mathbb{E}\left\{\sum_{j=1}^{z_{S,m}}\log\frac{f_X(x_{m,j}|H_1)}{f_X(x_{m,j}|H_0)}\,\middle|\,\mathbf{s}_m^{(1)},\hat{r}_m\right\}\right.\\
&\qquad\qquad\left.-\,\nu_m\,\mathbb{E}\left\{\sum_{j=1}^{z_{S,m}}\log\frac{f_X(x_{m,j}|H_1)}{f_X(x_{m,j}|H_0)}\,\middle|\,\mathbf{s}_m^{(0)},\hat{r}_m\right\}\right]. \qquad (66)
\end{aligned}$$

The expression in (66) is obtained from the fact that the conditional expectation given H_1 is positive, while the conditional expectation given H_0 is negative.

By using the IID assumption on the observations in Section 4.2.3 and Wald's

identity, the expectations in (66) can be expressed as

$$\mathbb{E}\Big\{ \sum_{j=1}^{z_{S,m}} \log \frac{f_X(x_{m,j}|H_1)}{f_X(x_{m,j}|H_0)} \,\Big|\, \mathbf{s}_m^{(i)}, \hat{r}_m \Big\}$$
$$= \mathbb{E}\Big\{ z_{S,m} \big| \mathbf{s}_m^{(i)}, \hat{r}_m \Big\} \mathbb{E}\Big\{ \log \frac{f_X(x|H_1)}{f_X(x|H_0)} \Big| \mathbf{s}_m^{(i)}, \hat{r}_m \Big\}, \tag{67}$$

for $i = 0, 1$. The first term is the expected number of successfully received observations, while the second term is related to the Kullback - Leibler (KL) divergence given $\mathbf{s}_m^{(i)}$ and $\hat{r}_m$. For the first term in (67), we can show that

$$\mathbb{E}\big\{ z_{S,m} \big| \mathbf{s}_m^{(i)}, \hat{r}_m \big\} = \mathbb{E}\Big\{ \mathbb{E}\{ z_{S,m} | n_m \} \Big| \mathbf{s}_m^{(i)}, \hat{r}_m \Big\}$$
$$= \mathbb{E}\left\{ \big(\tilde{b}_m + n_m\big) \Big(1 - \frac{1}{K}\Big)^{\left(\tilde{b}_m + n_m - 1\right)} \Big| \mathbf{s}_m^{(i)}, \hat{r}_m \right\}, \tag{68}$$

where $\mathbb{E}\big\{(\cdot)\big|\mathbf{s}_m^{(i)}, \hat{r}_m\big\}$ on the second line is the conditional expectation with respect to n_m, and the conditional probability $p(n_m|\mathbf{s}_m^{(i)}, \hat{r}_m)$ is shown in (59). The derivation of $\mathbb{E}\{z_{S,m}|n_m\} = \big(\tilde{b}_m + n_m\big)\Big(1 - \frac{1}{K}\Big)^{\left(\tilde{b}_m + n_m - 1\right)}$ can be found in Appendix B.

To compute the second term in (67), we need the conditional probability $p(x|\mathbf{s}_m^{(i)}, \hat{r}_m)$, which is quite complicated since a successfully received observation x in this frame might be from a backlogged node or a new active node. To overcome this problem, we apply the following assumption.

Assumption 3. *The successfully received observations are from the new active nodes. Specifically, we assume that* $x \in \mathcal{X}(\hat{r}_m, \gamma_m)$. □

Note that, by using Assumption 3, we underestimate the second term in (67). However, this gap will be decreased as the number of backlogged nodes decreases. As a result, we have

$$\mathbb{E}\Big\{ \log \frac{f_X(x|H_1)}{f_X(x|H_0)} \Big| \mathbf{s}_m^{(i)}, \hat{r}_m \Big\} = \mathbb{E}\Big\{ \log \frac{f_X(x|H_1)}{f_X(x|H_0)} \Big| H_i, x \in \mathcal{X}(\hat{r}_m, \gamma_m) \Big\}.$$

The conditional expectation $\mathbb{E}\big\{ \cdot \,\big|H_i, x \in \mathcal{X}(\hat{r}_m, \gamma_m)\big\}$ is with respect to x, whose conditional PDF is equal to $f_X(x|H_i) \big/ \int_{x \in \mathcal{X}(\hat{r}_m, \gamma_m)} f_X(x|H_i)\, dx$, for $x \in \mathcal{X}(\hat{r}_m, \gamma_m)$.

A summary of the proposed scheme's procedures is shown in Algorithm 1:

Algorithm 1 Proposed Scheme

1. m=1.
2. At the beginning of the mth frame, given the system state $\mathbf{s}_m$, find the reliability threshold $\hat{r}_m$ from the **1-SLA rule** shown in (66).
3. Follow the **channel access protocol** described in Section 4.3.1.
4. At the end of the mth frame, given $z_{S,m}$, $z_{I,m}$ and $\mathbf{x}_{z_{S,m}}$, update the system state to $\mathbf{s}_{m+1}$ as shown in Section 4.4.1 and the LLR value L_{m+1} in (53).
5. Follow the **stopping rule** in Section 4.3.2: if $L_{m+1} \notin (A,\ B)$, stop the collection process and announce the corresponding H_i, for $i = 0, 1$; otherwise, set $m = m + 1$ and go to Step 2).

4.5 Numerical Results

We use the following shift-in-mean model to evaluate the average collection time of the proposed scheme: $H_0 : x = \eta$, and $H_1 : x = \mu + \eta$, where μ is a constant and η is a Gaussian random variable with mean and variance equal to zero and σ^2, respectively. The prior probabilities $\Pr(H_0)$ and $\Pr(H_1)$ are set to $\frac{1}{2}$. The reliability of the observation x is $\left|\log \frac{f_X(x|H_1)}{f_X(x|H_0)}\right| = \frac{\mu}{\sigma^2}\left|x - \frac{\mu}{2}\right|$. Without loss of generality, in this case, we define the reliability of the observation x as $r = \left|x - \frac{\mu}{2}\right|$, i.e., we omit the scaling factor. Therefore, we have $\mathcal{X}(\hat{r}_m, \gamma_m) = \left(\frac{\mu}{2} - \gamma_m,\ \frac{\mu}{2} - \hat{r}_m\right] \cup \left[\frac{\mu}{2} + \hat{r}_m,\ \frac{\mu}{2} + \gamma_m\right)$. Since the PDF $f_X(x|H_1)$ is a shifted-version of the PDF $f_X(x|H_0)$, and the PDF $f_X(x|H_i)$ is symmetric about its mean, (66) is reduced to

$$\max_{\hat{r}_m \le \gamma_m} \mathbb{E}\left\{ \sum_{j=1}^{z_{S,m}} \log \frac{f_X(x_{m,j}|H_1)}{f_X(x_{m,j}|H_0)} \,\middle|\, \mathbf{s}_m^{(1)}, \hat{r}_m \right\},$$

where the expectation can be obtained from (67).

In Fig. 17, we compare the average collection times (ACTs) required by the proposed scheme ($K = 5$), a conventional SPRT scheme, the oracle SPRT scheme, and the proposed scheme's lower bound for various σ^2. The system is set up as follows:

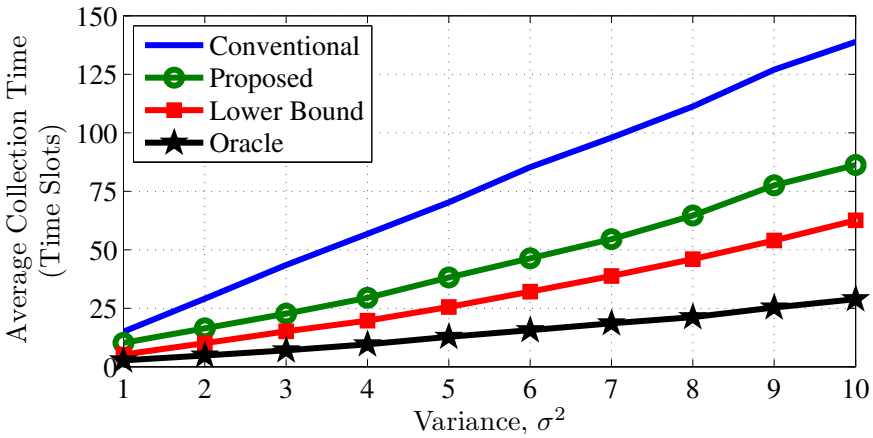

Figure 17: The average collection times of the proposed scheme, the conventional SPRT scheme, the oracle scheme, and the proposed scheme's lower bound for various σ^2. Other parameters are: $N = 500$, $P_{\text{FA}} = P_{\text{Miss}} = 0.001$, $\mu = 1$, $K = 5$.

$N = 500$ nodes,[5] $P_{\text{FA}} = P_{\text{Miss}} = 0.001$, and $\mu = 1$. In the conventional SPRT scheme, the local observations are sent to the FC in *random* order of the reliabilities, while, in the oracle SPRT scheme, the local observations are sent to the FC in *descending* order of the reliabilities. For both schemes, at the end of each time slot, the FC will update the LLR upon the received observation and follow the SPRT rule. There are no packet collisions in these two schemes. The lower bound of the proposed scheme's ACT ($K = 5$) is obtained from (56).

In Fig. 17, when we compare the ACTs between the proposed scheme and the conventional SPRT scheme, the result shows that the proposed scheme significantly outperforms the conventional SPRT scheme, even though the proposed scheme experiences packet collisions. The improvement gap increases as we increase the noise variance because the proposed scheme collects only the most reliable observations. Recall that the proposed scheme uses the suboptimal reliability threshold derived from (66). However, we can see that the ACT of the proposed scheme using even this suboptimal reliability threshold is close to the lower-bound ACT that the proposed

[5]To avoid the situation where the LLR L_m in (53) is still between A and B even all nodes have successfully sent their observations to the FC, we study the proposed scheme when N is large.

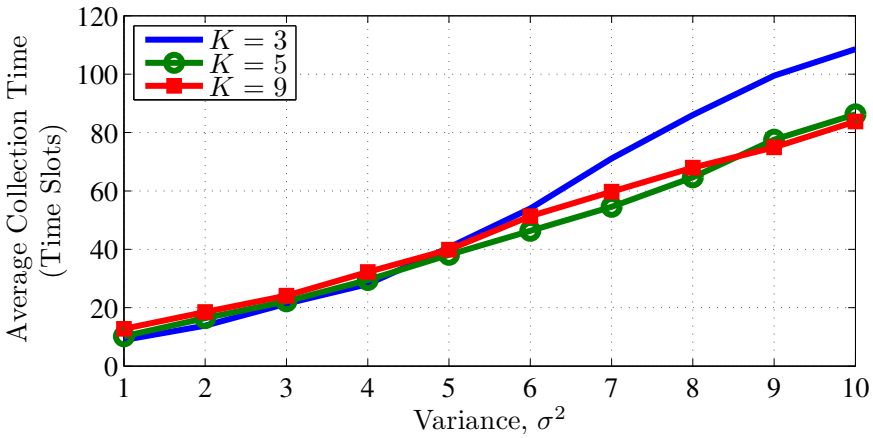

Figure 18: The average collection times of the proposed scheme for $K = 3, 5, 9$. Other parameters are: $N = 500$, $P_{\text{FA}} = P_{\text{Miss}} = 0.001$, $\mu = 1$.

scheme can achieve. The oracle scheme's ACT, shown as a reference, when perfect scheduling allows the FC to collect the local observations in perfectly descending order and without collisions or idle slots.

The variable K affects the proposed scheme's ACT on three aspects. First, a large K helps to estimate the current backlogged nodes $\tilde{b}_m$ more precisely. Second, a large K helps to resolve collisions when the actual active nodes in the current frame are larger than expected. Third, since the proposed scheme can stop the collection process only at the end of a frame, a large K introduces additional time slots to the proposed scheme's ACT. A tradeoff among these aspects is shown in Fig. 18, where the proposed scheme's ACTs for $K = 3, 5, 9$ are compared. When the noise variance σ^2 is small, only a few observations are required to stop the collection process. Therefore, for example, the proposed scheme with $K = 3$ gives the lowest ACT when $\sigma^2 = 1$. On the other hand, when the noise variance σ^2 is large, a long collection process is required to collect a large number of observations. There are a lot of chances that the actual active nodes will be larger than expected. The proposed scheme with a larger K will experience a lower effect of collisions than the proposed scheme with a smaller K does. As a result, the proposed schemes with $K = 5, 9$ outperform the proposed scheme with $K = 3$ when σ^2 is large.

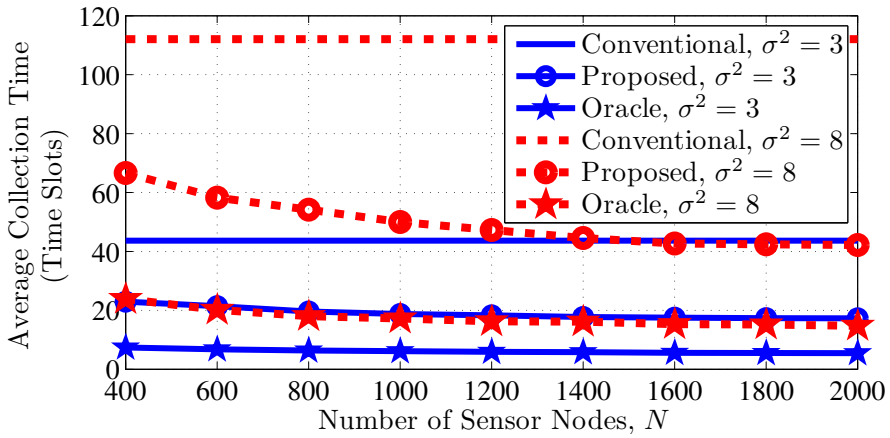

Figure 19: The average collection times of the proposed scheme, the conventional SPRT scheme, the oracle scheme for $\sigma^2 = 3$, $\sigma^2 = 8$, and various N. Other parameters are: $P_{\text{FA}} = P_{\text{Miss}} = 0.001$, $K = 5$, $\mu = 1$.

In Fig. 19, we plot the ACTs of the proposed scheme and the conventional SPRT scheme versus N for $\sigma^2 = 3$ and $\sigma^2 = 8$. The other parameters are set up as follows: $P_{\text{FA}} = P_{\text{Miss}} = 0.001$, $K = 5$ time slots, and $\mu = 1$. The ACT of the oracle scheme is also shown as a reference. Unlike the conventional SPRT scheme, the proposed scheme has an advantage when N increases because more nodes will have highly reliable observations. The improvement by increasing N is quite significant when σ^2 is large.

4.6 Conclusion

We proposed an ordered sequential detection scheme for large, single-hop WSNs. Under the considered scenarios, the numerical results showed that the proposed scheme significantly outperforms the conventional SPRT scheme. Furthermore, even though the proposed scheme uses a set of suboptimal reliability thresholds, the corresponding ACT is just slightly higher than its lower-bound ACT. Since slotted ALOHA is used as the transmission protocol, the proposed scheme experiences packet collisions. In fact, these collisions might infer some useful information on which hypothesis is happening. We will study how to exploit collisions to improve the proposed scheme's

performance in the next chapter. In addition, the framework of the proposed scheme can be extended to other applications such as estimation and tracking. The proposed scheme is also applicable to a WSN consisting of a small number of nodes; however, a modification is needed to avoid the situation where the observations run out before a decision is made. In this case, each sensor node should make and report a new observation after a maximum collection time has expired.

CHAPTER V

ADAPTIVE RELIABILITY-BASED SPLITTING ALGORITHMS WITH COLLISION INFERENCE FOR ORDERED SEQUENTIAL DETECTION

5.1 Introduction

An important application of wireless sensor networks (WSNs) is distributed detection [12, 79], where a fusion center (FC) collects the sensor nodes' local observations on the state of an event and processes them to make a global decision. Since it requires, on average, a smaller number of observations than a fixed-sample-size strategy does to achieve a level of confidence, a sequential probability ratio test (SPRT) [80] has been studied extensively in distributed detection [77, 95]. The average number of observations required by an SPRT scheme can be further reduced by incorporating an ordered-transmission strategy [13]. In such strategy, the FC collects the observations in descending order of their reliabilities, where the reliability of an observation is the magnitude of the log-likelihood ratio (LLR). To implement an ordered-transmission strategy in the presence of a bandwidth constrained channel, such as a single-transmission channel, a proper channel access protocol must be developed.

Random access protocols offer one way to achieve an ordered-transmission strategy in a finite-bandwidth system [19,44,92,93]. An inherent property of these protocols is, of course, transmission collisions. Generally, the collisions are treated as transmission errors and a retransmission strategy is exploited to retrieve the collided packets. Unfortunately, retransmissions consume both additional time and energy. On the other hand, in detection, these collisions might provide information about the event of interest.

In this chapter, we design an ordered sequential detection algorithm in which the FC is able to exploit the information in collisions to make a global decision. The proposed scheme combines a reliability-based splitting algorithm [44], an ordered-transmission strategy [13], and an SPRT [80]. The transmission channel's time is divided into frames – each frame consists of *two* subframes and each subframe consists of K time slots. At the beginning of each frame, the FC will sequentially update and announce a *reliability threshold* that is used as an admission control. The reliability threshold will be lowered with successive frames such that the observations with the highest reliabilities are collected first. Only the nodes that have observation reliabilities between the current reliability threshold and the previous reliability threshold will attempt transmissions in the current frame, using a framed version of slotted ALOHA. Nodes with a *negative* LLR will send their observations in the first subframe, while the nodes with a *positive* LLR will send their observations in the second subframe. These nodes will leave the collection process after sending their observations to the FC; there are no retransmissions. By designing the proposed scheme in this way, the FC is able to partially retrieve observations in the collided packets. At the end of each frame, based on the successfully received observations and these partially retrieved observations, the FC will decide whether to make a global decision or to continue collecting more local observations. We derive a set of good but suboptimal set of reliability thresholds for the sequence of frames and evaluate the performance of the proposed scheme.

The remainder of this chapter is organized as follows. The system model is provided in Section 5.2. We describe the proposed scheme in Section 5.3, where an algorithm to compute the reliability thresholds is derived in Section 5.4. The performance of the proposed scheme is shown and compared to other related schemes in Section 5.5. Finally, conclusions are given in Section 5.6.

5.2 System Model

We consider a distributed detection system with the following assumptions.

5.2.1 Centralized Fusion System

There are N sensor nodes deployed in an area to monitor events. The FC will broadcast an inquiry about an event of interest to start the data collection process. Each node will make an observation of this event, encapsulate it into a data packet, send it to the FC via a single-hop wireless channel, and then leave the collection process after it has transmitted its packet.[1] Note that we assume that the packet length is long enough that the effect of the observation's quantization can be omitted. Furthermore, we do not consider the effect of channel errors.

5.2.2 Transmission Channel

We assume that the sensor nodes share a transmission channel when sending their data packets to the FC. The channel is divided into time slots, where the FC and sensor nodes know when a time slot begins and ends (i.e., synchronous). A data packet will be successfully sent to the FC in a time slot if it is the only packet transmitted in that slot; otherwise the slot is idle or a collision occurs.[2] At the end of each transmission, the FC will send an acknowledgement packet to indicate whether a data packet was sent successfully or has collided with others.[3] The length of each time slot is equal to the data packet length plus the acknowledgement packet length. Therefore, the FC and the nodes are able to monitor the activity on the channel.

[1] Specifically, each node makes one observation on the event of interest.

[2] We assume that the collisions are solely from the transmissions of the nodes in the considered network.

[3] Since there are no retransmissions in the proposed scheme, this is an option.

5.2.3 Binary Hypothesis Testing Model

We assume that the noisy observation at a sensor node, x, is governed by the following binary hypothesis model:

$$H_0: \ x \sim f_X(x|H_0) \quad \text{and} \quad H_1: \ x \sim f_X(x|H_1),$$

where $f_X(x|H_i)$ is the conditional probability density function (PDF) of x. The observations are assumed to be *independent and identically distributed* (IID) given H_i, for $i = 0, 1$. The prior probability that H_0 happens, $\Pr(H_0)$, is equal to ν.

5.2.4 Observation Reliability

In detection, the reliability of an observation x can be defined as the magnitude of the log-likelihood ratio (LLR) of x. Therefore, the observation reliability r of the observation x is equal to $\left|\log \frac{f_X(x|H_1)}{f_X(x|H_0)}\right|$. Given the reliabilities r_A and r_B, where $r_A \leq r_B$, let $\mathcal{X}^{(-)}(r_A, r_B)$ be the set of observations x whose $\log \frac{f_X(x|H_1)}{f_X(x|H_0)} \in (-r_B, -r_A]$, and let $\mathcal{X}^{(+)}(r_A, r_B)$ be the set of observations x whose $\log \frac{f_X(x|H_1)}{f_X(x|H_0)} \in [r_A, r_B)$. Mathematically, we have

$$\begin{aligned} \mathcal{X}^{(-)}(r_A, r_B) &= \left\{ x : -r_B < \log \frac{f_X(x|H_1)}{f_X(x|H_0)} \leq -r_A \right\}, \\ \mathcal{X}^{(+)}(r_A, r_B) &= \left\{ x : r_A \leq \log \frac{f_X(x|H_1)}{f_X(x|H_0)} < r_B \right\}. \end{aligned} \tag{69}$$

5.3 Proposed Ordered Sequential Detection Algorithm

In this section, we explain the details of the proposed scheme, which combines a reliability-based splitting algorithm [44], an ordered-transmission strategy [13], and an SPRT [80] to achieve ordered sequential detection in a random-access WSN. The reliability-based splitting algorithm allows the FC to collect the local observations in descending order of their reliability. As a result, the collection process will reach its stopping condition earlier. The proposed scheme divides the transmission channel that the sensor nodes use to send their observations to the FC into frames, as shown

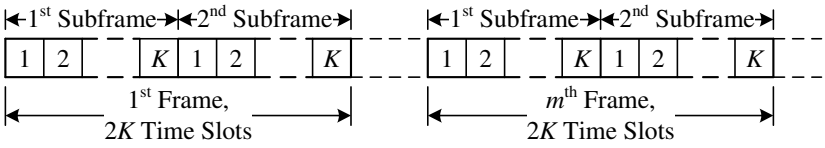

Figure 20: The transmission channel of the proposed scheme is divided into frames. Each frame is further divided into two subframes called the first and second subframes. Each subframe consists of K time slots.

in Fig. 20. Each frame is further divided into two subframes, where each subframe consists of K time slots. At the beginning of each frame, the FC will decide to either stop the collection process and make a global decision, or to continue the collection process with a new reliability threshold. If the FC continues the collection process, the nodes will follow the channel access protocol described in Section 5.3.1 to send their observations. The FC will decide whether to continue or stop the collection process based on the stopping rule in Section 5.3.2. We will show in Section 5.3.1 that *there is information in packet collisions* as well as in successful transmissions. In Section 5.3.2 we show how the FC can use the number of packet collisions in making a global decision.

5.3.1 Channel Access Protocol - Reliability-Based Splitting Algorithm

Assume that, at the beginning of the mth frame, the FC decides to continue the data collection process. It then selects a reliability threshold $\hat{r}_m$, where $\hat{r}_m \leq \hat{r}_{m-1}$ and $\hat{r}_0 = \infty$. An algorithm to find a suitable reliability threshold $\hat{r}_m$ will be introduced in Section 5.4.2.

The reliability threshold $\hat{r}_m$ is used as an admission control. The nodes that have the observations $x \in \mathcal{X}^{(-)}(\hat{r}_m, \hat{r}_{m-1})$ defined in (69) will send their packets in the *first* subframe. Each of these nodes will randomly choose one of the K time slots to send its packet, and leave the collection process afterward. On the other hand, the nodes that have the observations $x \in \mathcal{X}^{(+)}(\hat{r}_m, \hat{r}_{m-1})$ defined in (69) will send their packets in the *second* subframe. Each of these nodes will randomly choose one of the K time

slots to send its packet, and leave the collection process afterward. Note that there are no retransmissions. Similar to many papers [92], [93], the reliability threshold $\hat{r}_m$ will be sent to the sensor nodes through an *additional* control channel or at the end of each frame.

According to the transmission protocol above, we can partially retrieve observations involved in collisions. Given a collision, we know that: a) there are at least two packets sent in this time slot; b) if the collision is in a slot in the first subframe, the collided packets will contain observations $x \in \mathcal{X}^{(-)}(\hat{r}_m, \hat{r}_{m-1})$; c) if the collision is in a slot in the second subframe, the collided packets will contain observations $x \in \mathcal{X}^{(+)}(\hat{r}_m, \hat{r}_{m-1})$. Therefore, we can make the following inference from a collision time slot.

Assumption 4 (Collision Inference)**.** *We can approximate the observations in the collision time slots as follows. Assume that there are $z_{C,m}^{(-)}$ collision time slots in the first subframe, and $z_{C,m}^{(+)}$ collision time slots in the second subframe. There will be (at least) $2z_{C,m}^{(-)}$ packets collided at the first subframe, and $2z_{C,m}^{(+)}$ packets collided at the second subframe. Let $\tilde{\mathbf{x}}_{z_{C,m}}$ be the vector of the retrieved observations from the collided packets in the mth frame. We have*

$$\tilde{\mathbf{x}}_{z_{C,m}} = (\underbrace{\tilde{x}_m^{(-)}, \ldots, \tilde{x}_m^{(-)}}_{2z_{C,m}^{(-)}}, \underbrace{\tilde{x}_m^{(+)}, \ldots, \tilde{x}_m^{(+)}}_{2z_{C,m}^{(+)}}), \tag{70}$$

where $\tilde{x}_m^{(-)}$ is the least *reliable observation in $\mathcal{X}^{(-)}(\hat{r}_m, \hat{r}_{m-1})$, while $\tilde{x}_m^{(+)}$ is the* least *reliable observation in $\mathcal{X}^{(+)}(\hat{r}_m, \hat{r}_{m-1})$. Equivalently, $\tilde{x}_m^{(-)}$ is the value of $x \in \mathcal{X}^{(-)}(\hat{r}_m, \hat{r}_{m-1})$ such that $\log \frac{f_X(x|H_1)}{f_X(x|H_0)} = -\hat{r}_m$. If there are many values satisfying this condition, we just choose one. Similarly, $\tilde{x}_m^{(+)}$ is the value of $x \in \mathcal{X}^{(+)}(\hat{r}_m, \hat{r}_{m-1})$ such that $\log \frac{f_X(x|H_1)}{f_X(x|H_0)} = \hat{r}_m$.* □

5.3.2 Stopping Rule - Sequential Probability Ratio Test

Assume that the $(m-1)$st frame consists of $z^{(-)}_{S,m-1}$ successful time slots in the first subframe, $z^{(+)}_{S,m-1}$ successful time slots in the second subframe, $z^{(-)}_{C,m-1}$ collision time slots in the first subframe, and $z^{(+)}_{C,m-1}$ collision time slots in the second subframe. Let the observation vector $\mathbf{x}_{z_{S,m-1}}$ consist of the corresponding observations in the successful time slots. Therefore, we have $\mathbf{x}_{z_{S,m-1}}$ as

$$\big(x^{(-)}_{m-1,1}, \ldots, x^{(-)}_{m-1,z^{(-)}_{S,m-1}}, x^{(+)}_{m-1,1}, \ldots, x^{(+)}_{m-1,z^{(+)}_{S,m-1}} \big), \tag{71}$$

where $x^{(-)}_{m-1,j}$ is the observation in a successful time slot in the first subframe and $x^{(+)}_{m-1,j}$ is the observation in a successful time slot in the second subframe. Furthermore, let the observation vector $\tilde{\mathbf{x}}_{z_{C,m-1}}$ be the retrieved observations defined in (70) from the collision time slots. At the beginning of the mth frame, the FC will update the value of the LLR as

$$\begin{aligned} L_m &= \Upsilon(L_{m-1}, \mathbf{x}_{z_{S,m-1}}, \tilde{\mathbf{x}}_{z_{C,m-1}}) \\ &= L_{m-1} + \sum_{j=1}^{z^{(-)}_{S,m-1}} \log \frac{f_X(x^{(-)}_{m-1,j}|H_1)}{f_X(x^{(-)}_{m-1,j}|H_0)} + \sum_{j=1}^{z^{(+)}_{S,m-1}} \log \frac{f_X(x^{(+)}_{m-1,j}|H_1)}{f_X(x^{(+)}_{m-1,j}|H_0)} \\ &\qquad + 2\hat{r}_m \Big(z^{(+)}_{C,m-1} - z^{(-)}_{C,m-1} \Big), \end{aligned} \tag{72}$$

where L_{m-1} is the value of LLR at the beginning of the $(m-1)$st frame, and the summation in (72) is from the IID assumption on the observations in Section 5.2.3. The last term is obtained from the LLR of the retrieved observations $\tilde{\mathbf{x}}_{z_{C,m-1}}$:

$$\sum_{j=1}^{2z^{(-)}_{C,m-1}} \log \frac{f_X(\tilde{x}^{(-)}_{m-1,j}|H_1)}{f_X(\tilde{x}^{(-)}_{m-1,j}|H_0)} + \sum_{j=1}^{2z^{(+)}_{C,m-1}} \log \frac{f_X(\tilde{x}^{(+)}_{m-1,j}|H_1)}{f_X(\tilde{x}^{(+)}_{m-1,j}|H_0)}.$$

From Assumption 4, where, for all j, $\log \frac{f_X(\tilde{x}^{(-)}_{m-1,j}|H_1)}{f_X(\tilde{x}^{(-)}_{m-1,j}|H_0)} = -\hat{r}_m$ and $\log \frac{f_X(\tilde{x}^{(+)}_{m-1,j}|H_1)}{f_X(\tilde{x}^{(+)}_{m-1,j}|H_0)} = \hat{r}_m$, we have the last term in (72).

Thereafter, the FC will make a decision from the following SPRT rule: if $L_m \le A$, the FC announces H_0; if $L_m \ge B$, the FC announces H_1; and if $A < L_m < B$,

the FC selects a reliability threshold $\hat{r}_m$, and continues collecting the data packets in the mth frame. The values of A and B are obtained from Wald's approximation [80]: $A \approx \log\left(\frac{P_{\text{Miss}}}{1-P_{\text{FA}}}\right)$ and $B \approx \log\left(\frac{1-P_{\text{Miss}}}{P_{\text{FA}}}\right)$, where P_{Miss} and P_{FA} are the desired probabilities of miss detection and false alarm, respectively. Assume that the FC terminates the collection process at the beginning of the Mth frame. The *collection time* is equal to $2K(M-1)$ time slots, where $M = \min\left\{m \geq 1 : L_m \notin (A, B)\right\}$. The value M is an unknown random variable.

5.4 Adaptive Reliability Threshold

The performance of the proposed scheme - i.e., the collection time - depends on the set of reliability thresholds used in the system. The set of optimal reliability thresholds can be derived from the dynamic programming algorithm, which will map the system state to the optimal reliability threshold. However, since the system state of the proposed scheme (shown in Section 5.4.1) consists of many variables that are continuous or hidden, the computation of the optimal thresholds is highly complicated. Therefore, we propose a simple but efficient algorithm to derive suboptimal reliability thresholds instead. This algorithm, which is shown in Section 5.4.2, is based on the one-step look-ahead (1-SLA) rule. It will be shown in Section 5.5 that the proposed scheme using these suboptimal reliability thresholds significantly outperforms a conventional SPRT scheme.

5.4.1 System State and Evolution

In this section, we introduce the system state at the beginning of the mth frame, $\mathbf{s}_m$, of the proposed scheme, and study its evolution when a reliability threshold $\hat{r}_m$ is used. This relationship will be used to derive the suboptimal reliability threshold based on the 1-SLA rule in the next section. We define the system state at the beginning of the mth frame as $\mathbf{s}_m = (\tilde{N}_m, \gamma_m, \nu_m)$. The entries in $\mathbf{s}_m$ are defined as follows. The variable $\tilde{N}_m$ is an estimate of the residual number of nodes that do not

attempt transmissions yet. The variable γ_m is equal to the reliability threshold used in the previous frame, i.e., $\hat{r}_{m-1}$. The variable ν_m is the posterior probability that H_0 happens given all previous successfully received observations $\mathbf{x}_{z_{S,j}}$ and all previous retrieved observations $\tilde{\mathbf{x}}_{z_{C,j}}$, for $j = 1, \ldots, m-1$. Note that, for $m = 1$, we have $\tilde{N}_1 = N$, $\gamma_1 = \infty$, and $\nu_1 = \nu$. In the rest of the chapter, for clarity, we will write a probability of random variables given the system state and reliability threshold in the conditional form. This will also be applied to the expectation.

At the beginning of the mth frame, assume that the system state is $\mathbf{s}_m = (\tilde{N}_m, \gamma_m, \nu_m)$, and the FC continues the collection process with the reliability threshold $\hat{r}_m$. The system state evolution can be tracked as follows. Let $n_m^{(-)}$ be the number of nodes that have the observations $x \in \mathcal{X}^{(-)}(\hat{r}_m, \gamma_m)$ and $n_m^{(+)}$ be the number of nodes that have the observations $x \in \mathcal{X}^{(+)}(\hat{r}_m, \gamma_m)$. There will be $n_m^{(-)}$ nodes attempting transmissions in the first subframe and $n_m^{(+)}$ attempting transmissions in the second subframe with the joint probability

$$f\big(n_m^{(-)}, n_m^{(+)} | \mathbf{s}_m, \hat{r}_m\big) = \nu_m \, f\big(n_m^{(-)}, n_m^{(+)} | \mathbf{s}_m^{(0)}, \hat{r}_m\big) + (1-\nu_m) \, f\big(n_m^{(-)}, n_m^{(+)} | \mathbf{s}_m^{(1)}, \hat{r}_m\big), \quad (73)$$

where $0 \le n_m^{(-)} \le \tilde{N}_m$, $0 \le n_m^{(+)} \le \tilde{N}_m$, $0 \le n_m^{(-)} + n_m^{(+)} \le \tilde{N}_m$, and $\mathbf{s}_m^{(i)} = (\tilde{N}_m, \gamma_m, H_i)$ for $i = 0, 1$. The joint probability $f\big(n_m^{(-)}, n_m^{(+)} | \mathbf{s}_m^{(i)}, \hat{r}_m\big)$ can be expressed as

$$f\big(n_m^{(-)}, n_m^{(+)} | \mathbf{s}_m^{(i)}, \hat{r}_m\big) = f\big(n_m^{(-)} | \tilde{N}_m - n_m^{(+)}, \gamma_m, H_i, \hat{r}_m\big) \, f\big(n_m^{(+)} | \mathbf{s}_m^{(i)}, \hat{r}_m\big), \quad (74)$$

where $f\big(n_m^{(-)} | \tilde{N}_m - n_m^{(+)}, \gamma_m, H_i, \hat{r}_m\big) = \binom{\tilde{N}_m - n_m^{(+)}}{n_m^{(-)}} q^{n_m^{(-)}} (1-q)^{\tilde{N}_m - n_m^{(+)} - n_m^{(-)}}$ and $q = \int_{x \in \mathcal{X}^{(-)}(\hat{r}_m, \gamma_m)} f_X(x|H_i) \, dx$, for $i = 0, 1$, while $f\big(n_m^{(+)} | \mathbf{s}_m^{(i)}, \hat{r}_m\big) = \binom{\tilde{N}_m}{n_m^{(+)}} q^{n_m^{(+)}} (1-q)^{\tilde{N}_m - n_m^{(+)}}$ and $q = \int_{x \in \mathcal{X}^{(+)}(\hat{r}_m, \gamma_m)} f_X(x|H_i) \, dx$.

Assume that there are $n_m^{(-)}$ nodes attempting transmissions in the first subframe. Each of these nodes will randomly choose one of the K time slots to send their packets. As a result, the first subframe will consist of successful time slots, idle time slots, and collision time slots. Let $z_{S,m}^{(-)}$, $z_{I,m}^{(-)}$, and $z_{C,m}^{(-)}$ be the numbers of successful time slots, idle time slots, and collision time slots, respectively, where $z_{S,m}^{(-)} + z_{I,m}^{(-)} + z_{C,m}^{(-)} = K$.

Note that the number of successful nodes (or packets) in this frame is also equal to $z_{S,m}^{(-)}$. The joint probability that there are $z_{S,m}^{(-)}$ successful time slots and $z_{I,m}^{(-)}$ idle time slots given the number of active nodes $n_m^{(-)}$ is equal to

$$f\big(z_{S,m}^{(-)}, z_{I,m}^{(-)} | n_m^{(-)}\big) = f\big(z_{I,m}^{(-)} | z_{S,m}^{(-)}, n_m^{(-)}\big)\, f\big(z_{S,m}^{(-)} | n_m^{(-)}\big), \tag{75}$$

for $0 \le z_{S,m}^{(-)} + z_{I,m}^{(-)} \le K$, $0 \le z_{S,m}^{(-)} \le \min\big(K,\, n_m^{(-)}\big)$, $0 \le z_{I,m} \le K$, and we have [31, p. 102 and p. 112]

$$f\big(z_{S,m}^{(-)} | n_m^{(-)}\big) = \frac{(-1)^{z_{S,m}^{(-)}} K! n_m^{(-)}!}{z_{S,m}^{(-)}! K^{(\tilde{b}_m + n_m)}} \sum_{i \ge z_{S,m}^{(-)}}^{\min(K,\, n_m^{(-)})} \frac{(-1)^i \big(K-i\big)^{\left(n_m^{(-)} - i\right)}}{\big(i - z_{S,m}^{(-)}\big)!\big(K-i\big)!\big(n_m^{(-)} - i\big)!}, \tag{76}$$

$$f\big(z_{I,m}^{(-)} | z_{S,m}^{(-)}, n_m^{(-)}\big) = \binom{K - z_{S,m}^{(-)}}{z_{I,m}^{(-)}} \sum_{i=0}^{z_{C,m}^{(-)}} (-1)^i \binom{z_{C,m}^{(-)}}{i} \Big(1 - \frac{z_{I,m}^{(-)} + i}{K - z_{S,m}^{(-)}}\Big)^{n_m^{(-)}}, \tag{77}$$

where $z_{C,m}^{(-)} = K - z_{S,m}^{(-)} - z_{I,m}^{(-)}$. We use $z_{C,m}^{(-)}$ in (77) for brevity. Similarly, given that there are $n_m^{(+)}$ nodes attempting transmission in the second subframe, we can derive the joint probability $p\big(z_{S,m}^{(+)}, z_{I,m}^{(+)} | n_m^{(+)}\big)$ in the same manner, where $z_{S,m}^{(+)}$, $z_{I,m}^{(+)}$, and $z_{C,m}^{(+)}$ are the numbers of successful time slots, idle time slots, and collision time slots, respectively, and $z_{S,m}^{(+)} + z_{I,m}^{(+)} + z_{C,m}^{(+)} = K$.

At the end of the mth frame, assume that the FC has observed that there are $z_{S,m}^{(-)}$ successful time slots and $z_{I,m}^{(-)}$ idle time slots in the first subframe, and $z_{S,m}^{(+)}$ successful time slots and $z_{I,m}^{(+)}$ idle time slots in the second subframe. The corresponding successfully received observations are $\mathbf{x}_{z_{S,m}}$ defined in (71), and the corresponding retrieved observations are $\tilde{\mathbf{x}}_{z_{C,m}}$ defined in (70). The FC can update the system state at the beginning of the $(m+1)$st frame, $\mathbf{s}_{m+1} = (\tilde{N}_{m+1}, \gamma_{m+1}, \nu_{m+1})$, as follows. The value of γ_{m+1} is equal to $\hat{r}_m$ by its definition. The posterior probability ν_{m+1}, which is defined as $\Pr\big(H_0 | \mathbf{x}_{z_{S,1}}, \tilde{\mathbf{x}}_{z_{C,1}}, \ldots, \mathbf{x}_{z_{S,m}}, \tilde{\mathbf{x}}_{z_{C,m}}\big)$, can be computed recursively as [9, p. 266]

$$\nu_{m+1} = \frac{\nu_m f_X(\mathbf{x}_{z_{S,m}}, \tilde{\mathbf{x}}_{z_{C,m}} | H_0)}{\nu_m f_X(\mathbf{x}_{z_{S,m}}, \tilde{\mathbf{x}}_{z_{C,m}} | H_0) + (1-\nu_m) f_X(\mathbf{x}_{z_{S,m}}, \tilde{\mathbf{x}}_{z_{C,m}} | H_1)}, \tag{78}$$

where, $f_{\mathbf{X}}(\mathbf{x}_{z_{S,m}}, \tilde{\mathbf{x}}_{z_{C,m}}|H_i)$, for $i = 0, 1$, is

$$f_{\mathbf{X}}(\mathbf{x}_{z_{S,m}}, \tilde{\mathbf{x}}_{z_{C,m}}|H_i) = f_X(x_{m,1}^{(-)}|H_i)\cdots f_X(x_{m,z_{S,m}^{(-)}}^{(-)}|H_i) f_X(x_{m,1}^{(+)}|H_i)\cdots f_X(x_{m,z_{S,m}^{(+)}}^{(+)}|H_i)\times \Big(f_X(\tilde{x}_m^{(-)}|H_i)\Big)^{2z_{C,m}^{(-)}}\Big(f_X(\tilde{x}_m^{(+)}|H_i)\Big)^{2z_{C,m}^{(+)}},$$

from the IID assumption on the observations in Section 5.2.3.

The FC estimates the residual number of nodes from

$$\begin{aligned}\tilde{N}_{m+1} = \tilde{N}_m &- \text{nint}\Big(\mathbb{E}\big\{n_m^{(-)}|\tilde{N}_m, \gamma_m, \nu_{m+1}, \mathbf{z}_m^{(-)}, \hat{r}_m\big\}\Big) \\ &- \text{nint}\Big(\mathbb{E}\big\{n_m^{(+)}|\tilde{N}_m, \gamma_m, \nu_{m+1}, \mathbf{z}_m^{(+)}, \hat{r}_m\big\}\Big),\end{aligned} \tag{79}$$

where $\text{nint}(\cdot)$ is the nearest-integer function or round function, $\mathbf{z}_m^{(-)} = \big(z_{S,m}^{(-)}, z_{I,m}^{(-)}\big)$, and $\mathbf{z}_m^{(+)} = \big(z_{S,m}^{(+)}, z_{I,m}^{(+)}\big)$. The posterior probability of $n_m^{(-)}$ can be expressed as

$$\begin{aligned}&f\big(n_m^{(-)}|\tilde{N}_m, \gamma_m, \nu_{m+1}, \mathbf{z}_m^{(-)}, \hat{r}_m\big) \\ &\qquad = \frac{f\big(z_{S,m}^{(-)}, z_{I,m}^{(-)}, n_m^{(-)}|\tilde{N}_m, \gamma_m, \nu_{m+1}, \hat{r}_m\big)}{\sum_{n_m^{(-)} \geq z_{S,m}^{(-)}+2z_{C,m}^{(-)}}^{\tilde{N}_m} f\big(z_{S,m}^{(-)}, z_{I,m}^{(-)}, n_m^{(-)}|\tilde{N}_m, \gamma_m, \nu_{m+1}, \hat{r}_m\big)},\end{aligned} \tag{80}$$

where

$$\begin{aligned}&f\big(z_{S,m}^{(-)}, z_{I,m}^{(-)}, n_m^{(-)}|\tilde{N}_m, \gamma_m, \nu_{m+1}, \hat{r}_m\big) = f\big(z_{S,m}^{(-)}, z_{I,m}^{(-)}|n_m^{(-)}\big)\, f\big(n_m^{(-)}|\tilde{N}_m, \gamma_m, \nu_{m+1}, \hat{r}_m\big), \\ &f\big(n_m^{(-)}|\tilde{N}_m, \gamma_m, \nu_{m+1}, \hat{r}_m\big) = \sum_{n_m^{(+)}=0}^{\tilde{N}_m - n_m^{(-)}} f\big(n_m^{(-)}, n_m^{(+)}|\tilde{N}_m, \gamma_m, \nu_{m+1}, \hat{r}_m\big),\end{aligned}$$

$f\big(z_{S,m}^{(-)}, z_{I,m}^{(-)}|n_m^{(-)}\big)$ can be obtained from (75), and $f\big(n_m^{(-)}, n_m^{(+)}|\tilde{N}_m, \gamma_m, \nu_{m+1}, \hat{r}_m\big)$ can be obtained from (73) with using ν_{m+1} instead of ν_m. The posterior probability of $n_m^{(+)}$, $f\big(n_m^{(+)}|\tilde{N}_m, \gamma_m, \nu_{m+1}, \mathbf{z}_m^{(+)}, \hat{r}_m\big)$, can be obtained in a similar way.

5.4.2 One-Step Look-Ahead Rule

In this section, we find the reliability threshold $\hat{r}_m$ by using a simple strategy based on the 1-SLA rule. Assume that, at the beginning of the mth frame, where the system state is $\mathbf{s}_m$, the FC decides to continue the collection process; i.e., $L_m \in (A, B)$.

From the 1-SLA perspective, the FC will sequentially select the reliability threshold $\hat{r}_m$ that maximizes the expectation of the difference $\left|L_{m+1} - L_m\right|$. Therefore, given the system state $\mathbf{s}_m$, the reliability threshold $\hat{r}_m$ can be obtained from

$$\max_{\hat{r}_m \leq \gamma_m} \mathbb{E}\Bigg\{ \Bigg| \Upsilon(L_m, \mathbf{x}_{z_{S,m}}, \tilde{\mathbf{x}}_{z_{C,m}}) - L_m \Bigg| \Bigg| \mathbf{s}_m, \hat{r}_m \Bigg\} = \\ \max_{\hat{r}_m \leq \gamma_m} \Bigg[(1-\nu_m)\, \mathbb{E}\Bigg\{ \Upsilon(L_m, \mathbf{x}_{z_{S,m}}, \tilde{\mathbf{x}}_{z_{C,m}}) - L_m \Bigg| \mathbf{s}_m^{(1)}, \hat{r}_m \Bigg\} \\ - \nu_m\, \mathbb{E}\Bigg\{ \Upsilon(L_m, \mathbf{x}_{z_{S,m}}, \tilde{\mathbf{x}}_{z_{C,m}}) - L_m \Bigg| \mathbf{s}_m^{(0)}, \hat{r}_m \Bigg\} \Bigg], \tag{81}$$

where the function $\Upsilon(\cdot)$ is defined in (72). The expression in (81) is obtained from the fact that the conditional expectation given H_1 is positive, while the conditional expectation given H_0 is negative.

By substituting (72) into (81), using the IID assumption of the observations, and applying Wald's identity, we can express the expectation $\mathbb{E}\Big\{ \Upsilon(L_m, \mathbf{x}_{z_{S,m}}, \tilde{\mathbf{x}}_{z_{C,m}}) - L_m \Big| \mathbf{s}_m^{(i)}, \hat{r}_m \Big\}$ as

$$\mathbb{E}\Big\{ z_{S,m}^{(-)} \Big| \mathbf{s}_m^{(i)}, \hat{r}_m \Big\}\, \mathbb{E}\Bigg\{ \log \frac{f_X(x|H_1)}{f_X(x|H_0)} \Bigg| H_i, x \in \mathcal{X}^{(-)}(\hat{r}_m, \gamma_m) \Bigg\} \\ + \mathbb{E}\Big\{ z_{S,m}^{(+)} \Big| \mathbf{s}_m^{(i)}, \hat{r}_m \Big\}\, \mathbb{E}\Bigg\{ \log \frac{f_X(x|H_1)}{f_X(x|H_0)} \Bigg| H_i, x \in \mathcal{X}^{(+)}(\hat{r}_m, \gamma_m) \Bigg\} \\ + 2\hat{r}_m \Bigg[\mathbb{E}\Big\{ z_{C,m}^{(+)} \Big| \mathbf{s}_m^{(i)}, \hat{r}_m \Big\} - \mathbb{E}\Big\{ z_{C,m}^{(-)} \Big| \mathbf{s}_m^{(i)}, \hat{r}_m \Big\} \Bigg]. \tag{82}$$

The conditional expectation $\mathbb{E}\big\{ \cdot \,\big|\, H_i, x \in \mathcal{X}^{(-)}(\hat{r}_m, \gamma_m) \big\}$ is with respect to x, whose conditional PDF is equal to $f_X(x|H_i) \big/ \int_{x \in \mathcal{X}^{(-)}(\hat{r}_m, \gamma_m)} f_X(x|H_i)\, dx$, for $x \in \mathcal{X}^{(-)}(\hat{r}_m, \gamma_m)$. Similarly, the conditional expectation $\mathbb{E}\big\{ \cdot \,\big|\, H_i, x \in \mathcal{X}^{(+)}(\hat{r}_m, \gamma_m) \big\}$ is defined in a similar way. Furthermore, we can show that

$$\mathbb{E}\Big\{ z_{S,m}^{(-)} \Big| \mathbf{s}_m^{(i)}, \hat{r}_m \Big\} = \mathbb{E}\Big\{ \mathbb{E}\big\{ z_{S,m}^{(-)} \big| n_m^{(-)} \big\} \Big| \mathbf{s}_m^{(i)}, \hat{r}_m \Big\} = \mathbb{E}\Big\{ n_m^{(-)} \Big(1 - \frac{1}{K} \Big)^{(n_m^{(-)}-1)} \Big| \mathbf{s}_m^{(i)}, \hat{r}_m \Big\}, \\ \mathbb{E}\Big\{ z_{I,m}^{(-)} \Big| \mathbf{s}_m^{(i)}, \hat{r}_m \Big\} = \mathbb{E}\Big\{ \mathbb{E}\big\{ z_{I,m}^{(-)} \big| n_m^{(-)} \big\} \Big| \mathbf{s}_m^{(i)}, \hat{r}_m \Big\} = \mathbb{E}\Big\{ K \Big(1 - \frac{1}{K} \Big)^{n_m^{(-)}} \Big| \mathbf{s}_m^{(i)}, \hat{r}_m \Big\},$$

where the the conditional expectation $\mathbb{E}\big\{ \cdot \,\big|\, \mathbf{s}_m^{(i)}, \hat{r}_m \big\}$ on the right hand side is with

respect to $n_m^{(-)}$. The conditional probability $f\big(n_m^{(-)}\big|\mathbf{s}_m^{(i)},\hat{r}_m\big)$ is

$$f\big(n_m^{(-)}\big|\mathbf{s}_m^{(i)},\hat{r}_m\big)=\sum_{n_m^{(+)}=0}^{\check{N}_m-n_m^{(-)}} f\big(n_m^{(-)},n_m^{(+)}\big|\mathbf{s}_m^{(i)},\hat{r}_m\big),$$

where $f\big(n_m^{(-)},n_m^{(+)}\big|\mathbf{s}_m^{(i)},\hat{r}_m\big)$ is shown in (74). The derivations of $\mathbb{E}\big\{z_{S,m}^{(-)}\big|n_m^{(-)}\big\}=n_m^{(-)}\big(1-\frac{1}{K}\big)^{(n_m^{(-)}-1)}$ and $\mathbb{E}\big\{z_{I,m}^{(-)}\big|n_m^{(-)}\big\}=K\big(1-\frac{1}{K}\big)^{n_m^{(-)}}$ are shown in Appendix B. In addition, we have $\mathbb{E}\big\{z_{C,m}^{(-)}\big|\mathbf{s}_m^{(i)},\hat{r}_m\big\}=K-\mathbb{E}\big\{z_{S,m}^{(-)}\big|\mathbf{s}_m^{(i)},\hat{r}_m\big\}-\mathbb{E}\big\{z_{I,m}^{(-)}\big|\mathbf{s}_m^{(i)},\hat{r}_m\big\}$. The conditional expectations $\mathbb{E}\Big\{z_{S,m}^{(+)}\big|\mathbf{s}_m^{(i)},\hat{r}_m\Big\}$ and $\mathbb{E}\Big\{z_{C,m}^{(+)}\big|\mathbf{s}_m^{(i)},\hat{r}_m\Big\}$ can be derived in the same way.

A summary of the proposed scheme's procedures is shown in Algorithm 2.

Algorithm 2 Proposed Scheme

1. m=1.
2. At the beginning of the mth frame, given the system state $\mathbf{s}_m$, find the reliability threshold $\hat{r}_m$ from the **1-SLA rule** shown in (81).
3. Follow the **channel access protocol** described in Section 5.3.1.
4. At the end of the mth frame, given $\mathbf{z}_m^{(-)}$, $\mathbf{z}_m^{(+)}$, $\mathbf{x}_{z_{S,m}}$, and $\tilde{\mathbf{x}}_{z_{C,m}}$, update the system state to $\mathbf{s}_{m+1}$ as shown in Section 5.4.1, and the LLR value L_{m+1} as shown in (72).
5. Follow the **stopping rule** in Section 5.3.2: if $L_{m+1}\notin(A,\,B)$, stop the collection process and announce the corresponding H_i, for $i=0,1$; otherwise, set $m=m+1$ and go to Step 2).

5.5 Numerical Results

We use the following shift-in-mean model to evaluate the average collection time of the proposed scheme: $H_0: x=\eta$, and $H_1: x=\mu+\eta$, where μ is a constant, and η is a Gaussian random variable with mean and variance equal to zero and σ^2, respectively. The prior probabilities $\Pr(H_0)$ and $\Pr(H_1)$ are set to $\frac{1}{2}$. The reliability of the observation x is $\Big|\log\frac{f_X(x|H_1)}{f_X(x|H_0)}\Big|=\frac{\mu}{\sigma^2}\big|x-\frac{\mu}{2}\big|$. Without loss of generality,

in this case, we define the reliability of the observation x as $r = \left|x - \frac{\mu}{2}\right|$; i.e., we omit the scaling factor. Therefore, we have $\mathcal{X}^{(-)}(\hat{r}_m, \gamma_m) = \left(\frac{\mu}{2} - \gamma_m,\ \frac{\mu}{2} - \hat{r}_m\right]$ and $\mathcal{X}^{(+)}(\hat{r}_m, \gamma_m) = \left[\frac{\mu}{2} + \hat{r}_m,\ \frac{\mu}{2} + \gamma_m\right)$. Since the PDF $f_X(x|H_1)$ is a shifted-version of the PDF $f_X(x|H_0)$, and the PDF $f_X(x|H_i)$ is symmetric about its mean, (81) is reduced to $\max_{\hat{r}_m \leq \gamma_m} \mathbb{E}\Big\{\Upsilon(L_m, \mathbf{x}_{z_{S,m}}, \tilde{\mathbf{x}}_{z_{C,m}}) - L_m \left|\mathbf{s}_m^{(1)}, \hat{r}_m\right.\Big\}$, where the expectation can be obtained from (82).

In Fig. 21, we compare the average collection times (ACTs) required by the proposed scheme, a conventional SPRT scheme, and an oracle SPRT scheme for various values of σ^2. The other parameters' values are shown in the figure's caption. In the conventional SPRT scheme, the local observations are sent to the FC in *random* order and without collisions, while, in the oracle SPRT scheme, the local observations are sent to the FC in *descending* order of the reliabilities. For both schemes, at the end of each time slot, the FC will update the LLR upon the received observation and follow the SPRT rule. There are no packet collisions in these two schemes. The result shows that the proposed scheme significantly outperforms the conventional SPRT scheme, even though the proposed scheme experiences packet collisions. The improvement gap increases as we increase the noise variance since the proposed scheme collects only the most reliable observations. Note that the proposed scheme uses the suboptimal reliability threshold derived from (81). The oracle scheme's ACT, shown as a reference, occurs when perfect scheduling allows the FC to collect the local observations in perfectly descending order and without collisions or idle slots. The ACT of the proposed scheme is approximately two times higher than the ACT of the oracle scheme.

In Fig. 22, we show the average probability of successful transmission per time slot, $\bar{P}_{S,i}$, and the average probability of collision per time slot, $\bar{P}_{C,i}$, for the ith subframe, where $i = 1, 2$, when the hypothesis H_1 happens. The correct observations will be sent in the second subframe. We see that, since the proposed scheme can

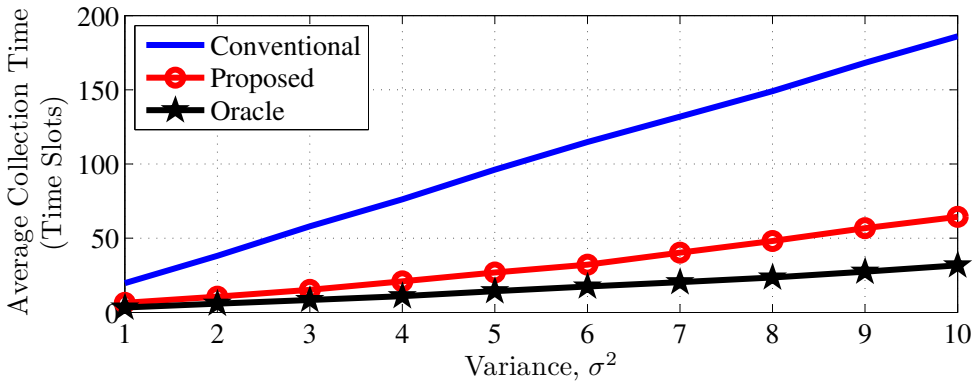

Figure 21: The average collection times of the conventional SPRT scheme, the proposed SPRT scheme, and the oracle scheme for various σ^2. The other parameters are $N = 1000$, $P_{\text{FA}} = P_{\text{Miss}} = 0.0001$, $K = 3$, $\mu = 1$.

retrieve two observations from a collision (from Assumption 4), the algorithm (81) prefers to choose the reliability thresholds that induce high collision rates in the second subframe. Note that, in this case, the resulting probabilities in the first subframe ($\bar{P}_{S,1}$ and $\bar{P}_{C,1}$) are by products that (81) is true. Recall that the retrieved observations are set to the lowest reliable observation in that frame (Assumption 4). Therefore, if we select a reliability threshold to obtain a higher number of collisions (i.e., a higher number of retrieved observations), we inevitably obtain a lower retrieved observation value. This tradeoff is also seen in Fig. 22, where the proposed scheme chooses the reliability thresholds to obtain lower $\bar{P}_{C,2}$ as the variance σ^2 increases. Note that, given the same γ_m and N, we have to adjust the reliability threshold $\hat{r}_m$ in a high variance case lower than that in a low variance case to obtain the same probability of collision in the second subframe.

In Fig. 23, we plot the ACTs of the proposed scheme and the oracle scheme versus N for $\sigma^2 = 3$ and $\sigma^2 = 8$. The other parameters' values are shown in the figure's caption. Since the ACT of the conventional SPRT scheme is independent of N, we have its ACTs equal to 57.16 and 150.67 time slots for $\sigma^2 = 3$ and $\sigma^2 = 8$, respectively, for all N. The proposed scheme and the oracle scheme have an advantage when N increases because more nodes will have highly reliable observations. The proposed

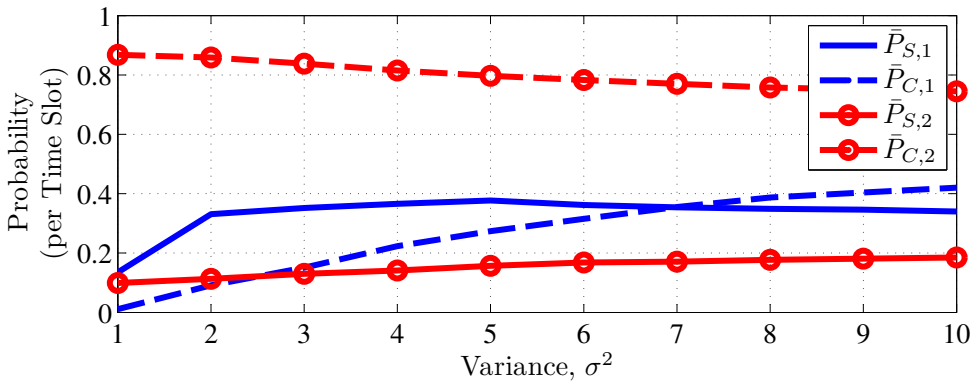

Figure 22: The average probabilities of successful transmission ($\bar{P}_{S,i}$) and collision ($\bar{P}_{C,i}$) per time slot for the ith subframe, where $i = 1, 2$, given the hypothesis H_1. The other parameters are $N = 1000$, $P_{\text{FA}} = P_{\text{Miss}} = 0.0001$, $K = 3$, $\mu = 1$.

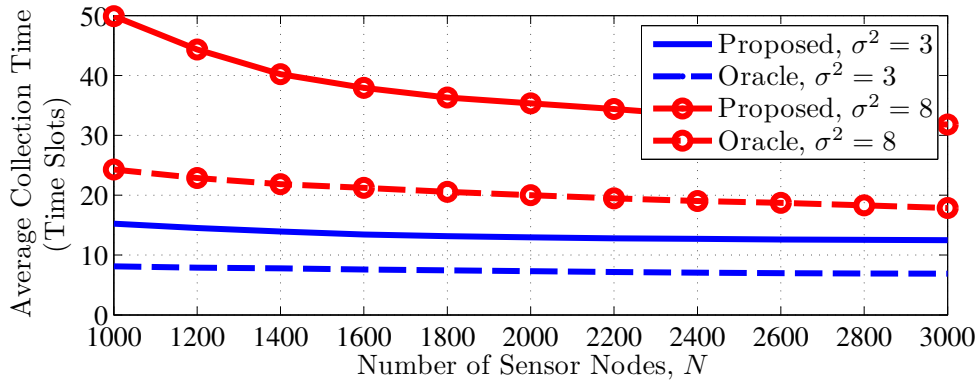

Figure 23: The average collection times (ACTs) of the proposed scheme and the oracle scheme for $\sigma^2 = 3$, $\sigma^2 = 8$, and various N. The other parameters are $P_{\text{FA}} = P_{\text{Miss}} = 0.001$, $K = 3$, $\mu = 1$. The ACTs of the conventional SPRT scheme for $\sigma^2 = 3$ and $\sigma^2 = 8$ are 57.16 time slots and 150.67 time slots, respectively.

scheme's improvement for increasing N is quite significant when σ^2 is large.

5.6 Conclusion

We proposed an ordered sequential detection scheme in which the FC is able to partially retrieve observations from collided packets. The FC will use both successfully received observations and these partially retrieved observations to decide whether to make a global decision or to continue collecting more local observations. As a result, under the considered scenarios, the proposed scheme requires as little as one-third of the conventional SPRT scheme's average collection time to achieve the same level of

confidence.

CHAPTER VI

THE USE OF RELIABILITY-BASED SPLITTING ALGORITHMS TO IMPROVE DISTRIBUTED ESTIMATION IN WSNS

6.1 Introduction

A wireless sensor network (WSN) performing distributed estimation consists of a number of small, inexpensive, and sensor-equipped nodes dispersed over a geographic area to estimate parameters of interest. These local estimates, which are quantized versions of noisy observations, are collected over a wireless channel by a fusion center (FC) that fuses them to produce a reliable global estimate.

Distributed estimation schemes have been studied extensively [91]. A popular approach is the best linear unbiased estimator (BLUE) [88], where the global parameter estimate is obtained by a weighted sum of the local estimates, and the weights can be computed from the local noise variances. Under resource constraints, e.g., power and number of bits, [47,86,88] have formulated optimization problems to find optimal allocation strategies that are functions of the local noise variances. However, these papers only considered the schemes in parallel access channels, where transmission scheduling and collisions are not considered.

For a collision channel, since the FC does not know the nodes' observation reliabilities in advance, a collision-free transmission scheduling cannot be properly managed without additional information exchanges among the nodes and the FC. Using a random access protocol, such as slotted ALOHA, in distributed detection/estimation is an alternative strategy that suffers packet loss from collisions. By applying the

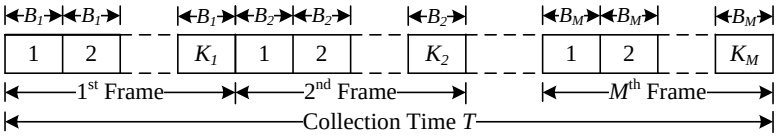

Figure 24: Time on the channel is divided into super-frames, where each super-frame has a length of T bits. A super-frame consists of M frames and each frame has K_m time slots with length B_m bits.

multiuser-diversity/opportunistic principle, threshold-based slotted ALOHA protocols that maximize the performance of distributed detection/estimation have been derived in [38, 44].

In this chapter, we consider distributed estimation in a *large*, *single-hop* WSN that uses a *collision* channel for transmission and is subject to a *fixed deadline* for making a global estimate. The sensor nodes monitor a scalar and deterministic parameter θ of a source in the network, quantize their observations, and send the estimates to the FC through a reliable (bit-error-free) link. The FC is allocated a collection time of T bits to gather the nodes' estimates, which are assumed to be ready at the beginning of the collection time and not updated during T. Since the network consists of a large number of nodes and has a time-delay constraint, the allocated collection time is generally not long enough to collect the estimates from all nodes.

To improve the performance of distributed estimation under the conditions above, we apply a reliability-based splitting algorithm [44]. Similar to [47,86–88], we assume that each node knows its instantaneous noise variance, σ^2.

Proposed distributed estimation: We divide T bits into M frames, where each frame consists of K_m time slots of length B_m bits (Fig. 24). The scheme performs the following steps.

1) *Reliability-based splitting strategy:* Given a set of reliability thresholds $\hat{\boldsymbol{\sigma}}^{\mathbf{2}} = [\hat{\sigma}_1^2, \ldots, \hat{\sigma}_M^2]$, where $\hat{\sigma}_0^2 < \hat{\sigma}_1^2 < \ldots < \hat{\sigma}_M^2 < \infty$, only nodes with instantaneous noise variances $\sigma^2 \in [\hat{\sigma}_{m-1}^2, \hat{\sigma}_m^2)$, where $m = 1, \ldots, M$, will transmit their local estimates in the mth frame. Therefore, the FC receives the local estimates almost in ascending

order of the observation noise variance.

2) *Sensor processing:* If a node's noise variance $\hat{\sigma}^2$ is such that $\sigma^2 \in [\hat{\sigma}^2_{m-1}, \hat{\sigma}^2_m)$, then it quantizes the observation by using a scalar uniform quantization, whose step size is $\frac{W}{2^{B_m}}$, where W is the considered range of the observation. Thereafter, the node schedules the transmission of this estimate (binary message) of length B_m within the mth frame.

3) *Channel access protocol:* Since the identities of nodes whose $\sigma^2 \in [\hat{\sigma}^2_{m-1}, \hat{\sigma}^2_m)$ are not known by the FC, slotted ALOHA is used as a channel access protocol. When the mth frame arrives, each node with $\sigma^2 \in [\hat{\sigma}^2_{m-1}, \hat{\sigma}^2_m)$ independently and randomly chooses one of the K_m slots to send its estimate.

4) *Fusion center processing:* The FC makes a global estimate by using a BLUE based on the received local estimates.

The performance of the proposed scheme is a function of the thresholds $\hat{\sigma}^2_m$, the number of bits B_m, and the number of time slots K_m. We formulate time-constrained optimization problems to find the optimal values of these parameters.

The chapter is organized as follows. Section 6.2 derives the mathematical expressions and performance measure of the proposed schemes. Methods to find the optimal parameter values are explained in Section 6.3. To remedy the effect of packet collisions, we introduce a modified frame structure in Section 6.4. In Section 6.5, we show the optimal parameter values and study the effects of these parameters on the proposed schemes. Conclusions are provided in Section 6.6.

6.2 System Model and Performance Measure

We assume that there are N nodes in the network. The local observation of the nth node is $x_n = \theta + v_n$, where v_n is an additive and independent noise with variance σ^2_n. Following the model introduced in [86–88], we define the noise variance as: $\sigma^2_n = \hat{\sigma}^2_0 + \kappa h_n$, where $\hat{\sigma}^2_0$ is a network-wide background noise variance, κ is a scaling variable,

and h_n is an independent and identical random variable characterizing the noise variance distribution in the network. Note that, in [86–88], h_n is modeled as a Chi-square random variable with degree 1 and κ is a function of a distance. Therefore, σ_n^2 is an independent and identical distributed random variable with the probability density function (PDF) $f_{\sigma^2}(\sigma^2)$.

The observation x_n with $\sigma_n^2 \in [\hat{\sigma}_{m-1}^2, \hat{\sigma}_m^2)$, is quantized to a binary message whose length is equal to B_m. Assume a scalar uniform quantizer is used. The estimate (quantized observation) $\tilde{x}_n$ can be modeled as: $\tilde{x}_n = \theta + v_n + w_n$, where w_n is quantization noise, which can be approximated as a uniform random variable with zero mean and variance equal to $\frac{W^2}{2^{2B_m}}$ [33], and W is the considered range of x_n.

The thresholds $\hat{\boldsymbol{\sigma}}^{\mathbf{2}}$ are also used to control nodes' channel access. Only the nodes with the noise variance $\sigma^2 \in [\hat{\sigma}_{m-1}^2, \hat{\sigma}_m^2)$ are allowed to send their estimates during the mth frame. Since we have $\hat{\sigma}_0^2 < \hat{\sigma}_1^2 < \ldots < \hat{\sigma}_M^2$, the estimates are sent to the FC approximately in order from lowest to highest noise variances. The number of nodes attempting transmission in the mth frame, n_m, is a random variable with mean $\bar{n}_m = N \int_{\hat{\sigma}_{m-1}^2}^{\hat{\sigma}_m^2} f_{\sigma^2}(\sigma^2)\, d\sigma^2$. Since the *identities* and the *number* of nodes that will attempt transmissions in the mth frame is unknown in advance, a slotted ALOHA protocol is used. Each node active in the mth frame will independently and randomly select one of the K_m slots to send its estimate.

At the end of the collection time T, the FC makes a global estimate $\hat{\theta}$, which is obtained by using a BLUE. Note that we assume a *worst-case scenario*, where all transmitted messages within a frame are assigned the highest noise variance associated with that frame, i.e., $\hat{\sigma}_m^2$. Let $y_{i,m}$ be the ith successfully received estimate in the mth frame, and s_m, which is a random variable, be the number of successfully received estimates in the mth frame. Given $s_1, \ldots, s_M$, the global estimate $\hat{\theta}$ and its variance

$var\big(\hat{\theta}\big)$ are

$$\hat{\theta} = \left(\sum_{m=1}^{M} \frac{s_m}{\hat{\sigma}_m^2 + \frac{W^2}{2^{2B_m}}}\right)^{-1} \sum_{m=1}^{M} \frac{\sum_{i=1}^{s_m} y_{i,m}}{\hat{\sigma}_m^2 + \frac{W^2}{2^{2B_m}}}, \qquad var\big(\hat{\theta}\big) = \left(\sum_{m=1}^{M} \frac{s_m}{\hat{\sigma}_m^2 + \frac{W^2}{2^{2B_m}}}\right)^{-1}.$$

The variance $var\big(\hat{\theta}\big)$ is a function of the random variables $s_1, \ldots, s_M$. Since a closed form of $\mathbb{E}\big\{var\big(\hat{\theta}\big)\big\}$ has not been found, where $\mathbb{E}\{\cdot\}$ is the expectation operator, we consider its lower bound instead. By applying Jensen's inequality and the fact that the function x^{-1} is a convex function for $x > 0$, we obtain $\mathbb{E}\big\{var\big(\hat{\theta}\big)\big\} \geq 1/\bar{I}_\theta$, where

$$\bar{I}_\theta = \sum_{m=1}^{M} \frac{\mathbb{E}\{s_m\}}{\hat{\sigma}_m^2 + \frac{W^2}{2^{2B_m}}}. \tag{83}$$

Since $\mathbb{E}\big\{var\big(\hat{\theta}\big)\big\}$ is inversely proportional to $\bar{I}_\theta$, then, we use $\bar{I}_\theta$ as the performance measure. Note that if v_n and w_n are Gaussian noise, $\bar{I}_\theta$ is the expectation of the Fisher information.

The expression for $\bar{I}_\theta$ can be obtained as follows. From (83), $\mathbb{E}\{s_m\} = \mathbb{E}_{n_m}\{\mathbb{E}_{s_m}\{s_m|n_m\}\}$ and s_m is a random variable with the conditional probability [31, p. 112]:

$$f(s_m|n_m) = \frac{(-1)^{s_m} K_m! n_m!}{s_m! K_m^{n_m}} \sum_{i \geq s_m}^{\tilde{K}_m} \frac{(-1)^i (K_m - i)^{n_m - i}}{(i - s_m)!(K_m - i)!(n_m - i)!},$$

for $0 \leq s_m \leq \tilde{K}_m$, where $\tilde{K}_m = \min(K_m, n_m)$. As shown in Appendix A, $\mathbb{E}_{s_m}\{s_m|n_m\} = n_m\big(1 - \frac{1}{K_m}\big)^{n_m - 1}$. Then, $\mathbb{E}_{n_m}\{\mathbb{E}_{s_m}\{s_m|n_m\}\} \simeq \bar{n}_m e^{-\frac{\bar{n}_m}{K_m}}$, and

$$\bar{I}_\theta(\hat{\boldsymbol{\sigma}}^{\mathbf{2}}, \mathbf{B}, \mathbf{K}) \simeq \sum_{m=1}^{M} \frac{\bar{n}_m e^{-\frac{\bar{n}_m}{K_m}}}{\hat{\sigma}_m^2 + \frac{W^2}{2^{2B_m}}}, \tag{84}$$

where $\hat{\boldsymbol{\sigma}}^{\mathbf{2}} = [\hat{\sigma}_1^2, \ldots, \hat{\sigma}_M^2]$, $\mathbf{B} = [B_1, \ldots, B_M]$, and $\mathbf{K} = [K_1, \ldots, K_M]$.

6.3 Optimal Parameter Values

In this section, we formulate a time-constrained optimization to find the optimal parameter values. We consider two approaches, which are distinguished by how we model the parameters $\mathbf{B}$ and $\mathbf{K}$: deterministic variables and random variables. For the first approach, we are finding integers $\mathbf{B}^*$ and $\mathbf{K}^*$, and, then, the optimization

problem based on this approach is a mixed integer nonlinear program. On the other hand, for the second approach, since $\mathbf{B}$ and $\mathbf{K}$ are random variables, we are seeking the joint probability mass function (PMF) $\mathbf{q}^*$ maximizing $\mathbb{E}_{\mathbf{B},\mathbf{K}}\big\{\bar{I}_\theta(\hat{\boldsymbol{\sigma}}^{\mathbf{2}}, \mathbf{B}, \mathbf{K})\big\}$, where $\mathbf{q}^* = [\mathbf{q}_1^*, \ldots, \mathbf{q}_M^*]$, $\mathbf{q}_m^* = [q_{b_m,k_m}^*]$, and q_{b_m,k_m}^* is the probability that, at the mth frame, $B_m = b_m$ and $K_m = k_m$, for integers $b_m, k_m \geq 1$. As a result, the optimization problem based on this approach is a mixed linear-nonlinear program. The details and algorithms to find $\hat{\boldsymbol{\sigma}}^{\mathbf{2}^*}$, $\mathbf{B}^*$, $\mathbf{K}^*$, and $\mathbf{q}^*$ of these approaches are shown in the following subsections.

6.3.1 Deterministic Approach

In this approach, the parameters $\mathbf{B}$ and $\mathbf{K}$ are modeled as integers. A time-constrained optimization problem to find the optimal $\hat{\boldsymbol{\sigma}}^{\mathbf{2}^*}$, $\mathbf{B}^*$, and $\mathbf{K}^*$ can be expressed as

$$\begin{aligned} P1: \max_{\hat{\boldsymbol{\sigma}}^{\mathbf{2}}} \max_{\mathbf{B},\mathbf{K}} \; & \bar{I}_\theta(\hat{\boldsymbol{\sigma}}^{\mathbf{2}}, \mathbf{B}, \mathbf{K}) \\ \text{s. t.} \; & \sum_{m=1}^{M} B_m K_m \leq T, \; B_m \geq 1, \; K_m \geq 1, \forall m; \\ & \hat{\sigma}_0^2 < \hat{\sigma}_1^2 < \ldots < \hat{\sigma}_M^2. \end{aligned}$$

The first constraint is from the allocated collection time. Finding the optimal solutions of these problems analytically is difficult. Therefore, we derive an algorithm to find efficient solutions instead. The algorithm consists of two steps. First, given $\hat{\boldsymbol{\sigma}}^{\mathbf{2}}$, we find the optimal $\mathbf{B}^*$ and $\mathbf{K}^*$. Second, we update $\hat{\boldsymbol{\sigma}}^{\mathbf{2}}$ and re-compute $\mathbf{B}^*$ and $\mathbf{K}^*$. The algorithm iterates until a convergence criterion is met. It can be illustrated as follows.

Given $\hat{\boldsymbol{\sigma}}^{\mathbf{2}}$, we define a function:

$$\bar{I}_{\theta,D}(\hat{\boldsymbol{\sigma}}^{\mathbf{2}}) = \max_{\mathbf{B},\mathbf{K}} \Big\{ \bar{I}_\theta(\hat{\boldsymbol{\sigma}}^{\mathbf{2}}, \mathbf{B}, \mathbf{K}) \Big| \sum_{m=1}^{M} B_m K_m \leq T, \; B_m \geq 1, \; K_m \geq 1, \forall m, \Big\}. \quad (85)$$

Instead of solving Primal Problem (85), we find the solutions $\mathbf{B}^*$ and $\mathbf{K}^*$ by using the dual decomposition method [8, p. 502], [59], which reduces computational complexity significantly. The Lagrange function of Problem (85), considering only the time

constraint, can be expressed as $L(\hat{\boldsymbol{\sigma}}^{\mathbf{2}}, \mathbf{B}, \mathbf{K}, \lambda) = \sum_{m=1}^{M} L_m + \lambda T$, where

$$L_m = \frac{\bar{n}_m e^{-\frac{\bar{n}_m}{K_m}}}{\hat{\sigma}_m^2 + \frac{W^2}{2^{2B_m}}} - \lambda B_m K_m,$$

λ is the dual variable. Note that L_m is a function of $\hat{\sigma}_{m-1}^2$, $\hat{\sigma}_m^2$, B_m, K_m, and λ. As a result, the dual function is

$$D(\hat{\boldsymbol{\sigma}}^{\mathbf{2}}, \lambda) = \max_{\mathbf{B},\mathbf{K}} \left\{ L(\hat{\boldsymbol{\sigma}}^{\mathbf{2}}, \mathbf{B}, \mathbf{K}, \lambda) \,\middle|\, B_m \geq 1, K_m \geq 1, \forall m \right\}.$$

The dual function can be decomposed into the following M separable problems, for $m = 1, \ldots, M$:

$$D_m(\hat{\sigma}_{m-1}^2, \hat{\sigma}_m^2, \lambda) = \max_{B_m, K_m} \left\{ L_m \,\middle|\, B_m \geq 1, K_m \geq 1 \right\}. \tag{86}$$

The values B_m^* and K_m^* from (86) can be found by a direct search method with a reasonable computational complexity.

The dual of Problem (85) is

$$D1: \min_{\lambda} D(\hat{\boldsymbol{\sigma}}^{\mathbf{2}}, \lambda) \text{ s. t. } \lambda \geq 0.$$

There are many methods to find λ^*, e.g., the subgradient method [8, 14, 59, 85]. However, in this work, λ^* can be obtained simply as shown in Algorithm 3, where $0 < \delta < 1$. With updated dual variable $\lambda^{(l+1)}$, $\mathbf{B}^*$ and $\mathbf{K}^*$ will be recomputed. As l increases, $\lambda^{(l)}$ decreases, while $\sum_{m=1}^{M} B_m^{(l)*} K_m^{(l)*}$ increases. Therefore, convergence typically occurs very quickly.

Algorithm 3 Finding $\mathbf{B}^*$ and $\mathbf{K}^*$ for given $\hat{\boldsymbol{\sigma}}^{\mathbf{2}}$.

1. Set $l = 1$ and $\lambda^{(1)} = \lambda^{(initial)}$.
2. For $m = 1, \ldots, M$, obtain $B_m^{(l)*}$ and $K_m^{(l)*}$ from (86).
3. If $T - \sum_{m=1}^{M} B_m^{(l)*} K_m^{(l)*} \leq \epsilon$, stop, and announce $\lambda^* = \lambda^{(l)}$, $\mathbf{B}^* = \mathbf{B}^{(l)*}$, $\mathbf{K}^* = \mathbf{K}^{(l)*}$; otherwise, set $l = l + 1$, $\lambda^{(l)} = \delta \lambda^{(l-1)}$, and go to Step 2).

Algorithm 4 Finding $\hat{\boldsymbol{\sigma}}^{\mathbf{2}^*}$.

1. Set $i = 1$. Randomly select $\hat{\boldsymbol{\sigma}}^{\mathbf{2}^{(1)}}$. Find $\bar{I}_{\theta,D}(\hat{\boldsymbol{\sigma}}^{\mathbf{2}^{(1)}})$, where, given $\hat{\boldsymbol{\sigma}}^{\mathbf{2}^{(1)}}$, $\mathbf{B}^*$ and $\mathbf{K}^*$ are found from Algorithm 3.

2. Set $i = i + 1$.

3. Update $\hat{\boldsymbol{\sigma}}^{\mathbf{2}^{(i)}}$ from the following procedures:

   (a) Set $m = 0$.

   (b) Set $m = m + 1$.

   (c) $\hat{\sigma}_m^{2^{(i)}} = \underset{\hat{\sigma}^2 \in (\hat{\sigma}_{m-1}^{2^{(i)}}, \hat{\sigma}_{m+1}^{2^{(i-1)}}]}{\arg\max} \bar{I}_{\theta,D}(\hat{\boldsymbol{\sigma}}^{\mathbf{2}^{(i)}}_m)$, where

   $$\hat{\boldsymbol{\sigma}}^{\mathbf{2}^{(i)}}_m = [\hat{\sigma}_1^{2^{(i)}}, \ldots, \hat{\sigma}_{m-1}^{2^{(i)}}, \hat{\sigma}^2, \hat{\sigma}_{m+1}^{2^{(i-1)}}, \ldots, \hat{\sigma}_M^{2^{(i-1)}}],$$

   and, given $\hat{\boldsymbol{\sigma}}^{\mathbf{2}^{(i)}}_m$, $\mathbf{B}^*$ and $\mathbf{K}^*$ are obtained from Algorithm 3.

   (d) Set $\hat{\boldsymbol{\sigma}}^{\mathbf{2}^{(i,m)}} = [\hat{\sigma}_1^{2^{(i)}}, \ldots, \hat{\sigma}_m^{2^{(i)}}, \hat{\sigma}_{m+1}^{2^{(i-1)}}, \ldots, \hat{\sigma}_M^{2^{(i-1)}}]$.

   (e) Repeat b) – d) until $m = M$. Set $\hat{\boldsymbol{\sigma}}^{\mathbf{2}^{(i)}} = \hat{\boldsymbol{\sigma}}^{\mathbf{2}^{(i,M)}}$.

4. Compute $\bar{I}_{\theta,D}(\hat{\boldsymbol{\sigma}}^{\mathbf{2}^{(i)}})$.

5. If $\bar{I}_{\theta,D}(\hat{\boldsymbol{\sigma}}^{\mathbf{2}^{(i)}}) - \bar{I}_{\theta,D}(\hat{\boldsymbol{\sigma}}^{\mathbf{2}^{(i-1)}}) \leq \varepsilon$, stop, and announce $\hat{\boldsymbol{\sigma}}^{\mathbf{2}^*} = \hat{\boldsymbol{\sigma}}^{\mathbf{2}^{(i)}}$; otherwise, go to Step 2).

In general, solving a dual problem gives an upper bound of the original solution. However, from [85, Proposition 10.2], if we obtain $\lambda^* > 0$ and $\sum_{m=1}^{M} B_m^* K_m^* = T$, there is no duality gap. As observed in the numerical results shown in Section 6.5, we achieve these conditions in most cases.

The next step is to find $\hat{\boldsymbol{\sigma}}^{\mathbf{2}^*}$ maximizing $\bar{I}_{\theta,D}(\hat{\boldsymbol{\sigma}}^{\mathbf{2}})$. However, the optimal thresholds of $\bar{I}_{\theta,D}(\hat{\boldsymbol{\sigma}}^{\mathbf{2}})$ are difficult to find analytically. Similar to [78], we derive an algorithm to find efficient solutions $\hat{\boldsymbol{\sigma}}^{\mathbf{2}^*}$ based on a Greedy principle, where we iteratively find $\hat{\sigma}_m^{2^*}$ maximizing $\bar{I}_{\theta,D}(\hat{\boldsymbol{\sigma}}^{\mathbf{2}})$ when fixing the rest of the thresholds. This algorithm is shown in Algorithm 4.

The following conditions can be used to verify whether $\hat{\boldsymbol{\sigma}}^{\mathbf{2}^*}$ from Algorithm 4 are candidates for the optimal values.

Proposition 16. *For given* $\mathbf{K}$*, necessary conditions for the optimal reliability thresholds* $\hat{\boldsymbol{\sigma}}^{\mathbf{2}^*} = [\hat{\sigma}_1^{2^*}, \ldots, \hat{\sigma}_M^{2^*}]$ *are* $\bar{n}_m \leq K_m$*, for all* m*.*

Proof. At the mth frame, we consider $\bar{n}_m e^{-\frac{\bar{n}_m}{K_m}} \big/ \big(\hat{\sigma}_m^2 + \frac{W^2}{2^{2B_m}}\big)$ for given $\hat{\sigma}_{m-1}^{2^*}$, B_m, and K_m. Let $\hat{\sigma}_m^{2^\circ}$ be the threshold that $\bar{n}_m = K_m$. Note that $\hat{\sigma}_m^{2^\circ}$ depends on $\hat{\sigma}_{m-1}^{2^*}$. The term $\bar{n}_m e^{-\frac{\bar{n}_m}{K_m}}$ is an nondecreasing function on $\hat{\sigma}_m^2$ for $\hat{\sigma}_m^2 \leq \hat{\sigma}_m^{2^\circ}$; otherwise, it is a decreasing function on $\hat{\sigma}_m^2$. The term $1\big/(\hat{\sigma}_m^2 + \frac{W^2}{2^{2B_m}})$ is a decreasing function on $\hat{\sigma}_m^2$. Therefore, the proposition is obtained by induction. □

The thresholds $\hat{\boldsymbol{\sigma}}^{\mathbf{2}^\circ} = [\hat{\sigma}_1^{2^\circ}, \ldots, \hat{\sigma}_M^{2^\circ}]$ in the proof above are called the *maximum throughput thresholds* [44], because, by using $\hat{\boldsymbol{\sigma}}^{\mathbf{2}^\circ}$, $\bar{n}_m$ is equal to K_m for all m. However, similar to [44], the thresholds, $\hat{\boldsymbol{\sigma}}^{\mathbf{2}^\circ}$, that maximize the channel efficiency, are *not always* optimal as shown in Section 6.5.

Since $\bar{I}_{\theta,D}(\hat{\boldsymbol{\sigma}}^{\mathbf{2}})$ is a nonlinear (possibly, nonconcave) function of $\hat{\boldsymbol{\sigma}}^{\mathbf{2}}$, there is no guarantee that the thresholds $\hat{\boldsymbol{\sigma}}^{\mathbf{2}^*}$ found from Algorithm 4 are globally optimal. However, since the initial thresholds $\hat{\boldsymbol{\sigma}}^{\mathbf{2}^{(1)}}$ are randomly chosen, we are likely to find the

globally optimal thresholds when repeating the algorithm several times. In our numerical results, we have always obtained the same solutions.

6.3.2 Randomized Approach

In this approach, we model the parameters $\mathbf{B}$ and $\mathbf{K}$ as random variables. Therefore, we are seeking $\hat{\boldsymbol{\sigma}}^{\mathbf{2}^*}$ and $\mathbf{q}^*$ maximizing $\mathbb{E}_{\mathbf{B},\mathbf{K}}\big\{\bar{I}_\theta(\hat{\boldsymbol{\sigma}}^{\mathbf{2}}, \mathbf{B}, \mathbf{K})\big\}$. A time-constrained optimization problem can be formulated as

$$\begin{aligned} P2: \ & \max_{\hat{\boldsymbol{\sigma}}^{\mathbf{2}}} \max_{\mathbf{q}} \mathbb{E}_{\mathbf{B},\mathbf{K}}\big\{\bar{I}_\theta(\hat{\boldsymbol{\sigma}}^{\mathbf{2}}, \mathbf{B}, \mathbf{K})\big\} \\ \text{s. t.} \ & \sum_{m=1}^{M} \mathbb{E}_{B_m,K_m}\big\{B_m K_m\big\} = T; \ \sum_{b_m=1}^{\infty}\sum_{k_m=1}^{\infty} q_{b_m,k_m} = 1, \ \forall m; \\ & 0 \leq q_{b_m,k_m} \leq 1, \forall b_m, k_m; \ \hat{\sigma}_0^2 < \hat{\sigma}_1^2 < \ldots < \hat{\sigma}_M^2. \end{aligned}$$

Similar steps explained in Section 6.3.1 are applied to find the solutions of Problem $P2$. Given $\hat{\boldsymbol{\sigma}}^{\mathbf{2}}$, we define

$$\bar{I}_{\theta,R}(\hat{\boldsymbol{\sigma}}^{\mathbf{2}}) = \max_{\mathbf{q}} \Bigg\{ \mathbb{E}_{\mathbf{B},\mathbf{K}}\big\{\bar{I}_\theta(\hat{\boldsymbol{\sigma}}^{\mathbf{2}}, \mathbf{B}, \mathbf{K})\big\} \Bigg| \sum_{m=1}^{M} \mathbb{E}_{\mathbf{B},\mathbf{K}}\big\{B_m K_m\big\} = T, \sum_{b_m=1}^{\infty}\sum_{k_m=1}^{\infty} q_{b_m,k_m} = 1, \ 0 \leq q_{b_m,k_m} \leq 1, \forall b_m, k_m \Bigg\}. \quad (87)$$

The optimal $\mathbf{q}^*$ for (87) can now be found by a linear program. As a result, since the member in $\mathbf{q}$ are probability measures, in general, we have at most two elements in $\mathbf{q}_m$, for all m, that are nonzero. Therefore, the randomized strategy might provide a deterministic solution. This suggests that, in terms of computational complexity, we might use the randomized strategy to approximate the integer solution.

Thereafter, we apply Algorithm 4, in which $\bar{I}_{\theta,R}(\hat{\boldsymbol{\sigma}}^{\mathbf{2}})$ is used instead of $\bar{I}_{\theta,D}(\hat{\boldsymbol{\sigma}}^{\mathbf{2}})$, to find efficient solutions $\hat{\boldsymbol{\sigma}}^{\mathbf{2}^*}$. The prior discussions about the solutions $\hat{\boldsymbol{\sigma}}^{\mathbf{2}^*}$ hold here as well.

6.4 Modified Frame Structure

By using the frame structure shown in Fig. 24, when a collision happens, entire transmitted packets are lost. To remedy this collision effect, we have modified the frame structure by decoupling the contention period from the estimates' transmissions as shown in Fig. 25, which is inspired by IEEE 802.15.3 and 802.15.4 frame structures. The modified frame structure is divided into three parts: contention access period (CAP), Beacon, and channel time allocation period (CTAP). In the mth frame, the CAP consists of K_m minislots with the length α bits, and the CTAP consists of J_m time slots with the length B_m bits. The Beacon period has a length equal to $\beta_m J_m$, where the length of β_m will be indicated below. The nodes with $\sigma^2 \in [\hat{\sigma}^2_{m-1}, \hat{\sigma}^2_m)$ will do the following channel access procedures at the mth frame.

1) *CAP:* Each active node independently and randomly chooses one of the K_m minislots to send its reservation. A reservation is successful if exactly one node sends a reservation in the minislot.

2) *Beacon:* This duration is exploited by the FC to schedule z_m nodes whose reservations are successfully received. The variable z_m is a random variable whose conditional PMF $f(z_m|n_m)$ is identical to $f(s_m|n_m)$ in Section 6.2. A simple schedule can be set up as follows. The Beacon period consists of J_m minislots with length equal to β_m bits. Let D_j be the decimal number of the binary message in the jth minislot. All competing nodes listen to the Beacon period. The decimal number D_j in the jth minislot indicates which minislot in CAP has been successfully reserved. As a result, the node that transmitted the reservation at the D_jth minislot in CAP is assigned the jth time slot in CTAP. A suitable length of β_m is $\lceil \log_2 K_m \rceil$. Since CTAP consists of a pre-designed J_m time slots, the following situations can happen: $z_m < J_m$, $z_m = J_m$, and $z_m > J_m$. If $z_m < J_m$, the remaining $J_m - z_m$ time slots are unused. On the other hand, if $z_m > J_m$, the FC will randomly assign the time slots to only J_m nodes from the total z_m successful reservations, while the others are

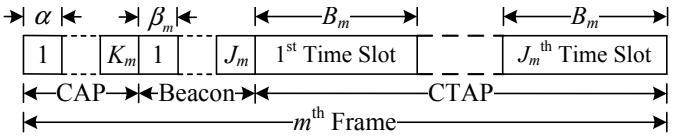

Figure 25: We modify the frame structure to reduce the effects of collisions.

neglected.

3) *CTAP:* The scheduled nodes, $s_m = \min(z_m, J_m)$, will transmit their estimates at their assigned time slots.

The proposed scheme using the modified frame structure is a function of $\hat{\boldsymbol{\sigma}}^{\mathbf{2}}$, $\mathbf{B}$, $\mathbf{J}$, and $\mathbf{K}$, where $\mathbf{J} = [J_1, \ldots, J_M]$. Similar to Section 6.2, the performance can be measured by $\bar{I}_\theta$ shown in (83), where $\mathbb{E}\{s_m\} = \mathbb{E}\{\min(z_m, J_m)\}$. Since there is no closed form for $\mathbb{E}\{\min(z_m, J_m)\}$, to facilitate in finding the optimal parameters, we will use an upper bound of $\mathbb{E}\{\min(z_m, J_m)\}$, i.e., $\min(\mathbb{E}\{z_m\}, J_m)$, instead. As a result, we have an upper bound of $\bar{I}_\theta$: $\bar{I}_\theta^U \geq \bar{I}_\theta$, where

$$\bar{I}_\theta^U(\hat{\boldsymbol{\sigma}}^{\mathbf{2}}, \mathbf{B}, \mathbf{J}, \mathbf{K}) = \sum_{m=1}^{M} \frac{\min\left(\bar{n}_m e^{-\frac{\bar{n}_m}{K_m}},\, J_m\right)}{\hat{\sigma}_m^2 + \frac{W^2}{2^{2B_m}}}. \tag{88}$$

We find $\hat{\boldsymbol{\sigma}}^{\mathbf{2}*}$, $\mathbf{B}^*$, $\mathbf{J}^*$, and $\mathbf{K}^*$ maximizing $\bar{I}_\theta^U(\hat{\boldsymbol{\sigma}}^{\mathbf{2}}, \mathbf{B}, \mathbf{J}, \mathbf{K})$ from the following time-constrained optimization problems. For the deterministic approach, we have

$$\begin{aligned} P3: \max_{\hat{\boldsymbol{\sigma}}^{\mathbf{2}}} \max_{\mathbf{B},\mathbf{J},\mathbf{K}} \; & \bar{I}_\theta^U(\hat{\boldsymbol{\sigma}}^{\mathbf{2}}, \mathbf{B}, \mathbf{J}, \mathbf{K}) \\ \text{s. t.} \; & \sum_{m=1}^{M} \left[\alpha K_m + (\beta_m + B_m) J_m\right] \leq T; \\ & B_m \geq 1,\, J_m \geq 1,\, K_m \geq 1, \forall m;\, \hat{\sigma}_0^2 < \hat{\sigma}_1^2 < \ldots < \hat{\sigma}_M^2. \end{aligned}$$

For the randomized approach, we have

$$
\begin{aligned}
P4: \quad & \max_{\hat{\boldsymbol{\sigma}}^{\mathbf{2}}} \max_{\mathbf{q}} \mathbb{E}_{\mathbf{B},\mathbf{J},\mathbf{K}}\left\{\bar{I}_{\theta}^{U}(\hat{\boldsymbol{\sigma}}^{\mathbf{2}}, \mathbf{B}, \mathbf{J}, \mathbf{K})\right\} \\
\text{s. t.} \quad & \sum_{m=1}^{M} \mathbb{E}_{B_m,J_m,K_m}\left\{\alpha K_m + (\beta_m + B_m) J_m\right\} = T; \\
& \sum_{b_m=1}^{\infty} \sum_{j_m=1}^{\infty} \sum_{k_m=1}^{\infty} q_{b_m,j_m,k_m} = 1, \, \forall m; \\
& 0 \leq q_{b_m,j_m,k_m} \leq 1, \forall b_m, j_m, k_m; \hat{\sigma}_0^2 < \hat{\sigma}_1^2 < \ldots < \hat{\sigma}_M^2,
\end{aligned}
$$

where $\mathbf{q} = [\mathbf{q}_1, \ldots, \mathbf{q}_M]$, $\mathbf{q}_m = [q_{b_m,j_m,k_m}]$, and q_{b_m,j_m,k_m} is the probability that $B_m = b_m$, $J_m = j_m$, and $K_m = k_m$, for integers $b_m, j_m, k_m \geq 1$. The solutions of Problems $P3$ and $P4$ can be found by the steps explained in Sections 6.3.1 and 6.3.2, respectively.

6.5 Numerical Results and Discussions

6.5.1 Optimal Parameter Values

In this section, we provide numerical results for the optimal parameters $\hat{\boldsymbol{\sigma}}^{\mathbf{2}*}$, $\mathbf{B}^*$, $\mathbf{J}^*$, and $\mathbf{K}^*$ obtained from the deterministic and randomized approaches explained in Section 6.3. The optimal parameter values according to both frame structures are shown in Table 6, where *Original Proposed Scheme* and *Modified Proposed Scheme* mean the proposed schemes using the frame structures shown in Fig. 24 and Fig. 25, respectively. The other variables are set up as shown in the table's caption. Note that $\bar{s}_m = \mathbb{E}\{s_m\}$ and $\bar{p}_{s,m} = \frac{\bar{s}_m}{\bar{n}_m}$ are the expected number of successfully received estimates and the probability of successfully received estimates at the FC, respectively. We see that the optimal parameter values obtained from these two approaches are only slightly different. As mentioned in Section 6.3.2, the randomized approach might return two sets of the optimal parameter values. In the context of computational complexity, the randomized approach has a much smaller computation time because it is based on linear programming.

As shown in Table 6, we notice that $B_1^* \geq \ldots \geq B_4^*$ and $\bar{p}_{s,1} \geq \ldots \geq \bar{p}_{s,4}$. These

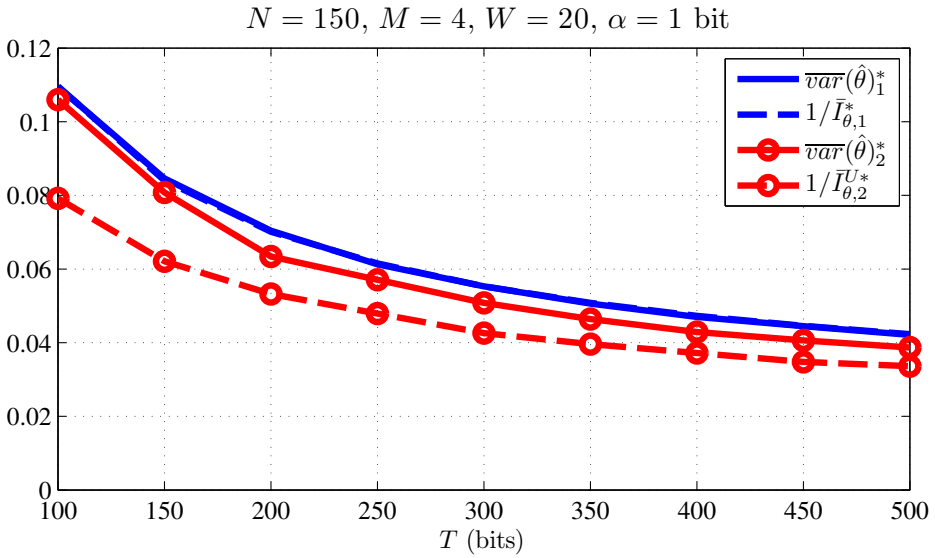

Figure 26: We verify that the estimate variances and their lower bounds (used in finding $\hat{\boldsymbol{\sigma}}^{\mathbf{2}^*}$, $\mathbf{B}^*$, $\mathbf{J}^*$, and $\mathbf{K}^*$) are acceptably close.

results suggest that the number of quantization levels and the probability of successful transmission depend on the reliabilities (noise variances) of the observations. An observation with a lower noise variance must be quantized with finer quantization and transmitted with a higher probability of successful transmission than an observation with a higher noise variance. A high probability of successful transmission in the proposed schemes can be achieved by allocating adequate K_m^* time slots larger than $\bar{n}_m$. As a result, similar to [44], the optimal thresholds $\hat{\boldsymbol{\sigma}}^{\mathbf{2}^*}$ for the proposed schemes *do not always maximize* the channel throughput. In the mth frame, since only a minislot with length α bits is wasted when a collision occurs, the modified proposed scheme allocates *more* minislots in the mth CAP period than the original proposed scheme allocates the number of time slots in the mth frame.

6.5.2 Variances of the Proposed Schemes' Estimates

Recall that we use $\bar{I}_\theta$ defined in (83) as the objective function to find $\hat{\boldsymbol{\sigma}}^{\mathbf{2}^*}$, $\mathbf{B}^*$, $\mathbf{J}^*$, and $\mathbf{K}^*$. We confirm the validity of our approximations by comparing the global estimate's variance $\mathbb{E}\{var(\hat{\theta})\}$ and the lower bound $1/\bar{I}_\theta$ in Fig. 26, where the following

Table 6: Optimal parameters: $\hat{\boldsymbol{\sigma}}^{\mathbf{2}^*}$, $\mathbf{B}^*$, $\mathbf{J}^*$ and $\mathbf{K}^*$ when $M = 4$, $N = 150$, $T = 200$ bits, $\alpha = 1$ bit, $W = 20$, $\sigma_n^2 = 0.25 + h_n$, $h_n \sim \chi^2(3)$.
Note †: $K_4^* = 10$ and $K_4^* = 11$ with probabilities 0.67 and 0.33. ‡: $(K_4^*, J_4*) = (8, 3)$ and $(K_4^*, J_4*) = (13, 4)$ with probabilities 0.63 and 0.36.

	Original Proposed Scheme							
	Deterministic Approach				Randomized Approach			
m	1	2	3	4	1	2	3	4
$\hat{\sigma}_m^{2^*}$	0.39	0.53	0.70	0.92	0.40	0.55	0.73	0.97
B_m^*	7	7	7	6	7	7	6	6
K_m^*	5	7	8	10	5	7	9	$(10, 11)^\dagger$
$\bar{n}_m$	2.05	3.43	5.00	7.65	2.18	3.73	5.71	8.12
$\bar{s}_m$	1.36	2.10	2.68	3.56	1.41	2.19	3.03	$(3.61, 3.88)$
$\bar{p}_{s,m}$	0.66	0.61	0.54	0.47	0.65	0.59	0.53	$(0.44, 0.48)$

	Modified Proposed Scheme							
	Deterministic Approach				Randomized Approach			
m	1	2	3	4	1	2	3	4
$\hat{\sigma}_m^{2^*}$	0.41	0.63	0.89	1.08	0.41	0.62	0.80	1.00
B_m^*	8	7	7	6	8	7	7	7
K_m^*	11	15	16	8	11	16	16	$(8, 13)^\ddagger$
J_m^*	2	4	5	3	2	4	4	$(3, 4)^\ddagger$
$\bar{n}_m$	2.51	5.93	8.55	6.80	2.49	5.68	5.77	6.79
$\bar{s}_m$	2.00	4.00	5.01	2.91	1.99	3.98	4.02	$(2.91, 4.03)$
$\bar{p}_{s,m}$	0.80	0.67	0.59	0.43	0.80	0.70	0.70	$(0.43, 0.59)$

notation is used in the figure and the subsequent numerical results: $\overline{var}(\hat{\theta})_1^*$ and $\overline{var}(\hat{\theta})_2^*$ are $\mathbb{E}\{var(\hat{\theta})\}$ (with using $\hat{\boldsymbol{\sigma}}^{\mathbf{2}^*}$, $\mathbf{B}^*$, $\mathbf{J}^*$, and $\mathbf{K}^*$ found by the randomized approach) of the original and modified proposed schemes (shown in Section 6.2 and 6.4, respectively); $\bar{I}_{\theta,1}^*$ and $\bar{I}_{\theta,2}^{U*}$ denote $\bar{I}_\theta(\hat{\boldsymbol{\sigma}}^{\mathbf{2}*}, \mathbf{B}^*, \mathbf{K}^*)$ in (84), and $\bar{I}_\theta^U(\hat{\boldsymbol{\sigma}}^{\mathbf{2}*}, \mathbf{B}^*, \mathbf{J}^*, \mathbf{K}^*)$ in (88), respectively. As shown in Fig. 26, the lower bound $1/\bar{I}_{\theta,1}^*$ and $\overline{var}(\hat{\theta})_1^*$ fit very well. On the other hand, there is an acceptable gap between the lower bound $1/\bar{I}_{\theta,2}^{U*}$ and $\overline{var}(\hat{\theta})_2^*$, which is reasonable since $\bar{I}_{\theta,2}^{U*}$ is an upper bound of $\bar{I}_\theta$ in (83).

The effects of the number of frames, M, the range of observations, W, the length, α, of a minislot, and the number of nodes, N, on the estimate variances $\overline{var}(\hat{\theta})_1^*$ and $\overline{var}(\hat{\theta})_2^*$ are demonstrated in Fig. 27. Note that $\hat{\boldsymbol{\sigma}}^{\mathbf{2}^*}$, $\mathbf{B}^*$, $\mathbf{J}^*$, and $\mathbf{K}^*$ are obtained from the randomized approach. The effect of M is shown in Fig. 27(a). Since the global estimate is computed from a weighted sum of the received local estimates, increasing M results in more suitable weight values. However, for the modified proposed scheme, because of the overhead CAP and Beacon (exploited in remedying the effect

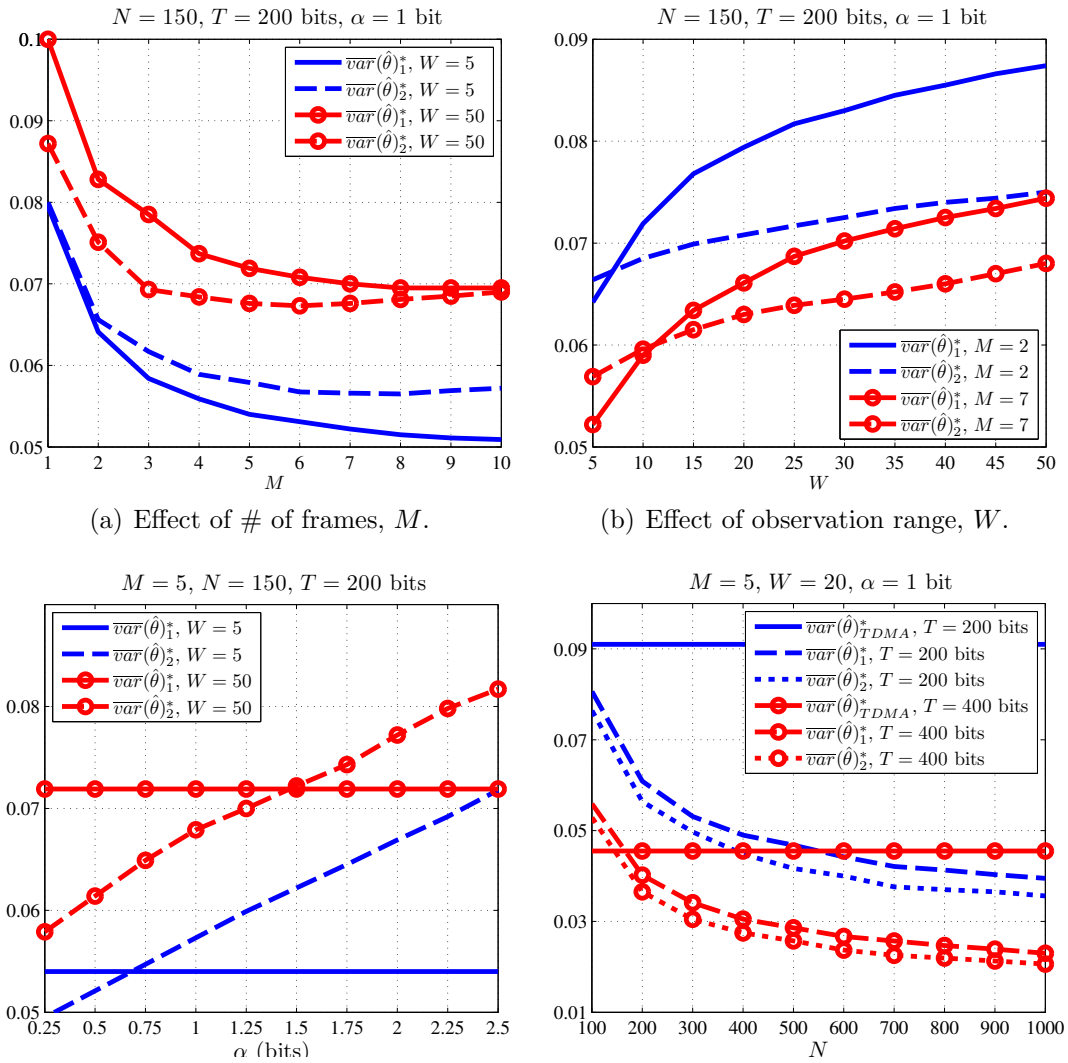

(a) Effect of # of frames, M.

(b) Effect of observation range, W.

(c) Effect of minislot length, α.

(d) Effect of # of nodes, N.

Figure 27: We show the effects of M, W, α, and N on $\overline{var}(\hat{\theta})_1^*$, the error variance for the original proposed scheme, and $\overline{var}(\hat{\theta})_2^*$, the error variance for the modified proposed scheme, when the noise variance's model is $\sigma_n^2 = 0.25 + h_n$, where $h_n \sim \chi^2(3)$.

of collisions), there exists an M^* minimizing $\overline{var}(\hat{\theta})_2^*$. We also notice that the original proposed scheme outperforms the modified proposed schemes when W is small. This effect of W is studied in Fig. 27(b). It shows that the original proposed scheme is suitable for small W. On the other hand, the modified proposed scheme is suitable for large W. It The reason can be explained as follows. Since the original proposed

scheme suffers from whole packet loss when a collision happens, it reluctantly allocates B_m^*, which is shorter than the modified proposed scheme's B_m^* (see Table 6, as an example).

The effect of α is shown in Fig. 27(c). Note that α has no effect on the original proposed scheme. In the modified proposed scheme, we partially remedy the effect of packet loss by allowing the nodes to compete for channel access only during the CAP, which consists of minislots of length α bits. Increasing α lowers the time left for the transmission of estimates in CTAP, which shortens B_m^*, and thus lowers the accuracy of the global estimate. As shown, the length α is a criterion to choose which proposed scheme should be used.

The effect of N is shown in Fig. 27(d). The proposed schemes exploit the reliability-based splitting algorithm, which is based on multi-user diversity. Increasing N helps improve the performance of the schemes since more nodes experience more reliable observations (lower noise variances). However, with a limited collection time, the improvement rate is negligible after a particular N. In addition, we show a lower bound of the estimate variances of a TDMA-based scheme, $\overline{var}\{\hat{\theta}\}_{TDMA}^{L^*} = \left(\lfloor \frac{T}{B^*} \rfloor \mathbb{E}_{\sigma^2}\left\{\frac{1}{\sigma^2+W^2/2^{2B^*}}\right\}\right)^{-1}$, where B^* minimizes this term, in Fig. 27(d). Since the TDMA-based scheme perfectly schedules the nodes' transmissions, there are no collisions happening. However, for a large number of nodes, a limited collection time, and no advanced knowledge of individual nodes' reliabilities, the TDMA-based scheme has to schedule the nodes' transmissions blindly. Comparing the performances of the proposed schemes and the TDMA-based scheme explicitly shows a tradeoff between two collection strategies: blind collection with a perfect transmission schedule and reliability-ordered collection with collisions. As shown in Fig. 27(d), the proposed schemes outperform the TDMA-based scheme for large N.

6.6 Conclusion

We proposed distributed estimation schemes incorporating a reliability-based splitting algorithm into slotted ALOHA for WSNs whose FC uses a BLUE and must collect the local estimates within a limited time. We formulated the time-constrained optimization problems and derived two numerical methods to find the optimal parameter values. In addition, a modified frame structure is introduced. The numerical results showed: the interesting characteristics of the optimal parameter values; the effects of these parameters on the proposed schemes; and the comparisons between the proposed schemes.

CHAPTER VII

CONCLUSION

7.1 Summary of Contributions

We have proposed reliability-based splitting algorithms for a large, shared-channel, single-hop WSN performing distributed detection and estimation when the network's FC is not able to collect local decisions/observations/estimates from all sensor nodes. We summarize the contributions of this dissertation as follows.

- We applied the reliability-based splitting algorithm to a time-constrained distributed detection scheme. Since no closed-forms have been found, we derived approximations of the DEP, efficacy, and ARE of the proposed scheme. We, then used these approximations to:

  (a) find the optimal parameter values (reliability thresholds and weights),

  (b) show when the proposed scheme can achieve any desired efficacy (asymptotic performance) by increasing N for a fixed T,

  (c) find the range of T over which the proposed scheme asymptotically outperforms the TDMA-based scheme.

  In addition, we showed that the reliability thresholds that maximize the channel throughput (which we call the maximum-throughput thresholds) are not always optimal. However, the numerical results showed that the maximum-throughput thresholds are optimal in many cases. When the maximum-throughput thresholds are not optimal, they yield slightly lower performance than the optimal thresholds do.

- We derived collision-aware fusion rules for a time-constrained distributed detection using the reliability-based splitting algorithm. The FC computes a global decision using both the successfully received local decisions, the number of successful time slots, and the number of collision time slots. At the present time, this is the first work introducing the use of collisions in distributed detection in the collision-channel model.

- We proposed an ordered sequential detection approach that is based on the reliability-based splitting algorithm. The reliability thresholds are dynamically adjusted based on the numbers of successful transmissions and collisions (or idle time slots). We provided an algorithm based on the one-step look-ahead rule to compute suboptimal but efficient reliability thresholds. In addition, we also considered an order sequential detection approach that is aware of packet collisions.

- We applied the reliability-based splitting algorithm to a time-constrained distributed estimation scheme whose FC uses a BLUE to compute a global estimate. The performance of the proposed scheme depends on the number of bits in an estimate, the number of time slots in a frame, and the reliability thresholds. We provided algorithms to find these parameter values. However, the algorithms might return locally optimal values. In addition, we proposed a modified frame structure to improve the performance of this distributed estimation approach.

7.2 Future Research Extensions

The work on this dissertation is focused on a cross-layer design between random access and distributed detection/estimation applications. It has opened up many possible research extensions, including:

- *Physical layer:* In this work, we studied the proposed schemes in a pessimistic channel model; namely, one in which collided packets are lost. If, however, the FC is still able to decode the local decisions inside the collided packets up to a certain signal-to-interference ratio, as is the case in multipacket reception [76], the performances of the proposed schemes would be improved, but different sets of optimal thresholds would be required. In addition, the knowledge of the fading-channel's statistics will lead to a different fusion rule.

- *Other distributed detection/estimation strategies:* The reliability-based splitting algorithm has enabled the use of the ordered-transmission strategy [13] in finite-bandwidth distributed detection and estimation. It is interesting to apply the reliability-based splitting algorithm to other distributed detection and estimation applications incorporating the ordered-transmission strategy – including, for example, repeated significance tests [34,35] and sequential estimation [11,34].

- *CSMA:* Since a short packet length (equal to a time slot) is assumed, we used slotted ALOHA as the channel access protocol. If we consider an application with a large number of events/parameters, which may result in long packet lengths, using a CSMA protocol will definitely improve the performance of all of the distributed detection/estimation applications we have considered.

APPENDICES

APPENDIX A

POWER ALLOCATION FOR DISTRIBUTED DETECTION IN A MULTIPLE-RING CLUSTER

In addition to the distributed detection and estimation schemes proposed in Chapter 2 to 6, we also studied transmission power allocation in distributed detection. The details are presented as follows.

A.1 Introduction

In distributed detection, a number of battery-powered sensor nodes are dispersed over or move around a geographic area to detect events. The local decisions made by these nodes are collected over wireless channels by a Fusion Center (FC) to produce a reliable global decision [12,79]. Traditionally, each node will transmit its decision with the same power regardless of local decision quality and channel gains, so each node's contribution to the final Detection Error Probability (DEP) can vary significantly. This uniform Power Allocation (PA) strategy is inefficient; significant power might be spent on transmitting very low quality local decisions over poor channels. We propose *intelligent* PA strategies to overcome this problem.

The problem of PA has been studied extensively in distributed detection/estimation [26,84,88,89,98]. By formulating and solving optimization problems, the optimal PA is found in the form of a water-filling solution [26, 84, 88, 89] that depends on the observation noise and channel quality at the nodes. Some PA strategies for distributed detection have been proposed. In [98], distributed detection with binary local decisions was considered. A weighted water-filling algorithm was proposed to maximize the sum of the J-divergence of all received signals at the FC. The PA for distributed

detection with amplify-and-forward nodes was examined in [84], and an analytical expression for the optimal power was derived. Both [98] and [84] assumed that all nodes' *instantaneous* observation quality and channel gains are known at the FC.

In this appendix, we consider the PA for distributed detection in a Wireless Sensor Network (WSN) when observation and channel *statistics* are known. We assume that nodes in the WSN form a single-hop, multiple-ring cluster with the FC at the center. The effect of node-FC distances is included and modeled as path loss. The nodes observe an event and make initial binary local decisions which are transmitted through parallel fading channels. A global decision is made at the FC from a weighted sum of the hard decisions of the received signals. We formulate optimization problems to find a PA that maximizes the total expected *Deflection Coefficient* (DC) of the received signals [62]. By using the Karush-Kuhn-Tucker (KKT) conditions, we obtain two explicit expressions, (93) and (96), for the optimal power under two different constraints: a total power constraint and a per-ring power constraint. Furthermore, whether a node will transmit its local decision depends on the product of the local decision quality and the channel gain, as shown in (94) and (97).

The proposed PA strategies perform two steps: censoring [65] and amplifying. First, only the nodes with observation and channel Signal-to-Noise Ratios (SNRs) exceeding the requisite thresholds are allowed to send their local decisions (censoring step). Second, these nodes will transmit with the proposed transmission power (amplifying step) to combat the channel inhospitality. As a result, the local decisions received at the FC according to the proposed PA are more reliable than those from the uniform PA.

The appendix is organized as follows. Section A.2 illustrates the system model and formulates the DEP. The proposed PA strategies are explained and derived in Section A.3. In Section A.4, the DEP comparisons between the uniform PA and the proposed PA are shown for various parameters. Finally, conclusions are given in

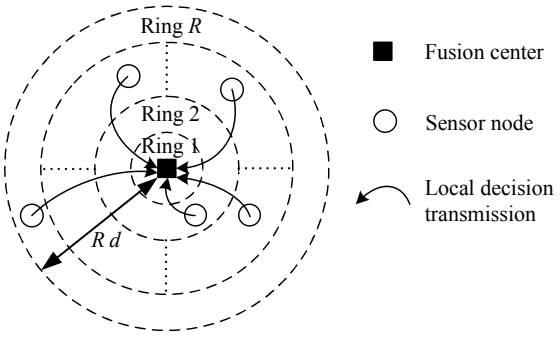

Figure 28: Network topology: a single-hop, R-ring cluster.

Section A.5.

A.2 Assumptions and System Model

We consider a binary hypothesis testing problem in a circular monitoring area where N sensor nodes are uniformly deployed with a density δ; see Fig. 28. These N nodes form an R-ring cluster with a FC at the center. We define the rth ring as the circular area between the radii $(r-1)d$ and rd, where $r = 1, 2, \ldots, R$ and d is an arbitrary distance. Then, the number of nodes within the rth ring, N_r, is equal to $\delta\pi(2r-1)d^2$. Note that $d = 1$ is used in Section A.4.

The nth node in the rth ring has the following observation $x_{n,r}$ under two hypotheses; $H_0 : x_{n,r} = v_{n,r}$ and $H_1 : x_{n,r} = \sqrt{\xi_{n,r}} + v_{n,r}$, where the noise $v_{n,r}$ is modeled as an Independent Identically Distributed (IID) Gaussian random variable with zero mean and unit variance and $\xi_{n,r}$ is the observation SNR modeled as an IID random variable with the Probability Density Function (PDF) $f_\xi(\xi_{n,r})$. Then, the observations $\{x_{n,r}\}$ are homogeneous and independent. We assume, for simplicity only, that $P(H_0) = P(H_1) = 0.5$.

The system model is shown in Fig. 29. A binary decision $u_{n,r}$ is made from the optimum decision rule given $\xi_{n,r}$, where $u_{n,r} = 1$ if $x_{n,r} \geq \sqrt{\xi_{n,r}}/2$; otherwise,

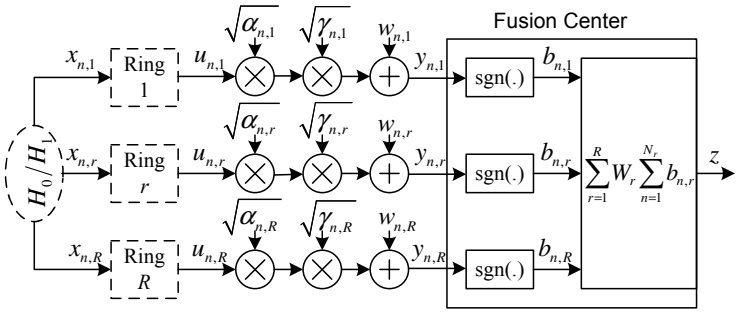

Figure 29: System model.

$u_{n,r} = -1$. Then, the conditional Probability Mass Functions (PMFs) of $u_{n,r}$ are

$$P(u_{n,r} = 1|H_1, \xi_{n,r}) = P(u_{n,r} = -1|H_0, \xi_{n,r}) = \Phi\left(\sqrt{\xi_{n,r}}/2\right),$$
$$P(u_{n,r} = 1|H_0, \xi_{n,r}) = P(u_{n,r} = -1|H_1, \xi_{n,r}) = \Phi\left(-\sqrt{\xi_{n,r}}/2\right),$$

where $\Phi(\cdot)$ is the Gaussian Cumulative Distribution Function.

The local decision $u_{n,r}$ is amplified with gain $\sqrt{\alpha_{n,r}}$ and, then, transmitted through fading and Gaussian additive parallel access channels. The received baseband signal at the FC, $y_{n,r}$, can be expressed as: $y_{n,r} = u_{n,r}\sqrt{\alpha_{n,r}\gamma_{n,r}} + w_{n,r}$, where the noise $w_{n,r}$ is an IID Gaussian random variable with zero mean and unit variance and the channel SNR $\gamma_{n,r}$ is an independent random variable from fading effects. We assume that, within the rth ring, $\gamma_{n,r}$ is an IID random variable with the PDF $f_{\gamma_r}(\gamma_{n,r})$ with mean $\bar{\gamma}_r$. Furthermore, according to a simple path-loss model, we have $\bar{\gamma}_r = G\bar{\gamma}_1\left(\frac{0.5}{r-0.5}\right)^a$, where G is an equipment gain, a is the attenuation index, and $r - 0.5$ is used as the average distance from the FC for the rth ring. Note that $G = 1$ and $a = 2$ is used in Section A.4. Then, $y_{n,r}$ is IID within the same ring and also independent among the rings. The conditional PDFs of $y_{n,r}$ are written as the following Gaussian mixture PDFs, for $i = 0$ or 1,

$$f_{y_r}(y_{n,r}|H_i, \xi_{n,r}, \gamma_{n,r}) = \sum_{u_{n,r}} f_{y_r}(y_{n,r}|u_{n,r}, \gamma_{n,r}) P(u_{n,r}|H_i, \xi_{n,r}),$$

where $f_{y_r}(y_{n,r}|u_{n,r}, \gamma_{n,r}) \sim \mathcal{N}\left(u_{n,r}\sqrt{\alpha_{n,r}\gamma_{n,r}}, 1\right)$.

As shown in the next section, the proposed PA strategies have the thresholds $\hat{\xi}$ and $\hat{\gamma}_r$ such that only the nodes whose $\xi_{n,r} > \hat{\xi}$ and $\gamma_{n,r} > \hat{\gamma}_r$ will transmit their local decisions to the FC. As a result, the number of active nodes in the rth ring, $N_{A,r}$, is less than or equal to N_r and the FC receives $N_{A,r}$ local decisions from the rth ring. In comparison, for the uniform PA, $\hat{\xi} = 0$, $\hat{\gamma}_r = 0$, and $N_{A,r} = N_r$.

At the FC, the received signals $\{y_{n,r}\}$ are decoded into binary bits $\{b_{n,r}\}$, where $b_{n,r} = \mathrm{sgn}(y_{n,r}) \in \{+1, -1\}$ and the operator $\mathrm{sgn}(\cdot)$ is the sign function. The conditional probabilities of $b_{n,r}$ are

$$\begin{aligned} P(b_{n,r} = 1|H_1, \xi_{n,r}, \gamma_{n,r}) &= P(b_{n,r} = -1|H_0, \xi_{n,r}, \gamma_{n,r}) \\ &= \sum_{u\in\{1,-1\}} \Phi\left(u\sqrt{\alpha_{r,n}\gamma_{n,r}}\right) \Phi\left(u\sqrt{\xi_{n,r}}/2\right), \end{aligned}$$

and, $P(b_{n,r} = 1|H_0, \xi_{n,r}, \gamma_{n,r}) = P(b_{n,r} = -1|H_1, \xi_{n,r}, \gamma_{n,r}) = 1 - P(b_{n,r} = 1|H_1, \xi_{n,r}, \gamma_{n,r})$. Since $y_{n,r}$ is independent and homogeneous within the same ring, the average conditional probability of $b_{n,r}$ for the rth ring is

$$\begin{aligned} P(b_{n,r} = 1|H_1) &= P(b_{n,r} = -1|H_0) \\ &= \sum_{u\in\{1,-1\}} \mathbb{E}_{\xi,\gamma_r}^{\hat{\xi},\hat{\gamma}_r} \left\{ \Phi\left(u\sqrt{\alpha_{r,n}\gamma_{n,r}}\right) \Phi\left(u\sqrt{\xi_{n,r}}/2\right) \right\}, \end{aligned} \tag{89}$$

where $\mathbb{E}_{\xi,\gamma_r}^{\hat{\xi},\hat{\gamma}_r}\{\cdot\} = \mathbb{E}_{\xi,\gamma_r}\left\{ \cdot \,\middle|\, \xi > \hat{\xi}, \gamma_r > \hat{\gamma}_r \right\}$.[1] Similarly, $P(b_{n,r} = 1|H_0) = P(b_{n,r} = -1|H_1) = 1 - P(b_{n,r} = 1|H_1)$. In other words, (89) is the average probability of detection $\bar{P}_{D,r}$ of the *received* local decisions from the rth ring at the FC. Then, $b_{n,r}$ is a Bernoulli random variable with the success probability $\bar{P}_{D,r}$.

The test statistic z at the FC is constructed from a weighted sum of $\{b_{n,r}\}$, i.e., $z = \sum_{r=1}^{R} W_r \sum_{n=1}^{N_r} b_{n,r}$, where W_r is a weight for $b_{n,r}$ from the rth ring. The optimal weight W_r^* can be obtained via the Log-Likelihood Ratio (LLR): $W_r^* = \log \frac{\bar{P}_{D,r}}{1-\bar{P}_{D,r}}$. The DEP of the global decision P_E is $P(H_1)P(z < 0|H_1) + P(H_0)P(z \geq 0|H_0)$ and

[1] The notation $\mathbb{E}_{s,t}\{\cdot\,|\,\cdot\}$ is the conditional expectation operator with respect to the random variables s and t.

can be computed from

$$P_E = \sum_{\sum_{r=1}^{R} W_r n_r < \tau} \prod_{r=1}^{R} \binom{N_{A,r}}{n_r} \bar{P}_{D,r}^{n_r} \left(1 - \bar{P}_{D,r}\right)^{N_{A,r} - n_r}, \tag{90}$$

where $\tau = \frac{\sum_{r=1}^{R} W_r N_{A,r}}{2}$, and n_r is the number of $b_{n,r} = 1$.

A.3 Proposed Power Allocation with Known Observation and Channel Statistics

Since the analysis is based on knowing statistics, i.e., PDFs, we declare the following changes on the variables. According to the homogeneous assumptions on the observation SNR for all nodes and the channel SNR for all nodes in the same ring, we will use ξ, γ_r, and y_r instead of $\xi_{n,r}$, $\gamma_{n,r}$, and $y_{n,r}$, respectively, from now on.

We are interested in finding a PA that improves the DEP P_E shown in (90), which can be formulated as an optimization problem. However, using the DEP as the objective function leads to a complicated and intractable solution. Instead, other functions related to the DEP have been used as criteria in performance analysis; e.g., divergence [98], error exponent [68], and DC [74].

In this paper, we will use the DC of the received signal y_r,

$$D_{y_r} = \frac{\left(\mathbb{E}\left\{y_r | H_1, \xi, \gamma_r\right\} - \mathbb{E}\left\{y_r | H_0, \xi, \gamma_r\right\}\right)^2}{\mathbb{V}ar\left\{y_r | H_0, \xi, \gamma_r\right\}},$$

as a function that α_r maximizes, where

$$D_{y_r} = \frac{4\left[2\Phi\left(\sqrt{\xi}/2\right) - 1\right]^2 \gamma_r \alpha_r}{1 + 4\Phi\left(\sqrt{\xi}/2\right)\left[1 - \Phi\left(\sqrt{\xi}/2\right)\right]\gamma_r \alpha_r}, \tag{91}$$

which is a measure of the FC's ability to differentiate the two hypotheses based on the analog signals, y_r, received from nodes in the rth ring. The underlying idea is that higher D_{y_r} increases $\bar{P}_{D,r}$ and, thus, helps improve the DEP. Note that D_{y_r} in (91) is a direct function of α_r, while α_r in (90) appears only in argument of Φ as shown in (89). The effect of this fact will be discussed below and can be observed in Section A.4.

Since the statistics are given, we are working under long-term average conditions. Let $\{\alpha_r^*\}$ be the proposed PA strategies which are applied to all nodes in the rth ring. They are found by maximizing the total sum of the $\mathbb{E}_{\xi,\gamma_r}\{D_{y_r}\}$ of all received signals at the FC. Furthermore, two different constraints are considered: a total power constraint and a per-ring power constraint.

First, we formulate the optimization problem with the long-term, total power constraint as follows:

$$\begin{aligned} &\max_{\{\alpha_r\}} \sum_{r=1}^{R} N_r \mathbb{E}_{\xi,\gamma_r}\{D_{y_r}\} \\ &\text{s. t.} \quad \sum_{r=1}^{R} N_r \mathbb{E}_{\xi,\gamma_r}\{\alpha_r\} \leq \mathcal{P}_T \text{ and } \alpha_r \geq 0, \forall r, \end{aligned} \tag{92}$$

where $\mathcal{P}_T$ is the total power, and $\mathbb{E}_{\xi,\gamma_r}\{\cdot\}$ is a joint expectation with respect to ξ and γ_r. Since (92) is a convex optimization problem, the optimal power α_r^* can be found by applying the KKT conditions and in the form of a water-filling solution. The results are summarized in the theorem below. Because of the space limitation, we omit the proof but techniques similar to those used in [26, 84, 88, 89] are applied. Note that in Theorem 1, the optimal power α^* is independent of r.

Theorem 1. *Consider an R-ring WSN cluster monitoring an event as modeled in Section A.2. Let ξ and γ be the observation SNR and channel SNR, respectively, at a node. The optimal power α^*, which is the strategy used by all nodes, for the problem* (92) *is*

$$\alpha^* = \frac{1}{4\Phi\left(\frac{\sqrt{\xi}}{2}\right)\left[1-\Phi\left(\frac{\sqrt{\xi}}{2}\right)\right]\gamma}\left[\frac{2\left[2\Phi\left(\frac{\sqrt{\xi}}{2}\right)-1\right]\sqrt{\gamma}}{\sqrt{\lambda}}-1\right], \tag{93}$$

if $\xi > \hat{\xi}$ and $\gamma > \hat{\gamma}$; $\alpha^* = 0$, otherwise. The Lagrange multiplier λ is computed from

$$\sqrt{\lambda} = \frac{\sum_{r=1}^{R} N_r \mathbb{I}_{\xi,\gamma_r}^{(\hat{\xi},\hat{\gamma})}\left\{\frac{\left[2\Phi\left(\sqrt{\xi}/2\right)-1\right]}{2\Phi\left(\sqrt{\xi}/2\right)\left[1-\Phi\left(\sqrt{\xi}/2\right)\right]\sqrt{\gamma_r}}\right\}}{\mathcal{P}_T + \sum_{r=1}^{R} N_r \mathbb{I}_{\xi,\gamma_r}^{(\hat{\xi},\hat{\gamma})}\left\{\frac{1}{4\Phi\left(\sqrt{\xi}/2\right)\left[1-\Phi\left(\sqrt{\xi}/2\right)\right]\gamma_r}\right\}},$$

$\mathbb{I}_{\xi,\gamma_r}^{(\hat{\xi},\hat{\gamma})}\{\cdot\}$ *is defined for every function* $H(\xi,\gamma_r)$ *as*

$$\mathbb{I}_{\xi,\gamma_r}^{(\hat{\xi},\hat{\gamma})}\{H(\xi,\gamma_r)\} = \int_{\hat{\xi}}^{\infty}\int_{\hat{\gamma}}^{\infty} H(\xi,\gamma_r) f_{\xi}(\xi) f_{\gamma_r}(\gamma_r)\, d\xi d\gamma_r.$$

The thresholds $\hat{\xi}$ *and* $\hat{\gamma}$ *are found from the following equality:*

$$2\left[2\Phi\left(\sqrt{\hat{\xi}}\big/2\right)-1\right]\sqrt{\hat{\gamma}} = \sqrt{\lambda}. \tag{94}$$

From Theorem 1, a node will compare its measured ξ and γ to the thresholds $\hat{\xi}$ and $\hat{\gamma}$ to decide whether its local decision is worth transmitting (censoring). When $\xi > \hat{\xi}$ and $\gamma > \hat{\gamma}$, the optimal power α^* is spent transmitting the local decision (amplifying). Note that the criterion used to find the thresholds is a product of the local decision quality $\left[2\Phi\big(\sqrt{\xi}/2\big)-1\right]$ and the channel gain $\sqrt{\gamma}$.

However, two immediate difficulties arise. First, under a high observation SNR, a very large λ (i.e., large $\hat{\xi}$ and $\hat{\gamma}$) is obtained. Then, there are only a few active nodes and they use very high transmission power. This results in lowering the DEP (which will be shown in Section 2.6) and inappropriately consuming nodes' power. Imposing a sensor power constraint can alleviate this difficulty.

Second, since the nodes close to the FC suffer little path loss, under the homogeneous observation SNR, these nodes will be frequently active and their power will be depleted faster than the nodes farther away from the FC. This *power-depletion fairness* can be solved by imposing a per-ring power constraint. The corresponding optimization problem can be formulated as

$$\begin{aligned} &\max_{\{\alpha_r\}} \sum_{r=1}^{R} N_r \mathbb{E}_{\xi,\gamma_r}\{D_{y_r}\} \\ &\text{s. t.} \quad N_r \mathbb{E}_{\xi,\gamma_r}\{\alpha_r\} \le \mathcal{P}_r \text{ and } \alpha_r \ge 0,\ \forall r, \end{aligned} \tag{95}$$

where $\mathcal{P}_r$ is the total power for the rth ring. Similarly, since (95) is a convex optimization problem, the solution α_r^* can be found by using the KKT conditions and summarized as follows.

Theorem 2. *Consider an R-ring WSN cluster monitoring an event as modeled in Section A.2. Let ξ and γ_r be the observation SNR and channel SNR, respectively, at a node in the rth ring. The optimal power α_r^*, which is the strategy applied to the nodes in the rth ring, for the problem* (95) *is*

$$\alpha_r^* = \frac{1}{4\Phi\left(\frac{\sqrt{\xi}}{2}\right)\left[1-\Phi\left(\frac{\sqrt{\xi}}{2}\right)\right]\gamma_r}\left[\frac{2\left[2\Phi\left(\frac{\sqrt{\xi}}{2}\right)-1\right]\sqrt{\gamma_r}}{\sqrt{\lambda_r}}-1\right], \tag{96}$$

if $\xi > \hat{\xi}$ and $\gamma_r > \hat{\gamma_r}$; $\alpha_r^* = 0$, otherwise. The Lagrange multiplier λ_r is computed from

$$\sqrt{\lambda_r} = \frac{N_r \mathbb{I}_{\xi,\gamma_r}^{(\hat{\xi},\hat{\gamma})}\left\{\frac{\left[2\Phi(\sqrt{\xi}/2)-1\right]}{2\Phi(\sqrt{\xi}/2)\left[1-\Phi(\sqrt{\xi}/2)\right]\sqrt{\gamma_r}}\right\}}{\mathcal{P}_r + N_r \mathbb{I}_{\xi,\gamma_r}^{(\hat{\xi},\hat{\gamma})}\left\{\frac{1}{4\Phi(\sqrt{\xi}/2)\left[1-\Phi(\sqrt{\xi}/2)\right]\gamma_r}\right\}}.$$

The thresholds $\hat{\xi}$ and $\hat{\gamma}_r$ are found from the following equality:

$$2\left[2\Phi\left(\sqrt{\hat{\xi}}\Big/2\right)-1\right]\sqrt{\hat{\gamma}_r} = \sqrt{\lambda_r}. \tag{97}$$

A.4 Numerical Results and Discussions

This section illustrates the DEP improvement according to the proposed PA (93) and (96) by comparison with the uniform PA. The DEP is computed from (90). We assume that the observation SNR is homogeneous to all nodes and deterministic; i.e., a constant. The channel is suffering from Rayleigh fading and, then, the PDF of the channel SNR of the nodes in the rth ring is $f_{\gamma_r}(\gamma_r) = \frac{1}{\bar{\gamma}_r} e^{\gamma_r/\bar{\gamma}_r}$. Note that the unit dB of the power is with respect to the channel noise variance.

First we consider a single-ring cluster and study the effect of ξ, $\bar{\gamma} = \bar{\gamma}_1$, and N on the DEPs. Note that (93) and (96) are equivalent for this case since $R = 1$. When the proposed PA is used, because of the censoring property, not all nodes are active. We have found that the number of active nodes is proportional to $\bar{\gamma}$ and inversely proportional to ξ. When the channel is good, low power will be spent per node, which results in a large number of active nodes. On the other hand, when the observations

are good (i.e., good local decisions), only a few nodes are active and a large amount of power (per node) will be spent to combat the channel adversity.

We compare the DEPs obtained by using the proposed PA and the uniform PA in Figs. 30 and 31. In Fig. 30, the impacts of ξ and $\bar{\gamma}$ on the DEPs are presented. Compared to the DEPs from the uniform PA, significant DEP improvement is obtained by using the proposed PA and is higher for better $\bar{\gamma}$. Interestingly, the proposed PA gives a deteriorated DEP when $\xi = 16$ dB. The reason is that, in this case, the proposed PA activates only a few nodes. This is a side effect of optimizing the DC instead of the DEP, as mentioned in Section A.3.

The impact of N on the DEPs is considered in Fig. 31. The DEPs from the uniform PA slightly improve when N increases. Because of a fixed total power, increasing N lowers the quality of the received local decisions at the FC due to spending lower uniform power per node. As seen, there exist points such that increasing N does not improve the DEPs for the uniform PA anymore. In comparison, for the proposed PA, increasing N results in more nodes experiencing good observation and channel SNRs. We see that the DEPs from the proposed PA have significantly lower saturation points.

Second, we show the DEPs of an R-ring cluster with a uniform node density for two cases: fixed number of nodes and fixed node density. In each case, the DEPs obtained from the uniform PA (U), the proposed PA under the total power constraint (P-TP), and the proposed PA under the per-ring power constraint (P-RP) (each with both the uniform weights $\{W_r = 1\}$ and the optimal weights $\{W_r^*\}$) are compared. Fig. 32(a) shows the DEPs when a fixed number of nodes, $N = 150$, is deployed while R increases. For an R-ring cluster, we have $N_r = \frac{(2r-1)}{R^2}N$ and the per-ring power $\mathcal{P}_r = \frac{N_r}{N}\mathcal{P}_T$ in (95). Increasing R is equivalent to increasing the observed area, and, then, more nodes are suffering inferior channel SNRs from larger path loss. Both proposed PA strategies (P-RP and P-TP) yield better DEPs than the uniform PA

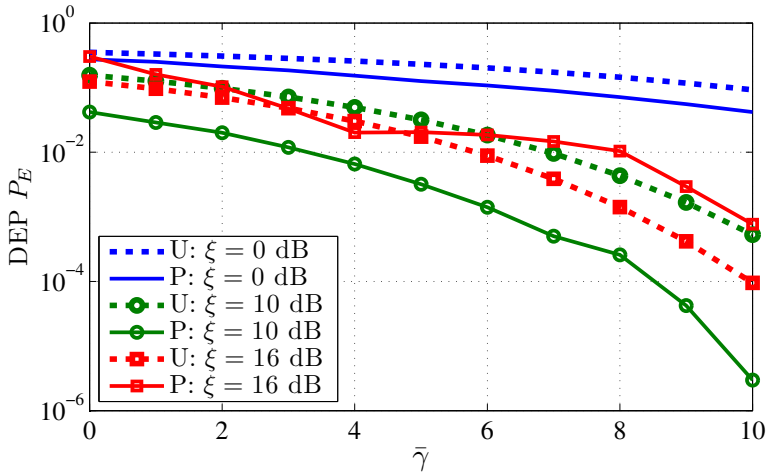

Figure 30: The DEP P_E versus the mean of the channel SNR $\bar{\gamma}$ when $R = 1$, $\mathcal{P}_T = 5$ dB, $N = 100$. ξ is the observation SNR, U is the uniform PA, and P is the proposed PA with the total power constraint. Since $R = 1$, the two proposed PA strategies are equivalent.

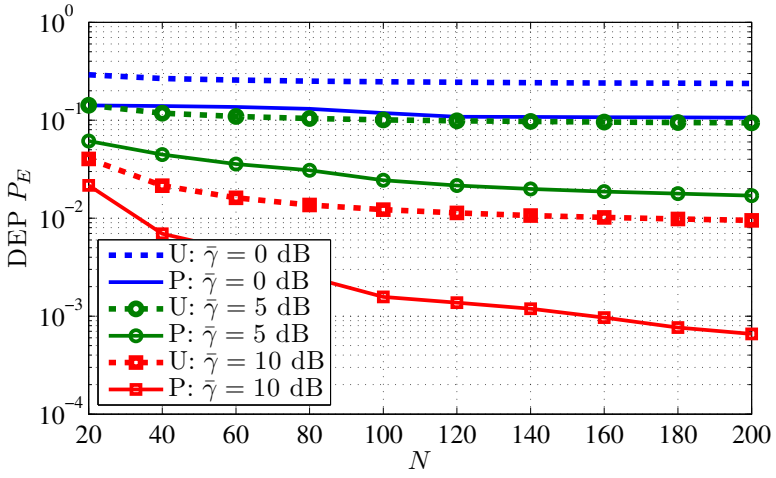

Figure 31: The DEP P_E versus the number of nodes N when $R = 1$, $\mathcal{P}_T = 5$ dB, and $\xi = 5$ dB. ξ is the observation SNR, $\bar{\gamma}$ is the mean of the channel SNR, U is the uniform PA, and P is the proposed PA with the total power constraint. Since $R = 1$, the two proposed PA strategies are equivalent.

does, since the proposed PA strategies will allow only the nodes with good observation and channel SNRs to be active and sharing the pooled power ($\mathcal{P}_T$ or $\mathcal{P}_r$). As a result, the FC receives only good local decisions with small channel errors.

Fig. 32(b) shows the DEPs for a fixed node density, i.e., $N_r = 10(2r - 1)$, and $\mathcal{P}_r = N_r \mathcal{P}_S$, where $\mathcal{P}_S$ is the power spent per node for the uniform PA. The number of

nodes and $\mathcal{P}_T$ (for P-TP) uniformly increase as R increases. Unlike the fixed number of nodes, increasing R provides more nodes and thus greater total power. Since the pooled power $\mathcal{P}_T$ and $\mathcal{P}_r$ are spent *intelligently* on sending good local decisions through good channels, the DEPs from the proposed strategies (P-RP, P-TP) yield large DEP improvements when compared with the DEPs from the uniform PA. For the uniform PA, since the received local decisions from the nodes in a large r (far from the FC) are susceptible to channel error, its DEPs slowly improve as R increases unless the optimal weights $\{W_r^*\}$ are used.

A.5 Conclusion

We have proposed two PA strategies for distributed detection in an R-ring cluster for homogeneous event observation, where the effects of fading, path loss, and observation error are also included. In the proposed strategies, two steps, censoring and amplifying, are performed; the nodes with observation and channel SNRs larger than the requisite thresholds send the local decisions with the proposed power. By using the power intelligently, the proposed PA strategies provide significantly better DEPs over the uniform PA under the considered parameters.

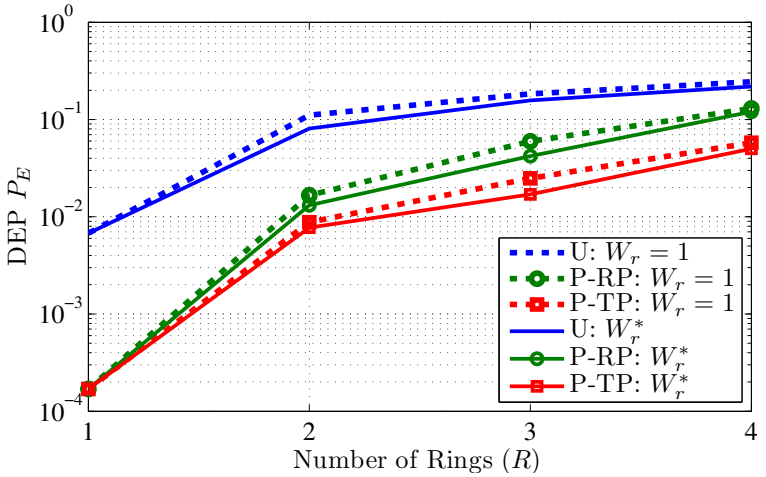

(a) For a fixed number of nodes, 150, when $\bar{\gamma}_1 = 10$ dB, $\xi = 5$ dB, and $\mathcal{P}_T = 5$ dB.

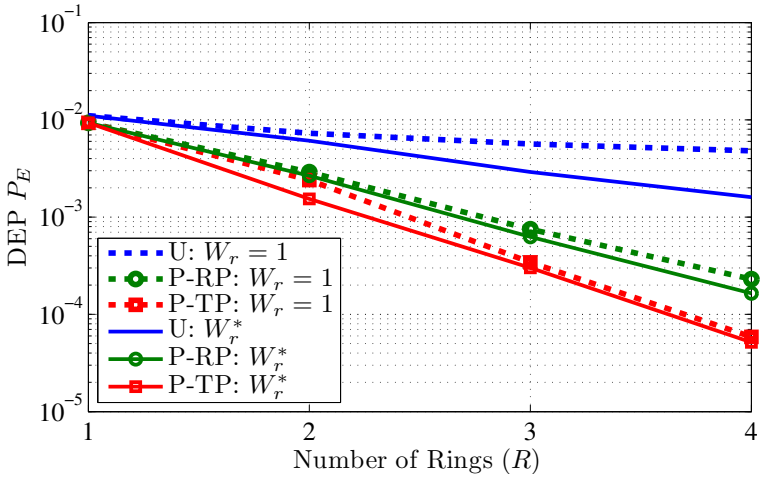

(b) For a fixed node density ($N_1 = 10$, $N_2 = 30$, $N_3 = 50$, and $N_4 = 70$) when $\bar{\gamma}_1 = 10$ dB, $\xi = 5$ dB, and $\mathcal{P}_S = -5$ dB.

Figure 32: The DEP P_E versus the number of rings (R). $\{W_r\}$ are the wights. $\{W_r^*\}$ are the optimal weights. U is the uniform PA. P-RP and P-TP are the proposed PAs with the per-ring power constraint and with the total power constraint, respectively.

APPENDIX B

EXPECTED NUMBERS OF SUCCESSFUL TIME SLOTS AND IDLE TIME SLOTS

Let us define the following variables:

- n is the number of nodes attempting transmissions in a frame,
- K is the number of time slots in a frame,
- z_S is the number of successful time slots, $0 \leq z_S \leq \min(K, n)$,
- z_I is the number of idle time slots, $0 \leq z_I \leq K$.

B.1 Expected Number of Successful Time Slots

From [31, p. 112], the conditional PMF of z_S given n is

$$f(z_S|n) = \frac{(-1)^{z_S} K!n!}{z_S! K^n} \sum_{i \geq z_S}^{\tilde{K}} \frac{(-1)^i (K-i)^{n-i}}{(i-z_S)!(K-i)!(n-i)!},$$

where $\tilde{K} = \min(K, n)$. The conditional expectation of z_S, $\mathbb{E}\{z_S|n\}$ can be written as

$$\mathbb{E}\{z_S|n\} = \sum_{z_S=1}^{\tilde{K}} \frac{K!n!}{(z_S-1)!K^n} \sum_{i=0}^{\tilde{K}-z_S} \frac{(-1)^i (K-i-z_S)^{n-i-z_S}}{i!(K-i-z_S)!(n-i-z_S)!}.$$

We can rewrite $\mathbb{E}\{z_S|n\}$ as $\mathbb{E}\{z_S|n\} = \sum_{c=1}^{\tilde{K}} A_c$, where

$$\begin{aligned} A_c &= \sum_{z_S+i=c} \left[\frac{K!n!}{(z_S-1)!K^n}\right] \left[\frac{(-1)^i (K-c)^{n-c}}{i!(K-c)!(n-c)!}\right], \\ &= \frac{K!n!(K-c)^{n-c}}{K^n (K-c)!(n-c)!} \sum_{z_S+i=c} \frac{(-1)^i}{(z_S-1)!i!}, \end{aligned}$$

for $1 \leq z_S \leq \tilde{K}$ and $0 \leq i \leq \tilde{K} - z_S$. For $2 \leq c \leq \tilde{K}$, we have

$$\sum_{z_S+i=c} \frac{(-1)^i}{(z_S-1)!i!} = \frac{1}{(c-1)!} \sum_{i=0}^{c-1} \frac{(-1)^i (c-1)!}{(c-1-i)!i!} = 0.$$

$$\mathbb{E}\{z_S|n\} = A_1 = \frac{K!n!(K-1)^{n-1}}{K^n(K-1)!(n-1)!} = n\left(1-\frac{1}{K}\right)^{n-1}.$$

B.2 Expected Number of Idle Time Slots

From [31, p. 102], the conditional PMF of z_I given n is

$$f(z_I|n) = \binom{K}{z_I} \sum_{i=0}^{K-z_I} (-1)^i \binom{K-z_I}{i} \left(1-\frac{z_I+i}{K}\right)^n.$$

The conditional expectation of z_S, $\mathbb{E}\{z_I|n\}$ can be written as

$$\begin{aligned}\mathbb{E}\big\{z_I\big|n\big\} &= \sum_{z_I=1}^{K} z_I \binom{K}{z_I} \sum_{i=0}^{K-z_I} (-1)^i \binom{K-z_I}{i} \left(1-\frac{z_I+i}{K}\right)^n, \\ &= \sum_{c=1}^{K} \frac{K!}{(K-c)!} \left(1-\frac{c}{K}\right)^n \sum_{z_I+i=c} \frac{(-1)^i}{(z_I-1)!i!}.\end{aligned}$$

We can show that $\sum_{z_I+i=c} \frac{(-1)^i}{(z_I-1)!i!}$ is 1 for $c=1$, and 0 for $2 \leq c \leq K$ as follows:

$$\begin{aligned}\sum_{z_I+i=c} \frac{(-1)^i}{(z_I-1)!i!} &= \sum_{z_I-1}^{c} \frac{(-1)^{(c-z_I)}}{(z_I-1)!(c-z_I)!}, \\ &= \sum_{z_I=0}^{c-1} \frac{(-1)^{(c-z_I-1)}}{z_I!(c-1-z_I)!} = \frac{(-1)^{(c-1)}}{(c-1)!} \sum_{z_I=0}^{c-1} (-1)^{z_I} \binom{c-1}{z_I},\end{aligned}$$

where the series in the last term is equal to 1 for $c=1$, and 0 for $2 \leq c \leq K$. Therefore, we have $\mathbb{E}\big\{z_I\big|n\big\} = K\left(1-\frac{1}{K}\right)^n$.

APPENDIX C

OPTIMAL FUSION RULE

Let a_m, b_m, and c_m be the numbers of $d_{k,m} = 1$, $d_{k,m} = -1$, and $d_{k,m} = 0$, respectively, where $c_m = K_m - a_m - b_m$. From Bayes' rule, we have

$$\log \frac{f\big(a_1, b_1, \ldots, a_M, b_M | H_1\big)}{f\big(a_1, b_1, \ldots, a_M, b_M | H_0\big)} \underset{H_0}{\overset{H_1}{\gtrless}} \log \frac{\Pr(H_0)}{\Pr(H_1)}. \tag{98}$$

The conditional probability $f\big(a_1, b_1, \ldots, a_M, b_M | H_i\big)$ is

$$\sum \cdots \sum_{n_1+\ldots+n_{M+1}=N} \prod_{m=1}^{M} f(a_m, b_m | n_m, H_i) f(n_1, \ldots, n_M). \tag{99}$$

By substituting (2), (5) and (99) into (98), and after some mathematical manipulation, we obtain

$$\begin{aligned} &\log \left[\frac{\sum \cdots \sum_{n_1+\ldots+n_{M+1}=N} \prod_{m=1}^{M} p_{s,m}^{a_m+b_m} \big(1-p_{s,m}\big)^{c_m} f(\mathbf{n})}{\sum \cdots \sum_{n_1+\ldots+n_{M+1}=N} \prod_{m=1}^{M} p_{s,m}^{a_m+b_m} \big(1-p_{s,m}\big)^{c_m} f(\mathbf{n})} \right] \\ &+ \sum_{m=1}^{M} \big(a_m - b_m\big) \log \Big(\frac{1-p_{e,m}}{p_{e,m}} \Big) \underset{H_0}{\overset{H_1}{\gtrless}} \log \frac{\Pr(H_0)}{\Pr(H_1)}. \end{aligned} \tag{100}$$

The first term in (100) is zero since $f(\mathbf{n})$ does *not* depend on H_i. As a result, the optimal fusion rule is a weighted sum of a_m and b_m.

APPENDIX D

APPROXIMATION OF THE DEP

D.1 Approximation of the DEP $P_E(\mathbf{W}, \hat{\mathbf{r}}, \mathbf{n})$

We will find an approximation of the DEP $P_E(\mathbf{W}, \hat{\mathbf{r}}, \mathbf{n})$, which can be done by using Gaussian approximations for (2) and (4). By using the Demoivre-Laplace theorem [61], (2) can be approximated as

$$f(\mathbf{n}) \approx \prod_{m=1}^{M} \frac{1}{\sqrt{2\pi}\sigma_m} e^{-\frac{(n_m-\mu_m)^2}{2\sigma_m^2}}, \tag{101}$$

where $\mu_m = N\Delta F_m(\theta) = \bar{n}_m$ and $\sigma_m^2 = N\Delta F_m(\theta)\big(1 - \Delta F_m(\theta)\big)$. Note that, since $T < N$, the independence among $\{n_m\}$ are reasonable.

For (4), the Demoivre-Laplace theorem is not applicable because strong correlations exist between a_m and b_m. Therefore, we approximate (4) by a conditional joint Gaussian PDF $\mathcal{N}\left(\boldsymbol{\mu}_{m,i}, \mathbf{C}_{m,i}\right)$, where

$$\boldsymbol{\mu}_{m,i} = \begin{bmatrix} \mathbb{E}\{a_m|n_m, H_i\} \\ \mathbb{E}\{b_m|n_m, H_i\} \end{bmatrix},$$

$$\mathbf{C}_{m,i} = \begin{bmatrix} \mathbb{V}ar\{a_m|n_m, H_i\} & \mathbb{C}ov\{a_m, b_m|n_m, H_i\} \\ \mathbb{C}ov\{a_m, b_m|n_m, H_i\} & \mathbb{V}ar\{b_m|n_m, H_i\} \end{bmatrix},$$

where $\mathbb{V}ar\{\cdot\}$ and $\mathbb{C}ov\{\cdot\}$ denote the variance and covariance, respectively, of the random variable inside. From (4), we have the mean $\mathbb{E}\{a_m|n_m, H_i\} = K_m p_{s,m} p_{m|i}$, the mean $\mathbb{E}\{b_m|n_m, H_i\} = K_m p_{s,m}(1-p_{m|i})$, the variance $\mathbb{V}ar\{a_m|n_m, H_i\} = K_m p_{s,m} p_{m|i}(1-p_{s,m}p_{m|i})$, the variance $\mathbb{V}ar\{b_m|n_m, H_i\} = K_m p_{s,m}(1-p_{m|i})\left[1 - p_{s,m}(1-p_{m|i})\right]$, and the covariance $\mathbb{C}ov\{a_m, b_m|n_m, H_i\} = -K_m p_{s,m}^2(1-p_{m|i})p_{m|i}$.

Consequently, for given n_m and H_i, $a_m - b_m$ can be approximated as a Gaussian random variable with the mean $K_m p_{s,m}(2p_{m|i}-1)$ and variance $K_m p_{s,m}\left[1 - p_{s,m}(2p_{m|i}-1)^2\right]$.

Since, for given $\{n_m\}$ and H_i, the random variables $\{a_m - b_m\}$ are independent, the FC's test statistic z_{ps} is approximated as a Gaussian random variable, whose PDF is

$$f_Z(z_{ps}|\mathbf{n}, H_i) \overset{approx}{\sim} \mathcal{N}\big(\mu_i, \sigma_i^2\big), \tag{102}$$

where $\mu_{z,i} = \sum_{m=1}^{M} W_m K_m p_{s,m}(2p_{m|i}-1)$ and $\sigma_{z,i}^2 = \sum_{m=1}^{M} W_m^2 K_m p_{s,m}\left[1 - p_{s,m}(2p_{m|i}-1)^2\right]$.

By using (102), an approximation of the DEP $P_E(\mathbf{W}, \hat{\mathbf{r}}, \mathbf{n})$ can be expressed as

$$\tilde{P}_E(\mathbf{W}, \hat{\mathbf{r}}, \mathbf{n}) = \Phi\left(-\sqrt{\frac{\mu_{z,1}^2}{\sigma_{z,1}^2}}\right).$$

Note that examples of using Gaussian approximation in distributed detection are [2] and [58].

D.2 Approximation of the DEP $P_E(\mathbf{W}, \hat{\mathbf{r}})$

We will find an approximation of the DEP $P_E(\mathbf{W}, \hat{\mathbf{r}})$. For convenience, we use

$$A_m(n_m) = W_m K_m p_{s,m}(1 - 2p_{e,m}),$$
$$B_m(n_m) = W_m^2 K_m p_{s,m}\left[1 - p_{s,m}(1-2p_{e,m})^2\right].$$

Recall that K_m and $p_{s,m}$ are functions of n_m: $K_m = \min(K, n_m)$ and $p_{s,m} = \frac{n_m}{K}\left(1 - \frac{n_m}{K}\right)^{n_m - 1}$. From Craig's formula [25], $Q(x) = \frac{1}{\pi}\int_0^{\pi/2} e^{-\frac{x^2}{2\sin^2\phi}}\, d\phi$, we rewrite

$$\tilde{P}_E(\mathbf{W}, \hat{\mathbf{r}}, \mathbf{n}) = \frac{1}{\pi}\int_0^{\pi/2} e^{-\frac{1}{2\sin^2\phi}\frac{\left[\sum_{m=1}^{M} A_m(n_m)\right]^2}{\sum_{m=1}^{M} B_m(n_m)}}\, d\phi. \tag{103}$$

From the approximation of the joint PDF of $\{n_m\}$ in (101), an approximation of the DEP $P_E(\mathbf{W}, \hat{\mathbf{r}}$ can be written as

$$\tilde{P}_E(\mathbf{W}, \hat{\mathbf{r}}) = \mathbb{E}_{\mathbf{n}}\left\{\tilde{P}_{E|\mathbf{n}}\right\} = \mathbb{E}_{n_M}\left\{\cdots \mathbb{E}_{n_1}\left\{\tilde{P}_E(\mathbf{W}, \hat{\mathbf{r}}, \mathbf{n})\right\}\cdots\right\}.$$

Applying Gauss-Hermite quadrature integration, $\int_{-\infty}^{\infty} g(x)e^{-x^2}\, dx = \sum_{j=1}^{J} C_j g(x_j)$, where J is the number of sample points, $\{x_j\}$ are the roots of Hermite polynomial, and $\{C_j\}$ are the associated weights, (103), and (101), we can show that

$$\mathbb{E}_{n_1}\left\{\tilde{P}_E(\mathbf{W}, \hat{\mathbf{r}}, \mathbf{n})\right\} = \frac{1}{\pi}\int_0^{\pi/2} \frac{1}{\sqrt{\pi}} \sum_{j_1=1}^{J_1} C_{j_1} e^{-\frac{1}{2sin^2\phi}\frac{\left[A_1(\sqrt{2}\sigma_1 x_{j_1} + \mu_1) + \sum_{m=2}^{M} A_m(n_m)\right]^2}{B_1(\sqrt{2}\sigma_1 x_{j_1} + \mu_1) + \sum_{m=2}^{M} B_m(n_m)}}\, d\phi$$

Repeating these steps, we have

$$\tilde{P}_E(\mathbf{W},\hat{\mathbf{r}}) = \frac{1}{\pi}\left(\frac{1}{\sqrt{\pi}}\right)^M \int_0^{\pi/2} \sum_{j_1=1}^{J_1} \cdots \sum_{j_M=1}^{J_M} C_{j_1}\cdots C_{j_M} e^{-\frac{1}{2sin^2\phi}\frac{\left[\sum_{m=1}^{M} A_m(\sqrt{2}\sigma_m x_{j_m}+\mu_m)\right]^2}{\sum_{m=1}^{M} B_m(\sqrt{2}\sigma_m x_{j_m}+\mu_m)}}\, d\phi.$$

Let $J_m = 1$, for all m. We have $C_{j_m} = \sqrt{\pi}$ and $x_{j_m} = 0$, for all m. Therefore,

$$\tilde{P}_E(\mathbf{W},\hat{\mathbf{r}}) = \frac{1}{\pi}\int_0^{\pi/2} e^{-\frac{1}{2sin^2\phi}\frac{\left[\sum_{m=1}^{M} A_m(\mu_m)\right]^2}{\sum_{m=1}^{M} B_m(\mu_m)}}\, d\phi.$$

Note that $\mu_m = \bar{n}_m$. By using Craig's formula, we can rewrite $\tilde{P}_E(\mathbf{W},\hat{\mathbf{r}})$ as shown in Proposition 1.

APPENDIX E

OPTIMAL WEIGHTS

The weights $\{W_m^*\}$ that minimize $\tilde{P}_E(\mathbf{W}, \hat{\mathbf{r}})$ are equivalent to those that maximize

$$\frac{\left[\sum_{m=1}^{M} W_m \bar{K}_m \bar{p}_{s,m}(1-2p_{e,m})\right]^2}{\sum_{m=1}^{M} W_m^2 \bar{K}_m \bar{p}_{s,m}\left[1-\bar{p}_{s,m}(1-2p_{e,m})^2\right]}, \tag{104}$$

which is the *deflection coefficient* of z_{ps} defined as $\frac{(\mathbb{E}\{z_{ps}|H_1\}-\mathbb{E}\{z_{ps}|H_0\})^2}{\mathbb{V}ar\{z_{ps}|H_0\}}$, when the approximation of the PDF of z_{ps} is used. Taking the partial derivative of (104) with respect to W_m and setting it to zero, after some mathematical manipulation, we can find the optimal weights $\{W_m^*\}$ from the following equalities, for $m = 1, \ldots, M$,

$$W_m^* \frac{\left[1-\bar{p}_{s,m}(1-2p_{e,m})^2\right]}{(1-2p_{e,m})} = \frac{\sum_{i=1}^{M} (W_i^*)^2 \bar{p}_{s,i} \bar{K}_i \left[1-\bar{p}_{s,i}(1-2p_{e,i})^2\right]}{\left[\sum_{i=1}^{M} W_i^* \bar{p}_{s,i} \bar{K}_i (1-2p_{e,i})\right]}. \tag{105}$$

We can show that the equalities in (105) hold for all m when the weights $W_m^* = \frac{(1-2p_{e,m})}{[1-\bar{p}_{s,m}(1-2p_{e,m})^2]}$ are plugged in.

APPENDIX F

EFFECT OF THE RELIABILITY THRESHOLDS

The threshold $\hat{r}_m$, for $m = 1, \ldots, M-1$, affects both the variables $\bar{K}_m$, $\bar{p}_{s,m}$, $p_{e,m}$ for the mth frame and the variables $\bar{K}_{m+1}$, $\bar{p}_{s,m+1}$, $p_{e,m+1}$ for the $(m+1)$th frame. We elucidate the impacts of the thresholds $\{\hat{r}_m\}$ on $\tilde{P}_E(\mathbf{W}^*, \hat{\mathbf{r}})$ in the following two remarks.

Remark 2. *Consider the mth frame, for $m = 1, \ldots, M$. For a given $\hat{r}_{m-1}$, let $\hat{r}^\dagger[\hat{r}_{m-1}]$ (i.e., depending on $\hat{r}_{m-1}$), where $\hat{r}^\dagger[\hat{r}_{m-1}] < \hat{r}_{m-1}$, be the threshold such that*

$$\int_{\frac{\theta}{2}-\hat{r}_{m-1}}^{\frac{\theta}{2}-\hat{r}^\dagger[\hat{r}_{m-1}]} f_X(x)\,dx + \int_{\frac{\theta}{2}+\hat{r}^\dagger[\hat{r}_{m-1}]}^{\frac{\theta}{2}+\hat{r}_{m-1}} f_X(x)\,dx = \frac{K}{N}.$$

The threshold $\hat{r}_m$ affects $\tilde{P}_E(\mathbf{W}^*, \hat{\mathbf{r}})$ through $\bar{K}_m$, $\bar{p}_{s,m}$, and $p_{e,m}$, which can be explained as follows.

1) Increasing $\hat{r}_m$ (from 0 towards $\hat{r}_{m-1}$) at first gives a constant $\bar{K}_m = K$. Increasing $\hat{r}_m$ beyond $\hat{r}^\dagger[\hat{r}_{m-1}]$ lowers $\bar{K}_m = \bar{n}_m = N\Delta F_m(\theta)$.

2) Increasing $\hat{r}_m$ (from 0 towards $\hat{r}_{m-1}$) at first also increases $\bar{p}_{s,m}$, which reaches its peak $\left(1-\frac{1}{K}\right)^{K-1}$ at $\hat{r}^\dagger[\hat{r}_{m-1}]$. Increasing $\hat{r}_m$ beyond $\hat{r}^\dagger_m[\hat{r}_{m-1}]$ lowers $\bar{p}_{s,m}$.

3) Increasing $\hat{r}_m$ (from 0 towards $\hat{r}_{m-1}$) lowers $p_{e,m}$.

Remark 3. *Similarly, consider the $(m+1)$th frame, for $m = 1, \ldots, M-1$. For a given $\hat{r}_{m+1}$, let $\hat{r}^\wr[\hat{r}_{m+1}]$ (i.e., depending on $\hat{r}_{m+1}$), where $\hat{r}^\wr[\hat{r}_{m+1}] > \hat{r}_{m+1}$, be the threshold such that*

$$\int_{\frac{\theta}{2}-\hat{r}^\wr[\hat{r}_{m+1}]}^{\frac{\theta}{2}-\hat{r}_{m+1}} f_X(x)\,dx + \int_{\frac{\theta}{2}+\hat{r}_{m+1}}^{\frac{\theta}{2}+\hat{r}^\wr[\hat{r}_{m+1}]} f_X(x)\,dx = \frac{K}{N}.$$

The threshold $\hat{r}_m$ affects $\tilde{P}_E(\mathbf{W}^*, \hat{\mathbf{r}})$ through $\bar{K}_{m+1}$, $\bar{p}_{s,m+1}$, and $p_{e,m+1}$, which can be explained as follows.

1) Increasing $\hat{r}_m$ (from $\hat{r}_{m+1}$) at first increases $\bar{K}_{m+1} = \bar{n}_{m+1} = N\Delta F_{m+1}(\theta)$. Increasing $\hat{r}_m$ beyond $\hat{r}^{\wr}[\hat{r}_{m+1}]$ gives a constant $\bar{K}_{m+1} = K$.

2) Increasing $\hat{r}_m$ (from $\hat{r}_{m+1}$) at first also increases $\bar{p}_{s,m+1}$, which reaches its peak $\left(1 - \frac{1}{K}\right)^{K-1}$ at $\hat{r}^{\wr}[\hat{r}_{m+1}]$. Increasing $\hat{r}_m$ beyond $\hat{r}^{\wr}[\hat{r}_{m+1}]$ lowers $\bar{p}_{s,m+1}$.

3) Increasing $\hat{r}_m$ (from $\hat{r}_{m+1}$) lowers $p_{e,m+1}$.

In Remark 2 (respectively, Remark 3), varying $\hat{r}_m$ affects the tradeoff between the throughput $\bar{K}_m\bar{p}_{s,m}$ (respectively, $\bar{K}_{m+1}\bar{p}_{s,m+1}$) and the average probability of local decision error $p_{e,m}$ (respectively, $p_{e,m+1}$) in the mth frame (respectively, $(m+1)$th frame). Using the remarks above, we derive the feasible regions for $\{\hat{r}_m^*\}$ as follows.

The proof can be shown by induction. Given the optimal threshold $\hat{r}_{m-1}^*$, where $\hat{r}_0^* = \infty$, we consider the term $\bar{K}_m \frac{\bar{p}_{s,m}(1-2p_{e,m})^2}{[1-\bar{p}_{s,m}(1-2p_{e,m})^2]}$ in (8). Let $\hat{r}^{\dagger}[\hat{r}_{m-1}^*]$ be the threshold such that

$$\int_{\frac{\theta}{2}-\hat{r}_{m-1}^*}^{\frac{\theta}{2}-\hat{r}^{\dagger}[\hat{r}_{m-1}^*]} f_X(x)\,dx + \int_{\frac{\theta}{2}+\hat{r}^{\dagger}[\hat{r}_{m-1}^*]}^{\frac{\theta}{2}+\hat{r}_{m-1}^*} f_X(x)\,dx = \frac{K}{N}. \tag{106}$$

From Remark 2, fixing $\hat{r}_{m-1} = \hat{r}_{m-1}^*$, $\bar{K}_m\bar{p}_{s,m}$ and $\frac{(1-2p_{e,m})^2}{[1-\bar{p}_{s,m}(1-2p_{e,m})^2]}$ are increasing functions for $0 \le \hat{r}_m < \hat{r}^{\dagger}[\hat{r}_{m-1}^*]$, i.e., decreasing $\hat{r}_m$ towards 0 lowers the value of $\bar{K}_m \frac{\bar{p}_{s,m}(1-2p_{e,m})^2}{[1-\bar{p}_{s,m}(1-2p_{e,m})^2]}$. Therefore, the optimal threshold $\hat{r}_m^*$ must be larger than or equal to $\hat{r}^{\dagger}[\hat{r}_{m-1}^*]$. As a result, we obtain the condition (9).

APPENDIX G

DERIVATION OF ARE

Substituting (24) and (25) into (23) and using the following relations: $\theta = \frac{\gamma}{\sqrt{N}}$, $\frac{T}{N} = \check{T}$, $\frac{T}{K} = M$, and $\frac{n_m}{N} = \check{n}_m$, we have

$$ARE(\mathbf{W}^*, \hat{\mathbf{r}}, \check{\mathbf{n}}) = \lim_{N\to\infty} \frac{4}{M} \frac{\bar{p}_e(1-\bar{p}_e)}{(1-2\bar{p}_e)^2} \sum_{m=1}^{M} \breve{K}_m \frac{p_{s,m}(1-2p_{e,m})^2}{[1-p_{s,m}(1-2p_{e,m})^2]}, \tag{107}$$

where $p_{e,m}$ and $\bar{p}_e$ are defined in (3) and Lemma 4, respectively. Now the $p_{e,m}$ and $\bar{p}_e$ are functions of N because of $\theta = \frac{\gamma}{\sqrt{N}}$, while $\breve{K}_m$ and $p_{s,m}$, which are shown in the proof of Lemma 2, are independent of N. The limit $\lim_{N\to\infty}$ in (107) results in an indeterminate form, $\frac{0}{0}$, since $\bar{p}_e = \frac{1}{2}$ and $p_{e,m} = \frac{1}{2}$ as $N \to \infty$.

To find (107), L´Hôpital's rule is applied. For convenience, the following notations are used: $A = \bar{p}_e(1-\bar{p}_e)$, $B_m = \frac{(1-2p_{e,m})^2}{1-\bar{p}_{s,m}(1-2p_{e,m})^2}$, and $C = (1-2\bar{p}_e)^2$. Therefore, we have

$$\begin{aligned} ARE(\mathbf{W}^*, \hat{\mathbf{r}}, \check{\mathbf{n}}) =& \frac{4}{M} \lim_{N\to\infty} \frac{\left(\frac{\partial}{\partial N}A\right) \sum_{m=1}^{M} \breve{K}_m p_{s,m} B_m}{\frac{\partial}{\partial N}C} \\ &+ \frac{4}{M} \lim_{N\to\infty} \frac{A \sum_{m=1}^{M} \breve{K}_m p_{s,m} \left(\frac{\partial}{\partial N}B_m\right)}{\frac{\partial}{\partial N}C}. \end{aligned} \tag{108}$$

Note that $A = \frac{1}{4}$, $B_m = 0$, and $C = 0$ as $N \to \infty$. The derivatives of A, B_m, and C are: $\frac{\partial}{\partial N}A = -\frac{\gamma}{4\sqrt{N^3}}(1-2p_c)c$, $\frac{\partial}{\partial N}B_m = \frac{\gamma}{\sqrt{N^3}}(1-2p_c)b_m$, and $\frac{\partial}{\partial N}C = \frac{\gamma}{\sqrt{N^3}}(1-2p_c)c$, where

$$\begin{aligned} b_m &= \frac{\left(1-2p_{e,m}\right)\left(f_{(-)}f'_{(+)} - f_{(+)}f'_{(-)}\right)}{\left[1-p_{s,m}(1-2p_{e,m})^2\right]^2\left(f_{(-)}+f_{(+)}\right)^2}, \quad c = \left(1-2\bar{p}_e\right) f_X\Big(\frac{\gamma}{2\sqrt{N}}\Big), \\ f_{(-)} &= f_X\Big(\frac{\gamma}{2\sqrt{N}} - \hat{r}_m\Big), \quad f_{(+)} = f_X\Big(\frac{\gamma}{2\sqrt{N}} + \hat{r}_m\Big), \\ f'_{(-)} &= f'_X\Big(\frac{\gamma}{2\sqrt{N}} - \hat{r}_m\Big), \quad f'_{(+)} = f'_X\Big(\frac{\gamma}{2\sqrt{N}} + \hat{r}_m\Big). \end{aligned}$$

Note that $b_m = 0$ and $c = 0$ as $N \to \infty$ (because of $\bar{p}_e$ and $p_{e,m}$). As a result, since the first term on the right hand side of (108) is equal to zero, we have

$$ARE(\mathbf{W}^*, \hat{\mathbf{r}}, \check{\mathbf{n}}) = \frac{4}{M} \lim_{N\to\infty} \frac{A \sum_{m=1}^{M} \breve{K}_m p_{s,m} b_m}{c}, \tag{109}$$

which is again in an indeterminate form, $\frac{0}{0}$.

To find (109), L´Hôpital's rule is applied. Therefore, we have

$$\begin{aligned} ARE(\mathbf{W}^*, \hat{\mathbf{r}}, \check{\mathbf{n}}) =& \frac{4}{M} \lim_{N\to\infty} \frac{\left(\frac{\partial}{\partial N} A\right) \sum_{m=1}^{M} \breve{K}_m p_{s,m} b_m}{\frac{\partial}{\partial N} c} \\ &+ \frac{4}{M} \lim_{N\to\infty} \frac{A \sum_{m=1}^{M} \breve{K}_m p_{s,m} \left(\frac{\partial}{\partial N} b_m\right)}{\frac{\partial}{\partial N} c}. \end{aligned} \tag{110}$$

The derivatives of b_m and c can be show as follows.

$$\frac{\partial}{\partial N} b_m = \frac{\gamma}{2\sqrt{N^3}} \frac{(1-2p_c)\left(f_{(-)} f'_{(+)} - f_{(+)} f'_{(-)}\right)^2}{\left[1 - p_{s,m}(1-2p_{e,m})^2\right]^2 \left(f_{(-)} + f_{(+)}\right)^4} + \frac{\gamma}{4\sqrt{N^3}} \left[\text{Don't-Care}\right], \tag{111}$$

$$\frac{\partial}{\partial N} c = \frac{\gamma}{4\sqrt{N^3}} \left\{ 2(1-2p_c) \left[f_X\left(\frac{\gamma}{2\sqrt{N}}\right) \right]^2 - (1-2\bar{p}_e) f'_X\left(\frac{\gamma}{2\sqrt{N}}\right) \right\}. \tag{112}$$

As $N \to \infty$, we have: the first term of (110) and the term "Don't-Care" are zeros, $\bar{p}_e = \frac{1}{2}$, $p_{e,m} = \frac{1}{2}$, $f_X(\frac{\gamma}{2\sqrt{N}}) = f_X(0)$, $f'_X(\frac{\gamma}{2\sqrt{N}}) = f'_X(0)$,

$$f_{(-)} = f_{(+)} = f_X(\hat{r}_m), \quad f'_{(-)} = -f'_{(+)} = f'_X(\hat{r}_m). \tag{113}$$

After substituting (111), (112), and (113) into (110) and some mathematical manipulation, we obtain (26).

REFERENCES

[1] Abramson, N., "Packet switching with satellites," in *Nat. Comput. Conf., AFIPS Conf. Proc.*, vol. 42, (Montvale, NJ), pp. 695–702, 1973.

[2] Addesso, P., Marano, S., and Matta, V., "Sequential sampling in sensor networks for detection with censoring nodes," *IEEE Trans. Signal Process.*, vol. 55, pp. 5497–5505, Nov. 2007.

[3] Adireddy, S. and Tong, L., "Exploiting decentralized channel state information for random access," *IEEE Trans. Inf. Theory*, vol. 51, pp. 537–561, Feb. 2005.

[4] Ahmadi, H. R. and Vosoughi, A., "Distributed detection with adaptive topology and nonideal communication channels," *IEEE Trans. Signal Process.*, vol. 59, pp. 2857–2874, Jun. 2011.

[5] Anandkumar, A. and Tong, L., "Type-based random access for distributed detection over multiaccess fading channels," *IEEE Trans. Signal Process.*, vol. 55, pp. 5032–5043, Oct. 2007.

[6] Berger, C. R., Guerriero, M., Zhou, S., and Willett, P., "PAC vs. MAC for decentralized detection using noncoherent modulation," *IEEE Trans. Signal Process.*, vol. 57, pp. 3562–3575, Sep. 2009.

[7] Bertsekas, D. and Gallager, R., *Data Networks*. Englewood Cliffs, NJ: Prentice-Hall, 2nd ed., 1992.

[8] Bertsekas, D. P., *Nonlinear Programming*. Belmont, MA: Athena Scientific, 3nd ed., 1999.

[9] Bertsekas, D. P., *Dynamic Programming and Optimal Control*. Belmont, MA: Athena Scientific, 3rd ed., 2005, vol. 1.

[10] Bianchi, G. and Tinnirello, I., "Kalman filter estimation of the number of competing terminals in an IEEE 802.11 network," in *Proc. IEEE INFOCOM'03*, (San Francisco, CA), pp. 844–852, Apr. 2003.

[11] Blum, R. S., "Ordering for estimation and optimization in energy efficient sensor networks," *IEEE Trans. Signal Process.*, vol. 59, pp. 2847–2856, Jun. 2011.

[12] Blum, R. S., Kassam, S. A., and Poor, H. V., "Distributed detection with multiple sensors: Part II–Advanced topics," *Proc. IEEE*, vol. 85, pp. 64–79, Jan. 1997.

[13] Blum, R. S. and Sadler, B. M., "Energy efficient signal detection in sensor networks using ordered transmission," *IEEE Trans. Signal Process.*, vol. 56, pp. 3229–3235, Jul. 2008.

[14] Boyd, S. and Mutapcic, A., "Subgradient methods," *Notes for EE364b*, vol. Stanford University, Winter 2006–07.

[15] Braca, P., Marano, S., and Matta, V., "Single-transmission distributed detection via order statistics," *IEEE Trans. Signal Process.*, vol. 60, pp. 2042–2048, Apr. 2012.

[16] Braca, P., Marano, S., Matta, V., and Willett, P., "Asymptotic optimality of running concensus in testing binary hypotheses," *IEEE Trans. Signal Process.*, vol. 58, pp. 814–825, Feb. 2010.

[17] Capetanakis, J. I., "Tree algorithms for packet broadcast channels," *IEEE Trans. Inf. Theory*, vol. IT-25, pp. 505–515, Sep. 1979.

[18] Chair, Z. and Varshney, P. K., "Optimal data fusion in multiple sensor detection systems," *IEEE Trans. Aerosp. Electron. Syst.*, vol. AES-22, pp. 98–101, Jan. 1986.

[19] Chang, T.-Y., Hsu, T.-C., and Hong, Y.-W. P., "Exploiting data-dependent transmission control and MAC timing information for distributed detection in sensor networks," *IEEE Trans. Signal Process.*, vol. 58, pp. 1369–1382, Mar. 2010.

[20] Chen, B., Jiang, R., Kasetkasem, T., and Varshney, P. K., "Channel aware decision fusion in wireless sensor networks," *IEEE Trans. Signal Process.*, vol. 52, pp. 3454–3458, Dec. 2004.

[21] Chen, H. and Varshney, P. K., "Performance limit for distributed estimation systems with identical one-bit quantizers," *IEEE Trans. Signal Process.*, vol. 58, pp. 466–471, Jan. 2010.

[22] Cheng, V. W. and Wang, T.-Y., "Performance analysis of distributed decision fusion using a multilevel censoring scheme in wireless sensor networks," *IEEE Trans. Veh. Technol.*, vol. 61, pp. 1610–1619, May 2012.

[23] Ciuonzo, D., Romano, G., and Rossi, P. S., "Channel-aware decision fusion in distributed MIMO wireless sensor networks: Decod-and-fuse vs. decode-then-fuse," *IEEE Trans. Wireless Commun.*, vol. 11, pp. 2976–2985, Aug. 2012.

[24] Ciuonzo, D., Romano, G., and Rossi, P. S., "Performance analysis and design of maximum ratio combining in channel-aware MIMO decision fusion," *IEEE Trans. Wireless Commun.*, vol. 12, pp. 4716–4728, Sep. 2013.

[25] Craig, J. W., "A new, simple and exact result for calculating the probability of error for two-dimensional signal constellations," in *Proc. MILCOM*, pp. 25.5.1 – 25.5.5, Nov. 1991.

[26] Cui, S., Xiao, J.-J., Goldsmith, A. J., Luo, Z.-Q., and Poor, H. V., "Estimation diversity and energy efficiency in distributed sensing," *IEEE Trans. Signal Process.*, vol. 55, pp. 4683–4695, Sep. 2007.

[27] DasGupta, A., *Asymptotic Theory of Statistics and Probability*. New York: Springer, 2008.

[28] del Angel, G. and Fine, T. L., "Optimal power and retransmission control policies for random access systems," *IEEE/ACM Trans. Netw.*, vol. 12, pp. 1156–1166, Dec. 2004.

[29] Delic, H., Papantoni-Kazakos, P., and Kazakos, D., "Fundamental structures and asymptotic performance criteria in decentralized binary hypothesis testing," *IEEE Trans. Commun.*, vol. 43, pp. 32–43, Jan. 1995.

[30] Fang, J. and Li, H., "Distributed adaptive quantization for wireless sensor networks: From delta modulation to maximum likelihood," *IEEE Trans. Signal Process.*, vol. 56, pp. 5246–5257, Oct. 2008.

[31] Feller, W., *An Introduction to Probability Theory and Its Applications*. NY: Wiley, 3rd ed., 1968, vol. 1.

[32] Fonseca, B. J. B. and Gubner, J. A., "Least favorable distributions for the design of randomly deployed sensor detection systems," *IEEE Trans. Inf. Theory*, vol. 60, pp. 661–680, Jan. 2014.

[33] Gersho, A. and Gray, R. M., *Vector Quantization and Signal Compression*. Norwell, MA: Kluwer Academic Publishers, 1992.

[34] Ghosh, B. K. and Sen, P. K., eds., *Handbook of Sequential Analysis*. NY: Marcel Dekker, Inc., 1991.

[35] Guerriero, M., Pozdnyakov, V., Glaz, J., and Willett, P., "A repeated significance test with applications to sequential detection in sensor networks," *IEEE Trans. Signal Process.*, vol. 58, pp. 3426–3435, Jul. 2010.

[36] Hajek, B. and Loon, T. V., "Decentralized dynamic control of a multiaccess broadcast channel," *IEEE Trans. Automat. Contr.*, vol. 27, pp. 559–569, Jun. 1982.

[37] Hesham, L., Sultan, A., Nafie, M., and Digham, F., "Distributed spectrum sensing with sequential ordered transmissions to a cognitive fusion center," *IEEE Trans. Signal Process.*, vol. 60, pp. 2524–2538, May 2012.

[38] Hong, Y.-W. P., Lei, K.-U., and Chi, C.-Y., "Channel-aware random access control for distributed estimation in sensor networks," *IEEE Trans. Signal Process.*, vol. 56, pp. 2967–2980, Jul. 2008.

[39] Kapnadak, V., Senel, M., and Coyle, E. J., "Distributed iterative quantization for interference characterization in wireless networks," *Digit. Signal Process.*, vol. 22, pp. 96–105, Jan. 2012.

[40] Kassam, S. A., "Optimum quantization for signal detection," *IEEE Trans. Commun.*, vol. COM-25, pp. 479–484, May 1977.

[41] Kassam, S. A., *Signal Detection in Non-Gaussian Noise*. New York: Springer, 1988.

[42] Kleinrock, L. and Tobagi, F. A., "Packet switching in radio channels: Part I – Carrier sense multiple-access modes and their throughput-delay characteristics," *IEEE Trans. Commun.*, vol. COM-23, pp. 1400–1416, Dec. 1975.

[43] Kwon, Y., Fang, Y., and Latchman, H., "Design of MAC protocols with fast collision resolution for wireless local area networks," *IEEE Trans. Wireless Commun.*, vol. 3, pp. 793–807, May 2004.

[44] Laitrakun, S. and Coyle, E. J., "Optimizing the collection of local decisions for time-constrained distributed detection in WSNs," in *Proc. IEEE INFOCOM*, pp. 1971–1979, Apr. 2013.

[45] Laitrakun, S. and Coyle, E. J., "The use of reliability-based splitting algorithms to improve distributed estimation in WSNs," in *Proc. MILCOM*, Nov. 2013.

[46] Li, F., Evans, J. S., and Dey, S., "Decision fusion over noncoherent fading multiaccess channels," *IEEE Trans. Signal Process.*, vol. 59, pp. 4367–4380, Sep. 2011.

[47] Li, J. and AlRegib, G., "Rate-contrained distributed estimation in wireless sensor networks," *IEEE Trans. Signal Process.*, vol. 55, pp. 1634–1643, May 2007.

[48] Li, W. and Dai, H., "Distributed detection in wireless sensor networks using a multiple access channel," *IEEE Trans. Signal Process.*, vol. 55, pp. 822–833, Mar. 2007.

[49] Lin, Y., Chen, B., and Varshney, P. K., "Decision fusion rules in multi-hop wireless sensor networks," *IEEE Trans. Aerosp. Electron. Syst.*, vol. 41, pp. 475–488, Apr. 2005.

[50] Liu, K. and Sayeed, A. M., "Type-based decentralized detection in wireless sensor networks," *IEEE Trans. Signal Process.*, vol. 55, pp. 1899–1910, May 2007.

[51] Marano, S., Matta, V., and Willett, P., "Asymptotic design of quantizers for decentralized MMSE estimation," *IEEE Trans. Signal Process.*, vol. 55, pp. 5485–5496, Nov. 2007.

[52] Marano, S., Matta, V., and Willett, P., "Nearest-neighbor distributed learning by ordered transmissions," *IEEE Trans. Signal Process.*, vol. 61, pp. 5217–5230, Nov. 2011.

[53] Marano, S., Matta, V., Willett, P., and Tong, L., "Cross-layer design of sequential detectors in sensor networks," *IEEE Trans. Signal Process.*, vol. 54, pp. 4105–4117, Nov. 2006.

[54] Mei, Y., "Asymptotic optimality theory for decentralized sequential hypothesis testing in sensor networks," *IEEE Trans. Inf. Theory*, vol. 54, pp. 2072–2089, May 2008.

[55] Msechu, E. J. and Giannakis, G. B., "Sensor-centric data reduction for estimation with WSNs via censoring and quantization," *IEEE Trans. Signal Process.*, vol. 60, pp. 400–414, Jan. 2012.

[56] Nevat, I., Peters, G. W., and Collings, I. B., "Distributed detection in sensor networks over fading channels with multiple antennas at the fusion centre," *IEEE Trans. Signal Process.*, vol. 62, pp. 671–683, Feb. 2014.

[57] Niu, R., Chen, B., and Varshney, P. K., "Fusion of decisions transmitted over Rayleigh fading channels in wireless sensor networks," *IEEE Trans. Signal Process.*, vol. 54, pp. 1018–1027, Mar. 2006.

[58] Niu, R. and Varshney, P. K., "Target location estimation in sensor networks with quantized data," *IEEE Trans. Signal Process.*, vol. 54, pp. 4519–4528, Dec. 2006.

[59] Palomar, D. P. and Chiang, M., "A tutorial on decomposition methods for network utility maximization," *IEEE J. Sel. Areas Commun.*, vol. 24, pp. 1439–1451, Aug. 2006.

[60] Papastavrou, J. D. and Athans, M., "Distributed detection by a large team of sensors in tandem," *IEEE Trans. Aerosp. Electron. Syst.*, vol. 28, pp. 639–653, Jul. 1992.

[61] Papoulis, A. and Pillai, S. U., *Probability, Random Variables, and Stochastic Processes*. McGraw-Hill, 4th ed., 2002.

[62] Picinbono, B., "On deflection as a performance criterion in detection," *IEEE Trans. Aerosp. Electron. Syst.*, vol. 31, pp. 1072–1081, Jul. 1995.

[63] Poor, H. V. and Thomas, J. B., "Memoryless quantizer-detectors for constant signals in m-dependent noise," *IEEE Trans. Inf. Theory*, vol. IT-26, pp. 423–432, Jul. 1980.

[64] Qin, X. and Berry, R. A., "Distributed approaches for exploiting multiuser diversity in wireless networks," *IEEE Trans. Inf. Theory*, vol. 52, pp. 392–413, Feb. 2006.

[65] Rago, C., Willett, P., and Bar-Shalom, Y., "Censoring sensors: A low-communication-rate scheme for distributed detection," *IEEE Trans. Aerosp. Electron. Syst.*, vol. 32, pp. 554–568, Apr. 1996.

[66] Ribeiro, A. and Giannakis, G. B., "Bandwidth-constrained distributed estimation for wireless sensor networks – Part I: Gaussian case," *IEEE Trans. Signal Process.*, vol. 54, pp. 1131–1143, Mar. 2006.

[67] S., R. and Kassam, S. A., "On the asymptotic relative efficiency of distributed detection schemes," *IEEE Trans. Inf. Theory*, vol. 41, pp. 523–527, Mar. 1995.

[68] Sun, X. and Coyle, E. J., "Low-complexity algorithms for event detection in wireless sensor networks," *IEEE J. Sel. Areas Commun.*, vol. 28, pp. 1138–1148, Sep. 2010.

[69] Sun, X. and Coyle, E. J., "Quantization, channel compensation, and optimal energy allocation for estimation in sensor networks," *ACM Trans. Sensor Netw.*, vol. 8, pp. 15:1–15:25, Mar. 2012.

[70] Sung, Y., Tong, L., and Swami, A., "Asymptotic locally optimal detector for large-scale sensor networks under the Poisson regime," *IEEE Trans. Signal Process.*, vol. 53, pp. 2005–2017, Jun. 2005.

[71] Swaszek, P. E., "On the performance of serial networks in distributed detection," *IEEE Trans. Aerosp. Electron. Syst.*, vol. 29, pp. 254–260, Jan. 1993.

[72] Tang, Z. B., Pattipati, K. R., and Kleinman, D. L., "Optimization of detection networks: Part I – Tandem structure," *IEEE Trans. Syst., Man, Cybern.*, vol. 21, pp. 1044–1059, Sep./Oct. 1991.

[73] Tantaratana, S. and Nasipuri, A., "Two-stage Wilcoxon detectors using conditional tests," *IEEE Trans. Inf. Theory*, vol. 38, pp. 1080–1090, May 1992.

[74] Tepedelenlioglu, C. and Dasarathan, S., "Distributed detection over Gaussian multiple access channels with constant modulus signaling," *IEEE Trans. Signal Process.*, vol. 59, pp. 2875–2886, Jun. 2011.

[75] Tian, Q. and Coyle, E. J., "Optimal distributed detection in clustered wireless sensor networks," *IEEE Trans. Signal Process.*, vol. 55, pp. 3892–3904, Jul. 2007.

[76] Tong, L., Zhao, Q., and Mergen, G., "Multipacket reception in random access wireless networks: From signal processing to optimal medium access control," *IEEE Commun. Mag.*, vol. 39, pp. 108–112, Nov. 2001.

[77] Veeravalli, V. V., Başar, T., and Poor, H. V., "Decentralized sequential detection with a fusion center performing the sequential test," *IEEE Trans. Inf. Theory*, vol. 39, pp. 433–442, Mar. 1993.

[78] Venkitasubramaniam, P., Tong, L., and Swami, A., "Quantization for maximin ARE in distributed estimation," *IEEE Trans. Signal Process.*, vol. 55, pp. 3596–3605, Jul. 2007.

[79] Viswanathan, R. and Varshney, P. K., "Distributed detection with multiple sensors: Part I–Fundamentals," *Proc. IEEE*, vol. 85, pp. 54–63, Jan. 1997.

[80] Wald, A., *Sequential Analysis*. NY: Wiley, 1947.

[81] Wang, T.-Y. and Wu, J.-Y., "Does more transmitting sensors always mean better decision fusion in censoring sensor networks with an unknown size?," *IEEE Trans. Commun.*, vol. 60, pp. 2313–2325, Aug. 2012.

[82] Wang, X., Tu, Y., and Giannakis, G. B., "Design and analysis of cross-layer tree algorithms for wireless random access," *IEEE Trans. Wireless Commun.*, vol. 7, pp. 909–919, Mar. 2008.

[83] Wang, Y. and Mei, Y., "Quantization effect on the log-likelihood ratio and its application to decentralized sequential detection," *IEEE Trans. Signal Process.*, vol. 61, pp. 1536–1543, Mar. 2013.

[84] Wimalajeewa, T. and Jayaweera, S. K., "Optimal power scheduling for correlated data fusion in wireless sensor networks via constrained PSO," *IEEE Trans. Wireless Commun.*, vol. 7, pp. 3608–3618, Sep. 2008.

[85] Wolsey, L. A., *Integer Programming*. New York: Wiley-Interscience Publication, 1998.

[86] Wu, J., Huang, Q., and Lee, T., "Minimal energy decentralized estimation via exploiting the statistical knowledge of sensor noise variance," *IEEE Trans. Signal Process.*, vol. 56, pp. 2171–2176, May 2008.

[87] Wu, J. and Wang, T.-Y., "Power allocation for robust distributed best-linear-unbiased estimation against sensing noise variance uncertainty," *IEEE Trans. Wireless Commun.*, vol. 12, pp. 2853–2869, Jun. 2013.

[88] Xiao, J.-J., Cui, S., Luo, Z.-Q., and Goldsmith, A. J., "Power scheduling of universal decentralized estimation in sensor networks," *IEEE Trans. Signal Process.*, vol. 54, pp. 413–422, Feb. 2006.

[89] Xiao, J.-J., Cui, S., Luo, Z.-Q., and Goldsmith, A. J., "Linear coherent decentralized estimation," *IEEE Trans. Signal Process.*, vol. 56, pp. 757–770, Feb. 2008.

[90] Xiao, J.-J. and Luo, Z.-Q., "Decentralized estimation in an inhomogeneous sensing environment," *IEEE Trans. Inf. Theory*, vol. 51, pp. 3564–3575, Oct. 2005.

[91] Xiao, J.-J., Ribeiro, A., Luo, Z.-Q., and Giannakis, G. B., "Distributed compression-estimation using wireless sensor networks," *IEEE Signal Process. Mag.*, vol. 23, pp. 27–41, Jul. 2006.

[92] Xu, D. and Yao, Y., "Contention-based transmission for decentralized detection," *IEEE Trans. Wireless Commun.*, vol. 11, pp. 1334–1342, Apr. 2012.

[93] Xu, D. and Yao, Y., "Splitting tree algorithm for decentralized detection in sensor networks," *IEEE Trans. Wireless Commun.*, vol. 12, pp. 6024–6033, Dec. 2013.

[94] Yao, Y., "Group-ordered SPRT for decentraized detection," *IEEE Trans. Inf. Theory*, vol. 58, pp. 3564–3574, Jun. 2012.

[95] Yilmaz, Y., Moustakides, G. V., and Wang, X., "Channel-aware decentralized detection via level-triggered sampling," *IEEE Trans. Signal Process.*, vol. 61, pp. 300–315, Jan. 2013.

[96] Yiu, S. and Schober, R., "Nonorthogonal transmission and noncoherent fusion of censored decisions," *IEEE Trans. Veh. Technol.*, vol. 58, pp. 263–273, Jan. 2009.

[97] Yuan, Y. and Kam, M., "Distributed decision fusion with a random-access channel for sensor network applications," *IEEE Trans. Instrum. Meas.*, vol. 53, pp. 1339–1344, Aug. 2004.

[98] Zhang, X., Poor, H. V., and Chiang, M., "Optimal power allocation for distributed detection over MIMO channels in wireless sensor networks," *IEEE Trans. Signal Process.*, vol. 56, pp. 4124–4140, Sep. 2008.